

Universal microscopic descriptions for statistics of particles and extended excitations

Ryohei Kobayashi,^{1,*} Yuyang Li,^{2,*} Hanyu Xue,^{2,3} Po-Shen Hsin,^{4,†} and Yu-An Chen^{2,‡}

¹*School of Natural Sciences, Institute for Advanced Study, Princeton, NJ 08540, USA*

²*International Center for Quantum Materials, School of Physics, Peking University, Beijing 100871, China*

³*Yuanpei College, Peking University, Beijing 100871, China*

⁴*Department of Mathematics, King's College London, Strand, London WC2R 2LS, UK*

(Dated: December 10, 2024)

Statistics of excitations play an essential role in understanding phases of matter. In this paper, we introduce a universal method for studying the generalized statistics of Abelian particles and extended excitations in lattices of any dimension. We compute the statistics using the Berry phase of a sequence of unitary operators that transports the excitations while canceling local ambiguities at each step. The sequence is derived from locality, using the Smith normal form. We show that the statistics are quantized invariants. Our method unifies the statistics for the braiding and fusion of particles and loops, and leads to the discovery of novel statistics for membrane excitations. The statistics can be interpreted as the quantum anomaly of a generalized global symmetry, which manifests as an obstruction to gauging the symmetry on lattices. Furthermore, we show that non-trivial statistics forbid short-range entangled states, establishing the dynamical consequence of anomalies in microscopic lattice models.

CONTENTS

I. Introduction	2	A. Deriving generalized statistics via locality identities	15
A. Summary of results	2	1. \mathbb{Z}_2 particles in (2+1)D	15
1. Universal microscopic description for statistics	2	2. \mathbb{Z}_2 loops in (3+1)D	16
2. Statistics as anomalies and their dynamical consequences	5	B. Computational algorithm using the Smith normal form	16
B. Examples	5	C. Generalized statistics as anomalies: computational approach	18
1. Particle Excitations	6	D. Stability of generalized statistics	19
2. Loop Excitations	7	IV. Statistics as Obstruction to Gauging	20
3. Membrane Excitations	9	V. Statistics as Obstruction to Short Range Entanglement: Dynamical Consequence of Anomalies	21
II. Framework for Generalized Statistics	9	A. Review: Anyons imply long-range entanglement	22
A. Review: T-junction of anyons in (2+1)D	9	B. Example: Fermionic loops imply long-range entanglement	22
B. Framework of invariants in generic dimensions	10	1. MPS representation of excitations in SRE states	22
1. Excitations and unitaries on simplicial complex	10	2. Decomposition of phases	23
2. Invariant Berry phases from unitary sequences	11	C. Nontrivial statistics imply long-range entanglement	24
3. Equivalence of Berry phases and genuine invariants	12	1. Patchwork of tensor network states at the excitations	25
4. Quantization of generalized statistics	13	2. Decomposition of phases	25
C. Generalized statistics for non-Abelian 0-form symmetries	13	3. Trivial invariants in SRE states	26
1. Generalized statistics for non-Abelian fusion groups	13	VI. Discussions	27
2. Quantization of invariants for non-Abelian fusion groups	14	Acknowledgements	28
III. Computation of Generalized Statistics	14	A. Simplicial complex, chains, and cochains	28
		B. Derivations for particle and loop statistics with fusion group \mathbb{Z}_2	28
		1. T-junction process in (2+1)D	28
		2. Loop-flipping process in (3+1)D	30

* These authors contributed equally to this work.

† E-mail: po-shen.hsin@kcl.ac.uk

‡ E-mail: yuanchen@pku.edu.cn

C. Detailed analysis on the structure of E_{id} 32

References 36

I. INTRODUCTION

Statistics of excitations underlie many physical phenomena in condensed matter and high-energy physics. For instance, nontrivial statistics of particles can forbid their condensation. Bosons can condense and lead to superfluidity or superconductivity [1–6], while fermions cannot condense [7–10]. In (2+1)D, particles can obey anyonic statistics that are neither bosons nor fermions, and this leads to interesting phenomena such as fractional quantum Hall effects [11–14], and has important applications to topological quantum computation [15–18], with deep mathematical connection to modular tensor categories and knot theory [19–23].

In addition to particles, there are extended excitations, such as flux loops in gauge theories and domain wall excitations. Unlike particles, where all data can be described by fusion category theory [10, 20, 23–28], research on the statistics of extended excitations remains ongoing [29–40]. There are recent works [41–45] describing the statistics of extended excitations as dependence on framing, i.e., choice of frame basis in the normal directions of the excitation. In particular, the statistics of loop excitations in \mathbb{Z}_2 gauge theories with fermionic particles, which can appear in superconducting phases, are related to certain discrete gravitational ’t Hooft anomalies [43–47]. These anomalies impose constraints on whether such theories can be consistently realized on a lattice. Such fermionic loop statistics also give rise to new quantum cellular automata [43, 48], which are locality-preserving maps that have fundamental importance in lattice quantum systems.

The statistics of topological excitations also provide ’t Hooft anomaly of the corresponding symmetry, which constrains the dynamics of the quantum systems and distinguishes different phases of matter. For instance, the 1-form global symmetry in (2+1)D is generated by Abelian anyons [27, 49], and the statistics determines whether the 1-form symmetry can be gauged. Any quantum system with such anyons cannot flow to a trivially gapped phase, as exemplified in numerous lattice models, including the emergent fermion in Kitaev’s honeycomb model [20] and its generalizations [50]. The ’t Hooft anomaly matching condition also allows us to distinguish different phases of matter by the statistics of topological excitations, as used extensively in Ref. [51–58].

In this work, we develop general processes on lattices to compute all possible statistics for excitations of general dimensions, including particles and extended excitations such as loop excitations. Statistics are extracted from multi-step operations on lattices that transform excitations back to themselves, such as moving particle excitations using string operators, and the statistics arise as the

Berry phase of the operation. In each step, there can be microscopic phase ambiguity that modifies the state at each site, and the operations are designed such that these ambiguities are canceled out to give well-defined universal statistics. Examples of such operations are discussed in Ref. [59, 60] for particle excitations and in Ref. [44] for loop excitations. However, these operations are not studied systematically and do not consider excitations in general dimensions.

We develop a systematic method based on the Smith normal form to construct sequences of unitary operators with clear physical interpretations. Using this method, we unify and improve known statistical processes for both particle and loop excitations and also uncover new statistics related to extended excitations, such as membrane excitations. The generalized statistics described within this framework include not only the conventional braiding processes but also F-symbol data associated with different fusion pathways.

Moreover, the statistics of excitations often imply a nontrivial low-energy spectrum, as particles with nontrivial statistics cannot condense. We find that these microscopic definitions of statistics are directly related to ’t Hooft anomalies in lattice models, and we demonstrate that these statistics prevent the realization of a short-range entangled state. This connection provides insight into the dynamical consequences of ’t Hooft anomalies in microscopic lattice models. We focus on invertible excitations, whose fusion follows group multiplication rules. The generalization to non-invertible excitations will be explored in future work.

A. Summary of results

1. Universal microscopic description for statistics

This work develops a universal framework to define generalized statistics on lattices across different space-time dimensions. We consider gapped local Hamiltonian systems in d spatial dimensions with tensor product Hilbert space,

$$H = \sum H_i, \quad (1)$$

where each Hamiltonian term H_i has support confined to a small ball of constant radius. Excitations are represented by the states that deviate from the ground state around their loci.

We consider systems exhibiting **invertible excitations**, where each excitation possesses an inverse, enabling mutual annihilation and forming a fusion group G . For simplicity, we summarize the results when G is an Abelian group. These results are generalized to the non-Abelian fusion groups as well. These excitations may extend spatially, spanning p dimensions. For instance, $p = 0$ corresponds to quasiparticles, while $p = 1$ represents loop excitations, such as magnetic flux loops, and so on.

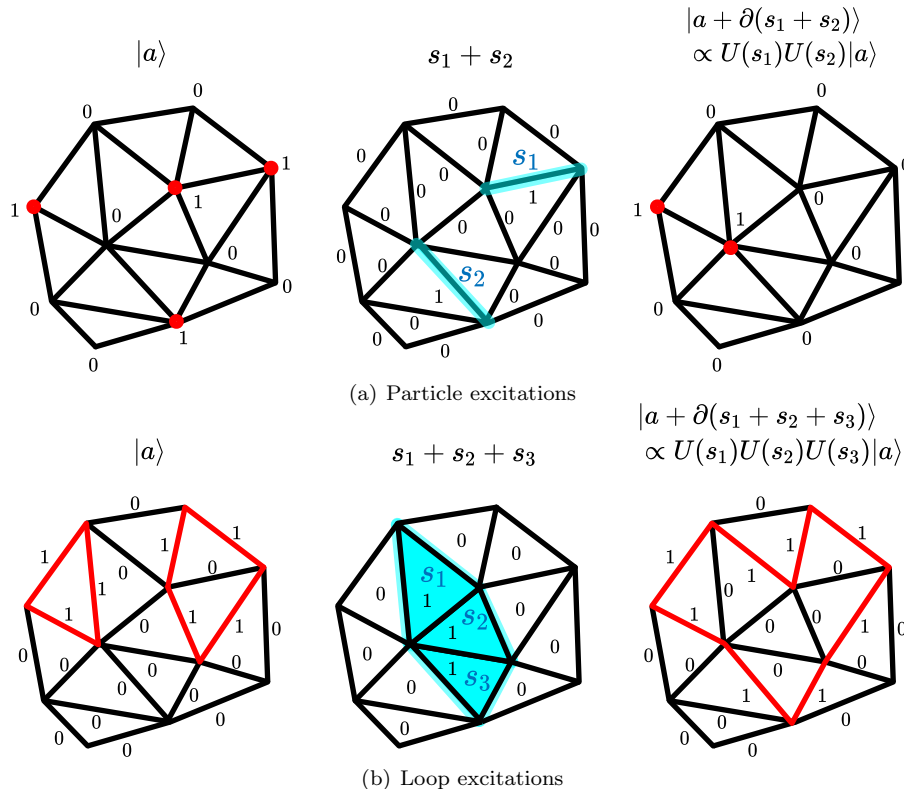


FIG. 1. Particles and loop excitations. (a) For simplicity, we consider particles with the fusion group $G = \mathbb{Z}_2$. The configuration state $|a\rangle$ is labeled by a \mathbb{Z}_2 field at each vertex, indicating the presence or absence of particle excitations. Edges s_1 and s_2 have coefficients $1 \in \mathbb{Z}_2$. The unitary operator $\prod_i U(s_i)$ is the string operator supported on these edges, creating particles at the endpoints. (b) For loop excitations with the fusion group $G = \mathbb{Z}_2$, the configuration state $|a\rangle$ is labeled by a \mathbb{Z}_2 field on each edge, with edges labeled by $1 \in \mathbb{Z}_2$ forming closed loops. Faces s_1, s_2, s_3 have coefficients $1 \in \mathbb{Z}_2$. The unitary operator $\prod_i U(s_i)$ is the membrane operator supported on these faces, creating loop excitations along the boundaries. Applying $\prod_i U(s_i)$ to $|a\rangle$ in both cases yields a configuration state proportional to $|a + \partial(\sum_i s_i)\rangle$. These examples can be generalized to any Abelian group G , with additional considerations for the branching structure.

Our framework begins by specifying the possible configurations of excitations, denoted by \mathcal{A} , on a simplicial complex X embedded in space. We consider the Hilbert space basis labeled by excitations $a \in \mathcal{A}$, where each p -dimensional simplex is associated with an element of the group G . Each configuration is represented by the **configuration state** $|a\rangle$. This state is not uniquely defined, as it can be redefined through the action of unitary operators supported at the locations of the excitations. To address this ambiguity, we fix a particular choice of states $|a\rangle$ and construct invariants that remain independent of these definitions.

Excitations are generated by local unitary operators $U(s)$, supported on a $(p+1)$ -dimensional simplex, where s represents the $(p+1)$ -simplex with a coefficient in G . We assume these excitations are deconfined, meaning that the operator $U(s)$ creates excitations only localized around its boundary ∂s . When a sum of s , such as $s_1 + \dots + s_n$, is closed (having no boundary), the combined operator $U(s_n) \dots U(s_1)$ commutes with the Hamiltonian and generates a (generalized) global symmetry of the system. Since the excitations are assumed to be invertible, this (generalized) global symmetry forms a group. In

general, the symmetries can form a higher group [62, 63], and they are symmetries support on subsystems on the lattice [64].

We will assume that the unitaries $U(s)$ generating the symmetry can be realized by a finite-depth quantum circuit—for example, the operator will not involve lattice isometries such as translation or rotation. This is always true for U that generates internal symmetries, and we will focus on such cases from now on. This assumption will later play an important role in our formulation of the invariants for generalized statistics.

The unitaries move the configuration of the excitations. In general, a unitary operator can be used to connect two states $|a\rangle$ and $|a'\rangle$ through the relation $U(s)|a\rangle \propto |a'\rangle$, where $a + \partial s = a'$ and $+$ represents the fusion of Abelian excitations. Once the states $|a\rangle$ and the unitary operators $U(s)$ are chosen, the phase factor $\theta(s, a)$ can be specified as:

$$U(s)|a\rangle = \exp[i\theta(s, a)]|a + \partial s\rangle, \quad (2)$$

with $\theta(s, a)$ depending on both the unitary operator $U(s)$ and the initial state $|a\rangle$. Note that each individual phase factor $\theta(s, a)$ does not have a direct physical meaning, as

	G -particles with $G = \prod_i \mathbb{Z}_{N_i}$	G -loops with $G = \prod_i \mathbb{Z}_{N_i}$	G -membranes with $G = \prod_i \mathbb{Z}_{N_i}$
(1+1)D	$H^3(BG, U(1))$ $= \prod_i \mathbb{Z}_{N_i} \prod_{i < j} \mathbb{Z}_{(N_i, N_j)}$ $\prod_{i < j < k} \mathbb{Z}_{(N_i, N_j, N_k)}$		
(2+1)D	$H^4(B^2G, U(1))$ $= \prod_i \mathbb{Z}_{(N_i, 2) \times N_i} \prod_{i < j} \mathbb{Z}_{(N_i, N_j)}$	$H^4(BG, U(1))$ $= \prod_{i < j} \mathbb{Z}_{(N_i, N_j)}^2 \prod_{i < j < k} \mathbb{Z}_{(N_i, N_j, N_k)}^2$ $\prod_{i < j < k < l} \mathbb{Z}_{(N_i, N_j, N_k, N_l)}$	
(3+1)D	$H^5(B^3G, U(1))$ $= \prod_i \mathbb{Z}_{(N_i, 2)}$	$H^5(B^2G, U(1))$ $= \prod_i \mathbb{Z}_{(N_i, 2)} \prod_{i < j} \mathbb{Z}_{(N_i, N_j)}$	$H^5(BG, U(1))$ $= \prod_i \mathbb{Z}_{N_i} \prod_{i < j} \mathbb{Z}_{(N_i, N_j)}^2$ $\prod_{i < j < k} \mathbb{Z}_{(N_i, N_j, N_k)}^4$ $\prod_{i < j < k < l} \mathbb{Z}_{(N_i, N_j, N_k, N_l)}^3$ $\prod_{i < j < k < l < m} \mathbb{Z}_{(N_i, N_j, N_k, N_l, N_m)}$

TABLE I. The cohomology of the Eilenberg–MacLane space $B^n G := K(G, n)$ for the finite Abelian group $G = \prod_i \mathbb{Z}_{N_i}$, as computed in Ref. [61]. The notation (N_i, N_j, \dots) denotes the greatest common divisor among the integers. This cohomology classifies the anomaly as an obstruction to gauging the higher-form G symmetry, which corresponds to symmetry-protected topological (SPT) phases in one higher dimensions. We conjecture that these data precisely match the generalized statistics of particle, loop, and membrane excitations as defined by Eq. (31) in Sec. II B. Specifically, p -dimensional excitations in $(d + 1)$ -dimensional spacetime have generalized statistics characterized by $H^{d+2}(B^{d-p}G, U(1))$. This conjecture has been verified for small groups G , with explicit sequences of unitary operators demonstrating the generalized statistics provided in Sec. I B.

it is sensitive to the specific choices of $\{|a\rangle\}$ and $\{U(s)\}$. On the other hand, certain combinations of the phase factors are independent of these choices and, therefore, correspond to physically meaningful quantities, which we refer to as **generalized statistics**. Changing the choices of $\{|a\rangle\}$ and $\{U(s)\}$ can be thought of as “gauge transformations” that affect the “Berry connection” $\theta(s, a)$. The gauge-invariant combinations of $\theta(s, a)$ yield the generalized statistics of the excitations, capturing their fundamental physical properties.

For example, in the case of quasiparticle excitations, the configuration state $|a\rangle$ can be represented by vertices labeled with elements of a group G . Each unitary $U(s)$ can be visualized as an edge labeled by a generator $g \in G$, connecting two vertices v_i and v_j . The operator $U(s)$ creates excitations g at v_j and g^{-1} at v_i , as shown in Fig. 1, with $G = \mathbb{Z}_2$. This concept similarly extends to loop excitations and higher-dimensional excitations.

We then consider the sequence of unitaries starting with the specific configuration of the excitations back to itself,

$$\begin{aligned} & \langle a_0 | U(s_{n-1}) \dots U(s_j) \dots U(s_0) | a_0 \rangle \\ &= \exp \left(i \sum_{j=0}^{n-1} \theta(s_j, a_j) \right), \end{aligned} \quad (3)$$

with $a_{j+1} := a_j + \partial s_j$. The above sequence can be regarded as the “closed path” in the Hilbert space, along which we measure the Berry phase associated with the family of states. For a practical purpose, it is convenient to treat the above phase as the formal sum of the objects

$\theta(s, a)$:

$$E = \bigoplus_{s, a} \mathbb{Z} \theta(s, a). \quad (4)$$

The phase defined above may or may not remain invariant under possible deformations of the states $|a\rangle$ and the unitaries $U(s)$, such as the redefinition by phases or local perturbations modifying the unitaries $U \rightarrow UU'$ at each step for unitaries U' close to the identity. The sequence needs to be carefully designed to be invariant under such deformations. We will see that the necessary and sufficient conditions for the invariance can be formulated as the constraints on the \mathbb{Z} coefficients in Eq. (4). We define the subgroup $E_{\text{inv}} \subset E$, which contains the elements that qualify as invariants associated with the excitations.

Some elements of E_{inv} correspond to trivial invariants that reduce to the identity operator. A trivial sequence of unitaries arises from the locality properties of the unitary operators. For instance, if the supports of two operators $U(s_1)$ and $U(s_2)$ do not overlap, i.e., $s_1 \cap s_2 = \emptyset$, their commutator is trivial

$$[U(s_1), U(s_2)] = 1, \quad (5)$$

where $[A, B] := A^{-1}B^{-1}AB$. This property extends to higher commutators involving multiple operators, such as:

$$[[[U(s_1), U(s_2)], \dots], U(s_n)] = 1, \quad (6)$$

if $s_1 \cap s_2 \cap \dots \cap s_n = \emptyset$. This property follows from the fact that each unitary is a finite-depth circuit, ensuring that the commutator $[U(s_1), U(s_2)]$ has support only around $s_1 \cap s_2$ due to the Lieb-Robinson bound [65, 66]. These

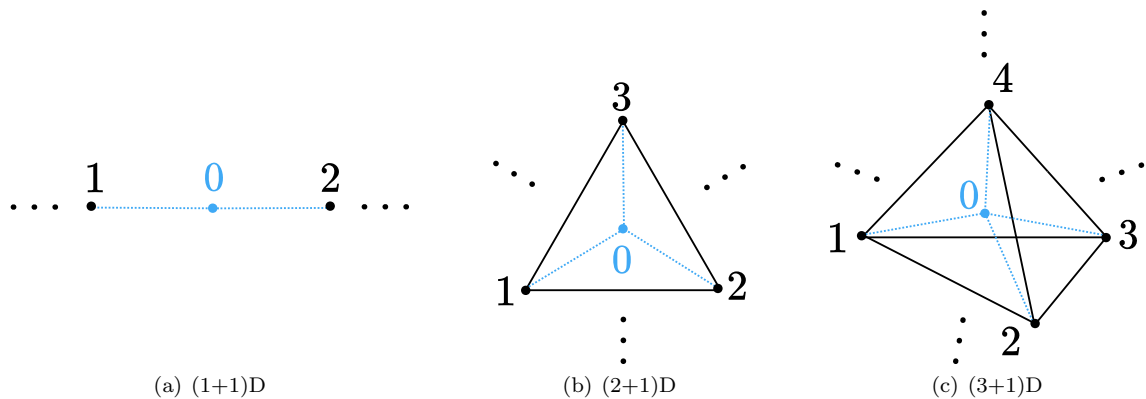


FIG. 2. In each dimension, we consider different simplicial complexes. In (1+1)D, we use a segment subdivided by a vertex; in (2+1)D, a triangle with a central vertex; and in (3+1)D, a tetrahedron subdivided by a central vertex. These complexes are embedded into a larger spatial manifold (omitted by \dots), with edge lengths chosen to be much longer than the system's correlation length. For computational convenience, we often compactify the manifold, wrapping the segment into a circle S^1 , the triangle into a 2-sphere S^2 , and the tetrahedron into a 3-sphere S^3 .

higher commutators acting on any initial configuration state $|a_0\rangle$, form the subgroup $E_{\text{id}} \subset E_{\text{inv}}$. The genuine invariants of the excitations are characterized by the quotient group $T := E_{\text{inv}}/E_{\text{id}}$, where the trivial phases due to locality have been factored out. We generally show that the invariants T with the finite group symmetry G become the finite Abelian group. This implies that the invariants T must be quantized into the discrete values.

This group of invariants can be explicitly computed using a computer, given the possible configurations of the excitations and the unitaries, as well as the group G describing the fusion of excitations.

2. Statistics as anomalies and their dynamical consequences

The above invariant $\Theta \in T$ gives a microscopic definition for the statistics of the excitations. At the same time, Θ is regarded as the microscopic definition of the 't Hooft anomalies for the global symmetry G . It is because each unitary $U(s)$ at a support s can be identified as the product of Gauss law operators that generates the symmetry restricted at s . The invariant Θ is the phase obtained from the product of the Gauss law operators, hence becomes an obstruction to the Gauss law constraints $U(s) = 1$ with any choice of s .

The presence of 't Hooft anomalies constrain the low energy spectrum of the theory. In particular, 't Hooft anomalies forbid a unique gapped ground state. We find that the invariants of microscopic lattice systems Θ directly lead to such a dynamical consequence: when the invariant Θ with the higher-form symmetry defects is nontrivial, the state cannot be a short-range entangled (SRE) state preserving the symmetry. We show that this statement is in full generality, assuming the tensor network representation of the state with excitations. This is reminiscent of the Lieb-Schultz-Mattis theorem [67–73],

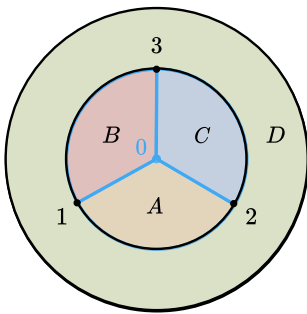
which constrains the low-energy spectrum of the state based on a given action of the internal and crystalline symmetries.

A large class of 't Hooft anomalies can be described through group cohomology by employing the group cohomology SPT phase in the bulk via bulk-boundary correspondence [74–76]. The mathematical results presented in Table I show the group cohomology of higher-form symmetry, i.e., the cohomology of the Eilenberg–MacLane space, for finite Abelian groups [61].¹ Our generalized statistics provides a microscopic perspective of 't Hooft anomalies on the lattice, and in all examples we have evaluated on a computer, its classification matches the results in Table I. Although the computational power limits us from verifying arbitrarily large groups G , the agreement in the small cases suggests the correspondence. This consistency leads us to conjecture that our generalized statistics are classified by the group cohomology of higher groups. In the following section, we explicitly demonstrate examples of generalized statistics for small groups G , illustrating their correspondence to the group cohomology of higher-form symmetries.

B. Examples

This work presents a general framework for defining the statistics of p -dimensional invertible excitations in d -dimensional spatial manifolds for arbitrary p and d . The condition of invertibility implies unitarity. Causality, governed by the Lieb-Robinson bound [65, 66], imposes locality requirements on these unitary operators, determining the structure of the statistics. We illustrate

¹ The cohomology of the Eilenberg–MacLane spaces have been computed up to $H^9(K(G, -), U(1))$ in Ref. [61].



$$Z_4^I(a, b) := (U(a)_{B+C})^{-N} \left(U(a)_{B+C} [U(a)_B, [U(a)_A, U(b)_{A+B+C+D}]] \right)^N, \quad (7)$$

$$Z_4^{II}(a, b) := (U(b)_{B+C})^{-N} \left(U(b)_{B+C} [U(b)_B, [U(b)_A, U(a)_{A+B+C+D}]] \right)^N.$$

FIG. 3. The statistics of loops in (2+1)D can be detected on an open disk. Let $U(i)_A$, $U(i)_B$, $U(i)_C$, and $U(i)_D$ represent membrane operators that create loop excitations labeled by i on their respective boundaries (with $i = a, b$ as generators of fusion group $G = \mathbb{Z}_N \times \mathbb{Z}_N$). $U(i)_{I+J+\dots}$ represents the membrane operator acting on the region $I \cup J \cup \dots$, defined as the product of individual membrane operators $U(i)_I U(i)_J \dots$.

the statistics of particles, loops, and membranes in spatial dimensions below three, using specific fusion groups as examples.

1. Particle Excitations

We consider particle excitations in (1+1), (2+1), and (3+1) spacetime dimensions.

- **(1+1)D:** Let the fusion groups of the particles be a finite group G , where each particle is labeled by an element $g \in G$. While G can be non-Abelian in general, we first focus on the Abelian case for demonstration. We define hopping operator $U(g)_{ij}$ as the operator which creates a particle g at vertex j and a particle g^{-1} at vertex i . The statistics of g -particles are defined by:

$$Z_3(g) := [U(g)_{01}^{|g|}, U(g)_{02}], \quad (8)$$

where the vertices 0, 1, and 2 are positioned along a segment, as shown in Fig. 2(a). Here, $|g|$ denotes the order of the element $g \in G$. This index corresponds to the third cohomology class $H^3(BG, U(1))$. This cohomology class is characterized by the partition function on the lens space

[77, 78]:

$$Z_3(g) = \prod_{n=1}^{|g|} F(g, g^n, g), \quad (9)$$

where the F -symbol $F(g_1, g_2, g_3)$ is defined microscopically in Ref. [60, 73]. Notably, when treating the particles as symmetry defects, the expression in Eq. (8) becomes equivalent to the topological invariants computed from the boundary of (2+1)D symmetry-protected topological (SPT) phases [79]. The nontrivial statistics described by Eq. (8) indicates an obstruction to satisfying $U(g)_{ij}^{|g|} = 1$, which aligns with the anomalous symmetry action outlined in Ref. [76]. We also emphasize that the statistics in Eq. (8) apply to non-Abelian groups. For instance, when $G = S_3$ is the symmetric group, which contains the Abelian subgroups \mathbb{Z}_2 and \mathbb{Z}_3 , we can substitute their generators into Eq. (8) to derive the \mathbb{Z}_2 and \mathbb{Z}_3 invariants, separately. These results are consistent with the cohomology class $H^3(S_3, U(1)) = \mathbb{Z}_6 = \mathbb{Z}_2 \times \mathbb{Z}_3$.

- **(2+1)D and (3+1)D:** Invertible particles in (2+1) and (3+1)-dimensional spacetime must have an Abelian fusion group G . The statistics of particles labeled by the group element $g \in G$ can be detected through the well-known T-junction process:

$$e^{i\Theta(g)} := U(g)_{02} U(g)_{03}^{-1} U(g)_{01} U(g)_{02}^{-1} U(g)_{03} U(g)_{01}^{-1}, \quad (10)$$

where the vertices 0, 1, 2, and 3 are shown in Fig. 2(b) and 2(c). This process represents the exchange of two identical particles. When $G = \mathbb{Z}_N$, we will show that the possible values of θ are:

$$e^{i\Theta} = \begin{cases} \exp\left(2\pi i \frac{k}{\gcd(2, N) \times N}\right) & \text{in (2+1)D,} \\ \pm 1 & \text{in (3+1)D,} \end{cases} \quad (11)$$

where $0 \leq k \leq \gcd(2, N) \times N$ is an integer. These values are characterized by the fourth cohomology class $H^4(B^2G, U(1))$ in (2+1)D and the fifth cohomology class $H^5(B^2G, U(1))$ in (3+1)D, both associated with the

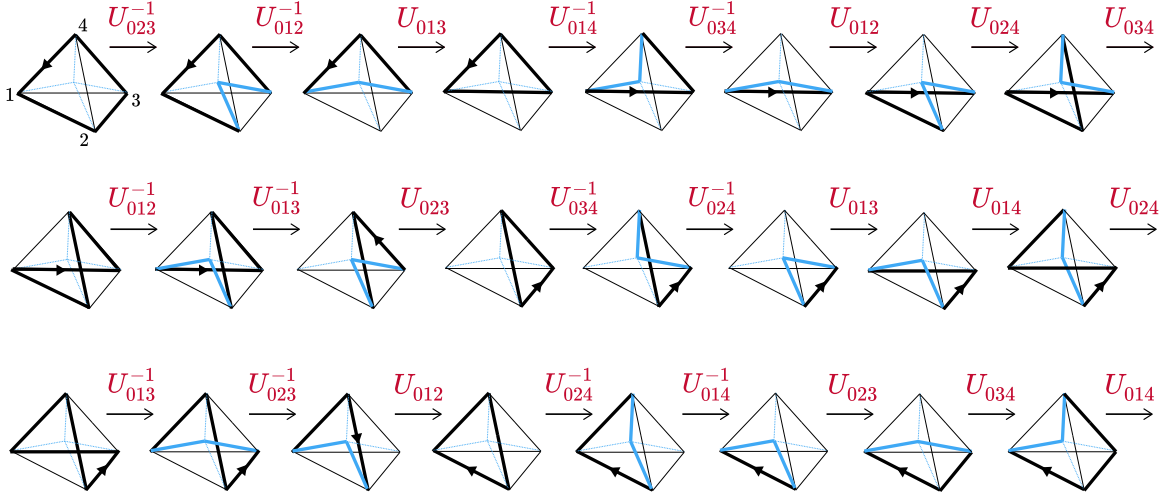


FIG. 4. The 24-step process for detecting the statistics of loops with $G = \mathbb{Z}_2$ fusion in (3+1)D. For \mathbb{Z}_2 loops, different orientations correspond to the same configuration state, indicating that the initial and final configurations are reversed and illustrating the loop-flipping process. This unitary sequence yields the same invariant as the 36-step unitary process proposed in Ref. [44]. We prove that this 24-step process is optimal, as no shorter sequence can achieve the same invariant.

1-form G symmetry. In (3+1)D and higher dimensions, the \pm sign corresponds to boson or fermion statistics, which are related to the second Stiefel-Whitney class w_2 [9, 80–85].

2. Loop Excitations

Loop excitations can be interpreted as defect lines or flux loops, and we consider loop excitations in (2+1) and (3+1) spacetime dimensions.

- **(2+1)D:** In this dimension, the "fusion" of loops also defines statistics, analogous to the F -symbol for particles. The simplest examples of nontrivial statistics arise when the fusion group is $G = \mathbb{Z}_N \times \mathbb{Z}_N$ (with generators labeled by a and b), and there are two invariants:

$$Z_4^I(a, b) := (U(a)_{023}U(a)_{013})^{-N} \left(U(a)_{023}U(a)_{013} [U(a)_{013}, [U(a)_{012}, U(b)_{012}U(b)_{013}U(b)_{023}U(b)_{123}]] \right)^N, \quad (12)$$

$$Z_4^{II}(a, b) := (U(b)_{023}U(b)_{013})^{-N} \left(U(b)_{023}U(b)_{013} [U(b)_{013}, [U(b)_{012}, U(a)_{012}U(a)_{013}U(a)_{023}U(a)_{123}]] \right)^N,$$

where the vertices 0, 1, 2, and 3 are arranged as shown in Fig. 2(b). In this process, we utilize the operators $U(a)_{123}$ and $U(b)_{123}$, which represent membrane operators acting on the region outside the triangle $\langle 123 \rangle$. These operators can also be interpreted as acting on the boundary surface of the tetrahedron $\langle 0123 \rangle$ for the compactified 2-manifold. Practically, we treat $U(a)_{123}$ and $U(b)_{123}$ as membrane operators acting in the annular region surrounding the triangle $\langle 123 \rangle$, where the annular width is much larger than the lattice spacing, as shown in Fig. 3, and the loop fusion statistics on an open disk can be expressed as Eq. (7).

Similar to particle fusion, we will show that the nontrivial statistics $Z_4(a)$ and $Z_4(b)$ are obstructions for

$$U(a)_{ijk}^N = U(b)_{ijk}^N = [U(a)_{ijk}, U(b)_{ijk}] = 1, \quad (13)$$

indicating an anomalous symmetry. We also highlight that the statistics in Eq. (12) corresponds to the fourth cohomology class $H^4(BG, U(1))$ of the global symmetry G .

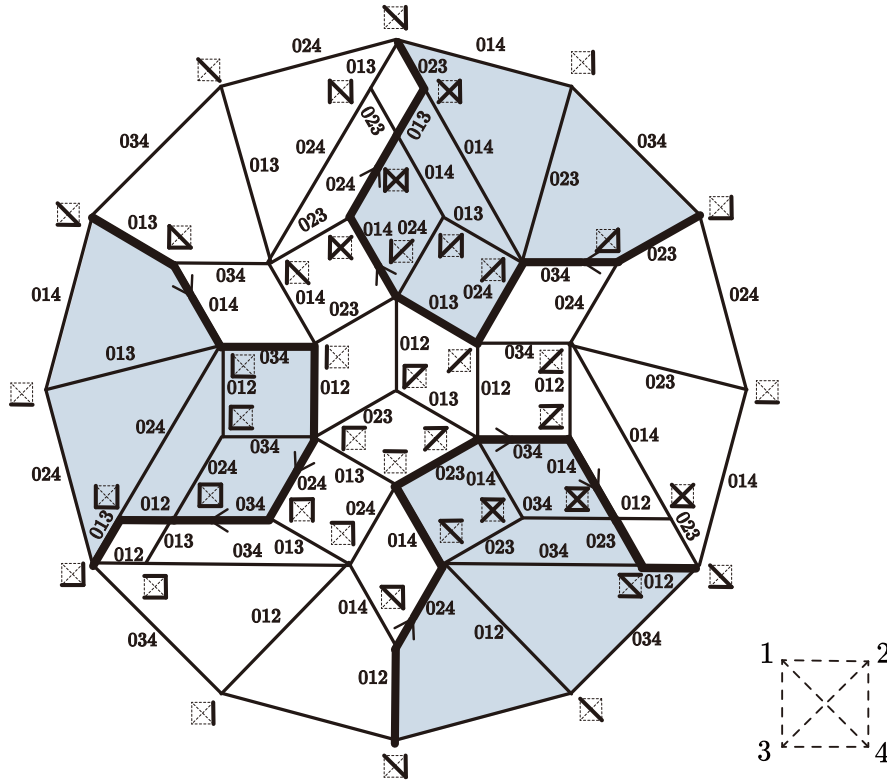


FIG. 5. The space of single-loop configuration states. Each vertex represents a single-loop configuration, where the loop is drawn only on edges between vertices 1, 2, 3, and 4 in Fig. 2(c) since the edges adjacent to vertex 0 can be inferred from these. Each edge of this space is labeled by $\langle 0ij \rangle$, and we can apply the operator U_{0ij} or U_{0ij}^{-1} to create or annihilate the loop on edge ij . This configuration space forms an \mathbb{RP}^2 structure [44], where antipodal vertices represent the same configuration state. The 24-step process is illustrated by the black directed line, exhibiting the C_3 rotational symmetry and corresponding to the nontrivial element of $\pi_1(\mathbb{RP}^2) = \mathbb{Z}_2$.

- **(3+1)D:** In (3+1)D, the loop statistics is determined by the loop-flipping process for $G = \mathbb{Z}_2$. We introduce a novel 24-step process to detect these statistics:

$$\begin{aligned}
 \mu_{24} := & U_{014}U_{034}U_{023}U_{014}^{-1}U_{024}^{-1}U_{012}U_{023}^{-1}U_{013}^{-1} \\
 & \times U_{024}U_{014}U_{013}U_{024}^{-1}U_{034}^{-1}U_{023}U_{013}^{-1}U_{012}^{-1} \\
 & \times U_{034}U_{024}U_{012}U_{034}^{-1}U_{014}^{-1}U_{013}U_{012}^{-1}U_{023}^{-1},
 \end{aligned} \tag{14}$$

which is shown in Fig. 4 explicitly. Each line in Eq. (14) is derived from the previous one by applying the substitutions $1 \rightarrow 2$, $2 \rightarrow 3$, and $3 \rightarrow 1$.² Therefore, the statistics μ exhibit an explicit rotational symmetry under $1 \rightarrow 2 \rightarrow 3$. The space of single-loop configurations forms an \mathbb{RP}^2 structure, as illustrated in Fig. 5. The 24-step process μ_{24} is represented on this \mathbb{RP}^2 , explicitly manifesting the C_3 rotational symmetry. We demonstrate that the 24-step process yields the same statistics as the 36-step process defined in Ref. [44], while being more efficient. Computational verification confirms that this 24-step sequence is the shortest way to obtain the loop statistics. These statistics correspond to the fifth cohomology class $H^5(B^2G, U(1))$ for the 1-form G symmetry and are also related to the third Stiefel-Whitney class w_3 for $G = \mathbb{Z}_2$. This process remains valid for the fusion group $G = \mathbb{Z}_N$ for even N , by choosing the operators U_{ijk} that create a loop labeled by $\frac{N}{2} \in \mathbb{Z}_N$, representing an element of order 2.

² In the case of loop excitations, the membrane operators U_{0ij} and

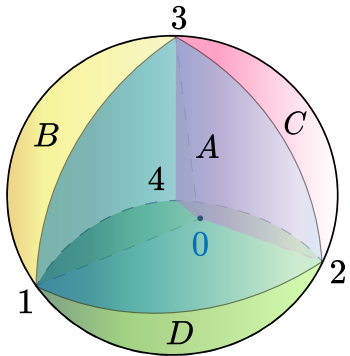
U_{0ji} represent the same operator.

3. Membrane Excitations

Finally, we consider membrane excitations in (3+1) spacetime dimensions. For fusion group G , the volume operator $U(g)_{0ijk}$ acting on tetrahedron $\langle 0ijk \rangle$ in Fig. 2 creates a g membrane excitation on its boundary surface. For $G = \mathbb{Z}_N$, the fusion of membranes gives rise to the statistics:

$$Z_5(g) := (U(g)_{0234}U(g)_{0124})^{-N} (U(g)_{0234}[U(g)_{0134}, U(g)_{0123}^N]^{-1}U(g)_{0124}[U(g)_{0134}, U(g)_{0123}^N])^N . \quad (15)$$

Similar to the (2+1)D fusion in Eq. (7), we can visualize the (3+1)D membrane fusion as Fig. 6, and the membrane fusion statistics on an open ball becomes Eq. (16).



$$Z_5(g) := (U(g)_{C+D})^{-N} (U(g)_{C+D}[U(g)_C, [U(g)_B, U(g)_A^N]])^N . \quad (16)$$

FIG. 6. The statistics of membranes in (3+1)D can be detected on an open ball. Let $U(g)_A$, $U(g)_B$, $U(g)_C$, and $U(g)_D$ represent volume operators that create g membrane excitations on their respective boundaries. $U(i)_{I+J+\dots}$ represents the volume operator acting on the region $I \cup J \cup \dots$, defined as the product of individual volume operators $U(i)_I U(i)_J \dots$.

The work is organized as follows. In section II, we define general statistics using a few axioms of invertible excitations, and show that the statistics generally take quantized values. In section III, we provide an algorithm for computing general statistics by producing microscopic processes as sequences of operators on lattice, which can be implemented on computers. In section IV we show that the general statistics gives a microscopic definition of 't Hooft anomalies as the obstructions to gauging the symmetries. In section V we prove that the non-trivial general statistics forbids short-range entangled states, which corresponds to dynamical consequences of anomalies. The reviews on background concepts used in this paper and detailed discussions are relegated to appendices.

II. FRAMEWORK FOR GENERALIZED STATISTICS

A. Review: T-junction of anyons in (2+1)D

Here we provide the microscopic description for the general statistics of invertible excitations in gapped phases. Before discussing the generic cases, we first review the microscopic description for the self-statistics (spins) of the Abelian anyons in (2+1)D.

Consider four points in the 2d space labeled by 0,1,2,3, with the 1,2,3 forming the triangle and 0 located at its

center (see Fig. 2(b)). These points specify the possible locations of the Abelian anyons. We then fix the unitary operator U_{jk} that moves the Abelian anyon from the location j to k . The spin of the anyon Θ is microscopically defined through the ‘‘T-junction’’ process, expressed as the sequence of unitaries [44, 59, 60]

$$U_{02}U_{03}^{-1}U_{01}U_{02}^{-1}U_{03}U_{01}^{-1} \left| \begin{array}{c} 3 \\ \triangle \\ 1 \quad 0 \quad 2 \end{array} \right\rangle = e^{i\Theta} \left| \begin{array}{c} 3 \\ \triangle \\ 2 \quad 0 \quad 1 \end{array} \right\rangle , \quad (17)$$

where the initial state contains two identical Abelian anyons a located at positions 1 and 2 of Fig. 2(b).³

By keeping track of the locations of two particles during the T-junction process, one can explicitly check that their positions are exchanged. This provides an intuition that this process measures the self-statistics of particles. Meanwhile, the exchange during the process does

³ Note that this state does not belong to the vacuum sector, as two identical anyons cannot annihilate each other unless $G = \mathbb{Z}_2$. In our setting, we consider only states within the same sector as the vacuum. Consequently, the state in Eq. (10) should be understood to implicitly include two inverse anyons, a^{-1} , located far from the triangle $\langle 123 \rangle$. One can generally show that the T junction invariant does not depend on the initial configuration of the anyons.

not guarantee that it defines an invariant that characterizes the self-statistics. The T-junction process (17) is carefully arranged so that it is invariant under the possible choices of the unitaries U_{jk} . For instance, it is invariant under the redefinition of U_{jk} by a phase $e^{i\phi}U_{jk}$; this is satisfied by Eq. (17) since U_{jk} and its inverse always appear in pair, canceling the phase ambiguity. One can further check that Eq. (17) is invariant under any local modifications of the unitary U_{jk} nearby its endpoints j, k [44, 60]. This invariance property also applies to the generalized statistics of loop and membrane excitations, as described by Eqs. (12), (14), and (15), defined in the previous section.

B. Framework of invariants in generic dimensions

We describe the invariants associated with extended excitations in generic dimensions. The T-junction process, previously discussed for particle excitations, will be generalized to extended excitations in any dimension using a sequence of unitaries that create these excitations.

Consider a system with a finite invertible $(d - p - 1)$ -form symmetry group G in a d -dimensional space. The group G is generated by unitary operators U supported on $(p + 1)$ -dimensional submanifolds. When the support has a boundary, the operator U creates a p -dimensional extended excitation at the boundary. For 0-form symmetry with $p = d - 1$, G can be a non-Abelian group; for all other cases, G must be Abelian. We first restrict ourselves to the Abelian fusion group G , and study the non-Abelian fusion in Sec. II C.

1. Excitations and unitaries on simplicial complex

Following the description of the T-junction process, the construction of the invariant starts with fixing the possible configurations of the excitations in the space. We define the **excitation model** as follows:

Definition II.1. An excitation model defined on a tensor product Hilbert space \mathcal{H} over a d -dimensional spatial manifold M consists of the following components:

1. A finite Abelian group \mathcal{A} . Each group element $a \in \mathcal{A}$ corresponds to a configuration of the excitations in the space M . For each configuration $a \in \mathcal{A}$, there exists a state $|a\rangle \in \mathcal{H}$, such that the states that correspond to different configurations are orthogonal.⁴

⁴ For simplicity, we typically assume that M is a sphere, ensuring that the ground state has no topological degeneracy. This assumption is valid since the generalized statistics is a local property and is insensitive to the global topology.

2. A finite set \mathcal{S} and a map $\partial : \mathcal{S} \rightarrow \mathcal{A}$, such that $\text{Im}\partial$ contains all generators of \mathcal{A} . Each element $s \in \mathcal{S}$ represents a unitary operator that creates the excitation ∂s . For each $s \in \mathcal{S}$, there is a unitary operator $U(s)$ such that $U(s)|a\rangle \propto |a + \partial s\rangle$ for all $s \in \mathcal{S}$ and $a \in \mathcal{A}$. The unitary $U(s)$ has a support at a $(p + 1)$ -dimensional locus $\text{supp}(s) \subset M$.

We note that the above definition assumes the invertible symmetry with group-like fusion rule, and further that the fusion group is finite and Abelian. One can extend the above definition to the case of invertible non-Abelian group symmetries, which will be studied in Sec. II C.

Let us take a concrete example of the excitation model based on the T-junction reviewed in Sec. II A. In that case, $\{U(s)|s \in \mathcal{S}\}$ is the set of operators that generate all string operators with the fusion group G support at fixed edges connecting the vertices 0,1,2,3 of Fig. 2(b). There are six edges $\langle jk \rangle$ with $0 \leq j < k \leq 3$, so \mathcal{S} is the set of generators of G^6 . \mathcal{A} is taken to be all configurations of the anyons created by the sequence of operators in $\{U(s)\}$ out of the vacuum. This is isomorphic to $\mathcal{A} = G^3$, which is the configuration of anyons at four vertices fusing into a vacuum. In the case of the T-junction, \mathcal{S} can be regarded as the set of generators of group 1-chains $C_1(X, G)$ in the simplicial complex X shown in Fig. 2(b), ∂ as the boundary map of the simplicial complex, and \mathcal{A} as the boundary $\mathcal{A} = B_0(X, G)$.

More generally, one can construct an excitation model on any finite simplicial complex X embedded in the space M , which can describe the extended excitations in generic dimensions. To illustrate these ideas, consider the excitation model on a simplicial complex. In this case, let \mathcal{A} be the group of p dimensional simplicial boundaries

$$\mathcal{A} = B_p(X, G). \quad (18)$$

We will take \mathcal{S} to be a minimal set of generators of $(p + 1)$ -chains of X with coefficients in G , i.e., generators of $C_{p+1}(X, G)$. Concretely, each element $s \in \mathcal{S}$ is given by $s = g\sigma_{p+1}$ where $g \in G$ is one of generators of G , and σ_{p+1} is a single $(p + 1)$ -simplex of X . Viewing X as a topological space embedded in the space M , $\text{supp}(s)$ gives the image of the simplex σ_{p+1} in M under the embedding map. The unitary $U(s)$ can then be expressed as $U(s) = U_g(\sigma_{p+1})$, namely the operator generating $g \in G$ symmetry at the simplex σ_{p+1} embedded in M . $\partial : \mathcal{S} \rightarrow \mathcal{A}$ is a homological boundary map of X , and we have $U(s)|a\rangle \propto |a + \partial s\rangle$ with $a \in \mathcal{A}$, $s \in \mathcal{S}$.

In general, different choices of the simplicial complex X extract the different invariants. If one wants to extract the whole set of invariants that can be observed in the spatial manifold M , one can choose X as the simplicial decomposition of M . Meanwhile, the generalized statistics of excitations are typically the local properties that can be extracted on the simplicial complex X support at a ball embedded in the whole space M . Such invariants include e.g., the T-junction of anyons, and are insensitive to the global topology of the space.

2. Invariant Berry phases from unitary sequences

Now we are ready to construct the invariants out of the sequence of unitaries $\{U(s)\}$ acting on the excited states $\{|a\rangle\}$. From now we assume that the excitation model is constructed on the simplicial complex X embedded in the space, according to Sec. II B 1.

For $a \in \mathcal{A}$, $s \in \mathcal{S}$, the unitary operator $U(s)$ transforms the state $|a\rangle$ into $|a + \partial s\rangle$ up to a phase:

$$U(s) |a\rangle = \exp[i\theta(s, a)] |a + \partial s\rangle . \quad (19)$$

Accordingly, the inverse of the unitary $U(s)$ acts on the states by

$$U(s)^{-1} |a + \partial s\rangle = \exp[-i\theta(s, a)] |a\rangle . \quad (20)$$

The invariant is then expressed as a sequence of unitary operators starting and terminating with the same configuration of excitations

$$\langle a_0 | U(s_{n-1})^\pm \dots U(s_j)^\pm \dots U(s_0)^\pm | a_0 \rangle , \quad (21)$$

where \pm is the sign which can be chosen for each unitary. This Berry phase will become the sum over the phases $\theta(s, a)$ with $s \in \mathcal{S}$, $a \in \mathcal{A}$.

To qualify the above phase as an invariant, one needs to establish the invariance of the above quantity against possible deformations of the states as well as unitaries. For the formulation of the invariants, it is convenient to express the above Berry phase as the element of the formal sum of the objects $\theta(s, a)$:

$$E = \bigoplus_{s \in \mathcal{S}, a \in \mathcal{A}} \mathbb{Z} \theta(s, a) , \quad (22)$$

which we call the **expression group** associated with the excitation model. Each element $e \in E$ is expressed as $e = \bigoplus_{(s,a)} \epsilon(s, a) \theta(s, a)$ with the integer coefficients $\epsilon(s, a) \in \mathbb{Z}$. The condition for e being the invariant will be compiled into a set of equations that the coefficients $\{\epsilon(s, a) | s \in \mathcal{S}, a \in \mathcal{A}\}$ need to satisfy. The invariants then correspond to a specific subgroup $E_{\text{inv}} \subset E$ which we now characterize.

The first condition for E_{inv} simply requires that the Berry phase corresponds to a sequence of unitaries initiating and terminating with the same state. This is equivalent to requiring the invariance under the redefinition of the states $|a\rangle \rightarrow e^{i\phi(a)} |a\rangle$ for $a \in \mathcal{A}$, shifting the phases as $\theta(s, a) \rightarrow \theta(s, a) - \phi(a) + \phi(a + \partial s)$. The element $e \in E$ is invariant under such redefinition of phases if and only if the coefficients $\{\epsilon(s, a)\}$ satisfy

$$\sum_{s \in \mathcal{S}} \epsilon(s, a) - \sum_{s \in \mathcal{S}} \epsilon(s, a - \partial s) = 0, \quad \text{for any } a \in \mathcal{A} . \quad (23)$$

This gives the first necessary condition for $e \in E_{\text{inv}}$.

The second condition for E_{inv} is that the Berry phase is invariant under the redefinition of unitaries $U(s)$ by a

phase $U(s) \rightarrow e^{i\phi(s)} U(s)$ for $s \in \mathcal{S}$, shifting the phases as $\theta(s, a) \rightarrow \theta(s, a) + \phi(s)$. The element $e \in E$ is invariant under such redefinition if and only if the coefficients $\{\epsilon(s, a)\}$ satisfy

$$\sum_{a \in \mathcal{A}} \epsilon(s, a) = 0, \quad \text{for any } s \in \mathcal{S} . \quad (24)$$

This gives the second necessary condition for $e \in E_{\text{inv}}$.

The rest of the conditions for E_{inv} is that the Berry phase is invariant under the deformations of the unitary $U(s)$ by a local operator near the boundary of the support of $U(s)$. Suppose that we add a local deformation at a point contained in the j -simplex $\sigma_j \in X$ embedded in the space M . This has the effect of locally modifying the symmetry operator $U(s)$ to the other unitary $U'(s)$, when the support $(p+1)$ -simplex $\sigma_{p+1} = \text{supp}(s)$ contains the simplex σ_j . Such an inclusion of a simplex is denoted by $\sigma_j \subset \sigma_{p+1}$, meaning that a set of vertices of σ_j is a subset of that of σ_{p+1} .

The phase $\theta(s, a)$ gets shifted according to the redefinition of the unitary. Since $U'(s)$ differs from $U(s)$ locally, the operator $U'(s)^\dagger U(s)$ is a local operator support on σ_j . The excited states $|a\rangle, |a + \partial s\rangle$ possibly get modified by $|a\rangle' = V |a\rangle, |a + \partial s\rangle' = \tilde{V} |a + \partial s\rangle$ with some local unitary V, \tilde{V} with the same support as $U'(s)^\dagger U(s)$. $|a\rangle$ is then an eigenstate of the operator $V^\dagger U'(s)^\dagger \tilde{V} U(s)$. Let us denote the eigenvalue as the phase $\exp(i\phi(s, a))$.

Due to the locality of the perturbation and finite correlation length in gapped phases, V, \tilde{V} only depend on the excitation a through the restriction of a at a set of p -simplices satisfying $\sigma_j \subset \sigma_p$. Further, the eigenvalue of the local operator $V^\dagger U'(s)^\dagger \tilde{V} U(s)$ also depends on a through p -simplices satisfying $\sigma_j \subset \sigma_p$. Let us define $a|_{\sigma_j}$ as a G -valued p -cochain defined by $a|_{\sigma_j} = a$ at σ_p satisfying $\sigma_j \subset \sigma_p$, otherwise zero. Then, the action of $V^\dagger U'(s)^\dagger \tilde{V} U(s)$ can be expressed as $V^\dagger U'(s)^\dagger \tilde{V} U(s) |a\rangle = \exp(i\phi(s, a|_{\sigma_j})) |a\rangle$, namely the dependence on a is only through the configuration of a nearby the simplex σ_j where the deformation occurs.

This implies that the action of $U'(s)$ is shifted from $U(s)$ by $\theta'(s, a) = \theta(s, a) + \phi(s, a|_{\sigma_j})$ when $\sigma_j \subset \text{supp}(s)$. Requiring the invariance of $e \in E$ under this shift of θ is equivalent to requiring that the coefficients $\{\epsilon(s, a)\}$ satisfy

$$\sum_{\substack{a \in \mathcal{A} \\ a|_{\sigma_j} = a_*^{(j)}}} \epsilon(s, a) = 0 , \quad (25)$$

for any possible choices of $s \in \mathcal{S}$, $\sigma_j \in X$ satisfying $\sigma_j \subset \text{supp}(s)$ and any $a_*^{(j)}$, with $0 \leq j \leq p$.

One can further see that Eq. (25) labeled by $0 \leq j \leq p$ gives a redundant set of constraints. To see this, pick a j -simplex σ_j and a 0-simplex (vertex) σ_0 of σ_j , i.e., $\sigma_0 \subset \sigma_j$. The chain $a_*^{(0)}$ then satisfies $(a_*^{(0)})|_{\sigma_j} = a_*^{(j)}$.

We get

$$\sum_{\substack{a \in \mathcal{A} \\ a|_{\sigma_j} = a_*^{(j)}}} \epsilon(s, a) = \sum_{\substack{a_*^{(0)} \\ (a_*^{(0)})|_{\sigma_j} = a_*^{(j)}}} \left(\sum_{\substack{a \in \mathcal{A} \\ a|_{\sigma_0} = a_*^{(0)}}} \epsilon(s, a) \right), \quad (26)$$

which implies that the equations for $j = 0$ are sufficient to fully characterize the constraints in Eq. (25). Thus, a refined version of the condition equivalent to Eq. (25) can be written as follows:

$$\sum_{\substack{a \in \mathcal{A} \\ a|_{\sigma_0} = a_*^{(0)}}} \epsilon(s, a) = 0, \quad (27)$$

for any possible choices of $s \in \mathcal{S}$, a 0-simplex $\sigma_0 \in X$ satisfying $\sigma_0 \subset \text{supp}(s)$ and any $a_*^{(0)}$.

The above requirements complete the description of E_{inv} ; the group $E_{\text{inv}} \subset E$ is defined as the group of $e \in E$ whose integral coefficients satisfy the conditions (23), (24), (27).

3. Equivalence of Berry phases and genuine invariants

Some elements of E_{inv} correspond to trivial invariants. One class of trivial invariants arises from the commutators of the unitaries. For instance, if two unitaries $U(s_1), U(s_2)$ have no overlap of their support $\text{supp}(s_1) \cap \text{supp}(s_2) = \emptyset$, the commutator (5) $[U(s_1), U(s_2)] = 1$ is trivial. This implies that the element of E_{inv} given by

$$\theta(s_1, a) + \theta(s_2, a + \partial s_1) - \theta(s_1, a + \partial s_2) - \theta(s_2, a) = 0 \pmod{2\pi}, \quad (28)$$

gives a trivial invariant. Hence, the set $\{\theta(s, a)\}$ is not entirely independent. More generally, let us take multiple unitaries $U(s_1), \dots, U(s_n)$ without common overlaps $\text{supp}(s_1) \cap \dots \cap \text{supp}(s_n) = \emptyset$. Noting that each unitary $U(s_j)$ is a local finite-depth circuit, the higher commutator (6), $[[[U(s_1), U(s_2)], \dots], U(s_n)]$, becomes trivial. Taking the expectation value of these higher commutators with any state $|a\rangle$ gives an element of E_{inv} that

is a trivial invariant:⁵

$$\langle a | [[U(s_1), U(s_2)], \dots], U(s_n) | a \rangle = 1, \\ \forall a \in \mathcal{A}, \forall s_1, s_2, \dots, s_n \in \mathcal{S} | s_1 \cap s_2 \cap \dots \cap s_n = \emptyset. \quad (30)$$

This equation follows from the fact that the commutator of two local finite-depth circuits are supported in the neighborhood of their intersection, due to the Lieb-Robinson bound [65, 66]. Eq. (30) is referred to as **locality identities**.

We define the subgroup $E_{\text{id}} \subset E_{\text{inv}}$ as the group generated by the locality identities in Eq. (30). It can be verified that E_{id} includes all invariants arising from the higher commutators of operators of the form $V = \prod_{s \in \mathcal{S}} (U(s))^{n_s}$, with $n_s \in \mathbb{Z}$. To classify the genuine invariants, we introduce the following quotient group:

Definition II.2. (Generalized statistics) The generalized statistics is defined as the quotient of E_{inv} by the subgroup E_{id} ,

$$T := E_{\text{inv}}/E_{\text{id}}, \quad (31)$$

which forms an Abelian group.

We now establish the following theorem about the property of this quotient group T :

Theorem II.3. (Initial state independence) The generalized statistics is uniquely determined by the sequence of unitaries, independent of the initial state $|a_0\rangle$ it acts upon:

$$\langle a_0 | \prod U(s_j)^\pm | a_0 \rangle = \langle a'_0 | \prod U(s_j)^\pm | a'_0 \rangle, \quad (32)$$

for all $\langle a_0 | \prod U(s_j)^\pm | a_0 \rangle \in E_{\text{inv}}$ and $a'_0 \in \mathcal{A}$.

To prove this, we first conjugate the entire sequence of unitaries in Eq. (21) by another unitary operator $U(s')$. Specifically, consider the equality of invariants:

$$\langle a_0 | \prod U(s_j)^\pm | a_0 \rangle = \langle a_0 + \partial s' | \prod \tilde{U}(s_j)^\pm | a_0 + \partial s' \rangle, \quad (33)$$

⁵ One can extend this Eq. (30) to more generic setup:

$$\langle a | [[U(s_1), U(s_2)], \dots], U(s_n) | a \rangle \\ = \langle b | [[U(s_1), U(s_2)], \dots], U(s_n) | b \rangle, \quad (29)$$

for all states $|a\rangle, |b\rangle$ that are identical at the mutual support of unitaries $\text{supp}(s_1) \cap \dots \cap \text{supp}(s_n)$. Note that this is equivalent to Eq. (30) when $X \setminus \{\text{supp}(s_1) \cap \dots \cap \text{supp}(s_n)\}$ is connected, allowing us to find an additional operator that connects states $|a\rangle$ and $|b\rangle$ without overlapping with the mutual support of unitaries. Therefore, when X is a triangulation of a closed manifold, such as a sphere S^d , it is sufficient to consider Eq. (30). This paper will focus on this case.

with $s' \in \mathcal{S}$ and $\tilde{U}(s_j) := U(s')U(s_j)U(s')^\dagger$. One can then write $\tilde{U}(s_j)$ as

$$\tilde{U}(s_j) = U(s_j)O(\partial s_j), \quad (34)$$

Here, an operator $O(\partial s_j) := [U(s_j), U(s')^\dagger]$ is supported at the neighborhood of ∂s_j . This is because for $s' \neq s_j$, the commutator of $U(s')$, $U(s_j)$ has a support at $s_j \cap s' \subset \partial s_j$. For $s' = s_j$, the symmetry operators of the Abelian fusion group is commutative in the bulk, so $O(\partial s_j)$ again has a support within ∂s_j . These $O(\partial s_j)$ can be treated as local perturbations acting on the boundary of each unitary $U(s)$. Then, by the definition of E_{inv} , we have

$$\begin{aligned} & \langle a_0 + \partial s' | \prod (U(s_j)O(\partial s_j))^\pm | a_0 + \partial s' \rangle \\ &= \langle a_0 + \partial s' | \prod (U(s_j))^\pm | a_0 + \partial s' \rangle. \end{aligned} \quad (35)$$

Combining Eq. (33), and noting that $\text{Im}\partial$ generates \mathcal{A} , this completes the proof of Theorem II.3. As a result, the ratio

$$\frac{\langle a_0 | \prod U(s_j)^\pm | a_0 \rangle}{\langle a'_0 | \prod U(s_j)^\pm | a'_0 \rangle} \quad (36)$$

with $\langle a_0 | \prod U(s_j)^\pm | a_0 \rangle \in E_{\text{inv}}$ and $a'_0 \in \mathcal{A}$ becomes a trivial phase. In Appendix C, we show that the above ratio (36) becomes an element of E_{id} by explicitly checking that it is given by a product of higher commutators.

4. Quantization of generalized statistics

One can show that the above group T with any finite simplicial complex X and finite Abelian group G always becomes a finite Abelian group. In particular, this implies that the invariants $e^{i\Theta}$ in T must generate a torsion group and take the quantized values.

Since the number of generators of T is finite upper bounded by $|\mathcal{S}| \times |\mathcal{A}|$, it suffices to show that T is a torsion, i.e., a direct sum of finite Abelian groups and do not contain a free part. Let us take an invariant $[e] \in E_{\text{inv}}/E_{\text{id}}$. Then take a representative $e \in E_{\text{inv}}$ expressed as $e = \sum_{(s,a)} \epsilon(s,a)\theta(s,a)$. Since (36) is included in E_{id} , the equivalence class of e is left invariant under the global shift of $a \rightarrow a + a_0$ with $a_0 \in \mathcal{A}$ in phases $\theta(s,a)$, which leads to the expression $e' = \sum_{(s,a)} \epsilon(s,a)\theta(s,a+a_0)$ with $[e] = [e']$. We then get

$$\begin{aligned} |\mathcal{A}|[e] &= \sum_{a_0 \in \mathcal{A}} \sum_{(s,a)} \epsilon(s,a)\theta(s,a+a_0) \\ &= \sum_{a_0 \in \mathcal{A}} \sum_{(s,a)} \epsilon(s,a-a_0)\theta(s,a) \\ &= \sum_{(s,a)} \left(\sum_{a_0 \in \mathcal{A}} \epsilon(s,a_0) \right) \theta(s,a) = 0 \pmod{2\pi}, \end{aligned} \quad (37)$$

where we used Eq. (24) in the last equation. Since $\mathcal{A} = B_p(X, G)$ is finite, this implies that any element of T has finite order which divides $|\mathcal{A}|$. This shows that T is a finite Abelian group.

Later in Sec. IV and Sec. V, the invariants in T will be identified as the microscopic definition of the 't Hooft anomalies of the global symmetry G . The above observation implies that the 't Hooft anomalies in the microscopic lattice models of the gapped phase generally become a torsion when G is finite. This is consistent with a generic conjecture that the 't Hooft anomalies realized in symmetry-preserving gapped theories must be a torsion [86].

C. Generalized statistics for non-Abelian 0-form symmetries

1. Generalized statistics for non-Abelian fusion groups

It is straightforward to extend the above formalism to the case of non-Abelian fusion group G , which can happen for the 0-form symmetry. Let us describe the excitation model for the non-Abelian G on a simplicial complex X embedded in a d -dimensional space. \mathcal{S} is again a set of a pair $s = (g_j, \sigma_d)$, where $\{g_j\}$ is a minimal set of generators of G and σ_d is a d -simplex of X . Each element $s \in \mathcal{S}$ corresponds to the unitary $U(s) = U_{g_j}(\sigma_d)$. Then \mathcal{A} is identified as the set of the states $\{|a\rangle\}$ obtained by the sequence of unitaries on a fixed G symmetric state $|0\rangle$. The unitary acts on the state by $U(s)|a\rangle = |a \times \partial s\rangle$ with the group fusion \times , i.e., fusing the excitations at the boundary of a d -simplex.

The expression groups $E, E_{\text{inv}}, E_{\text{id}}$ can be readily generalized to the non-Abelian group G .

There are slight modifications to the characteristic equations for $E_{\text{inv}}, E_{\text{id}}$ arising from the non-Abelian nature of fusion groups. The only modification to E_{inv} is that one of the conditions for E_{inv} (23) is expressed according to the fusion of non-Abelian groups as

$$\sum_{s \in \mathcal{S}} \epsilon(s,a) - \sum_{s \in \mathcal{S}} \epsilon(s, a \times (\partial s)^{-1}) = 0, \quad \text{for any } a \in \mathcal{A}. \quad (38)$$

For the definition of E_{id} , the non-Abelian fusion group has the effect of modifying Eq. (32). Instead of Eq. (32), for non-Abelian G we have the equation

$$\langle a_0 | \prod U(s_j)^\pm | a_0 \rangle = \langle a_0 \times \partial s' | \prod \rho_{s'}[U(s_j)]^\pm | a_0 \times \partial s' \rangle, \quad (39)$$

for all $\langle a_0 | \prod U(s_j)^\pm | a_0 \rangle \in E_{\text{inv}}$ and any choice of $s' = (g', \sigma'_d)$. Here, we write the conjugation action of $U(s')$

on $U(s)$ with $s = (g, \sigma_d)$ by

$$\rho_{s'}[U(s)] = \begin{cases} U_{g'gg'^{-1}}(\sigma_d) & \sigma_d = \sigma'_d \\ U_g(\sigma_d) & \sigma_d \neq \sigma'_d \end{cases}. \quad (40)$$

That is, $U(s')$ acts on $U(s)$ by an automorphism if these operators have the same support. (39) can be derived by a similar discussion to the proof of (32).

We define the group $E_{\text{id}} \subset E_{\text{inv}}$ as the group generated by the elements in the form of the ratio

$$\frac{\langle a_0 | \prod U(s_j)^\pm | a_0 \rangle}{\langle a_0 \times \partial s' | \prod \rho_{s'}[U(s_j)]^\pm | a_0 \times \partial s' \rangle} \quad (41)$$

with $\langle a_0 | \prod U(s_j)^\pm | a_0 \rangle \in E_{\text{inv}}$, $s' \in \mathcal{S}$, and the elements given by the higher commutators

$$\begin{aligned} \langle a | [[U(s_1), U(s_2)], \dots], U(s_n) | a \rangle &= 1, \\ \forall a \in \mathcal{A}, \forall s_1, s_2, \dots, s_n \in \mathcal{S} | s_1 \cap s_2 \cap \dots \cap s_n &= \emptyset. \end{aligned} \quad (42)$$

It is expected that the ratio (41) is again given by a product of higher commutators, and the above definition gives a redundant set of generators. Verifying this expectation is left for future studies.

2. Quantization of invariants for non-Abelian fusion groups

One can show the quantization of the invariants for non-Abelian fusion groups as well. For simplicity, let us take X to be a triangulation of a sphere S^d .

Let us take an element $[e] \in T = E_{\text{inv}}/E_{\text{id}}$. Since (41) is an element of E_{id} , the conjugation action by unitary $U(s')$ leaves the equivalence class $[e]$ invariant. Hence, the conjugation action by any unitary in the form of $\prod_{\sigma' \in X} U_{g'(\sigma')}(\sigma')$ leaves $[e]$ invariant, where $g'(\sigma')$ is any group element $g'(\sigma') \in G$ chosen for each d -simplex σ' . Each $U_{g'(\sigma')}(\sigma')$ is a product of operators $U(s)$ with $s \in \mathcal{S}$ support at the simplex σ' . Then, let us sum over all possible conjugation actions of $[e]$ by $\prod_{\sigma' \in X} U_{g'(\sigma')}(\sigma')$. This corresponds to summing over the choices of group elements $g'(\sigma')$ for each d -simplex, so there are $|G|^{N_d}$ such choices with N_d the number of d -simplices in X .

After this summation, we get a certain expression of $|G|^{N_d}[e]$, and we will show that it vanishes. To see this, let us pick a single d -simplex $\sigma_d \in X$, and focus on the coefficient of the phase $\theta(s, a)$ with s support at σ_d . Then, in the sum over conjugation actions, let us first sum over $N_d - 1$ of d -simplices except for $\sigma' = \sigma_d$,

$$|G|^{N_d-1}[e] = \sum_{\substack{\{g'(\sigma')\} \\ \sigma' \neq \sigma_d}} \sum_{a \in \mathcal{A}} \epsilon(s, a) \theta(s, a \times \prod_{\sigma' \neq \sigma_d} \partial(g'(\sigma'), \sigma')) + \dots \quad (43)$$

where \dots denotes the other phases θ . Note that while the excitation a is shifted by the conjugation action, s is invariant under conjugation since the conjugation action avoids the simplex σ_d . Here, since we take X to be a

triangulation of a sphere, $\text{Im}(\partial)$ with the domain $\sigma' \neq \sigma_d$ can generate the whole group \mathcal{A} . Therefore, one can rewrite

$$\begin{aligned} |G|^{N_d-1}[e] &= \sum_{a' \in \mathcal{A}} \sum_{a \in \mathcal{A}} \epsilon(s, a) \theta(s, a \times a') + \dots \\ &= \sum_{a' \in \mathcal{A}} \sum_{a \in \mathcal{A}} \epsilon(s, a \times a'^{-1}) \theta(s, a) + \dots \\ &= \sum_{a \in \mathcal{A}} \left(\sum_{a' \in \mathcal{A}} \epsilon(s, a') \right) \theta(s, a) + \dots \\ &= 0 + \dots, \end{aligned} \quad (44)$$

implying that the part in the sum involving each $s \in \mathcal{S}$ vanishes by looking at the sum over $N_d - 1$ of simplices avoiding s . This shows that $|G|^{N_d}[e]$ becomes zero.

Therefore, we conclude that the generalized statistics T becomes a finite Abelian group whose order divides $|G|^{N_d}$. The invariants are hence quantized into discrete values.

III. COMPUTATION OF GENERALIZED STATISTICS

In the previous section, we provided the conditions (Eqs. (23), (24), and (27)) under which a process remains invariant under any local deformation. Solving for $\epsilon(s, a)$ that satisfies these equations is generally challenging. For instance, Ref. [44] uses computational methods to solve similar equations for loop excitations in (3+1)D, with additional constraints (specifically, restricting to processes that flip a loop). However, extending this approach to other types of excitations is not straightforward. Therefore, we adopt an alternative approach. Instead of directly solving the equations, we investigate the ‘‘trivial solutions’’ and use them to construct new solutions for genuine generalized statistics.

Specifically, for each locality identity in Eq. (30) within E_{id} , a linear combination of $\theta(s, a)$ must be zero modulo 2π . The coefficients $\epsilon(s, a)$ satisfy the conditions given in Eqs. (23), (24), and (27) since the locality identities always hold, regardless of how $U(s)$ or $|a\rangle$ is deformed. Since the commutators of unitaries for non-overlapping simplexes always yield a phase factor of $+1$, the solution $\epsilon(s, a)$ derived from the locality identity is considered a trivial solution.

Next, note that these equations are linear in $\epsilon(s, a)$. Specifically, if $\{\epsilon(s, a)\}$ is a solution, then $\{\epsilon'(s, a) := \alpha \epsilon(s, a)\}$ is also a solution, provided that all $\alpha \epsilon(s, a)$ remain integers. If we find a combination of locality identities such that all coefficients $\{\epsilon(s, a)\}$ are multiples of an integer k , we can obtain a potentially non-trivial solution by dividing these coefficients by k . If this new solution cannot be expressed as a linear combination of identities in E_{id} , we categorize it as a genuine invariant. Moreover, this solution imposes a constraint on the generalized statistics, which can only take the form $\exp\left(\frac{2\pi i j}{k}\right)$,

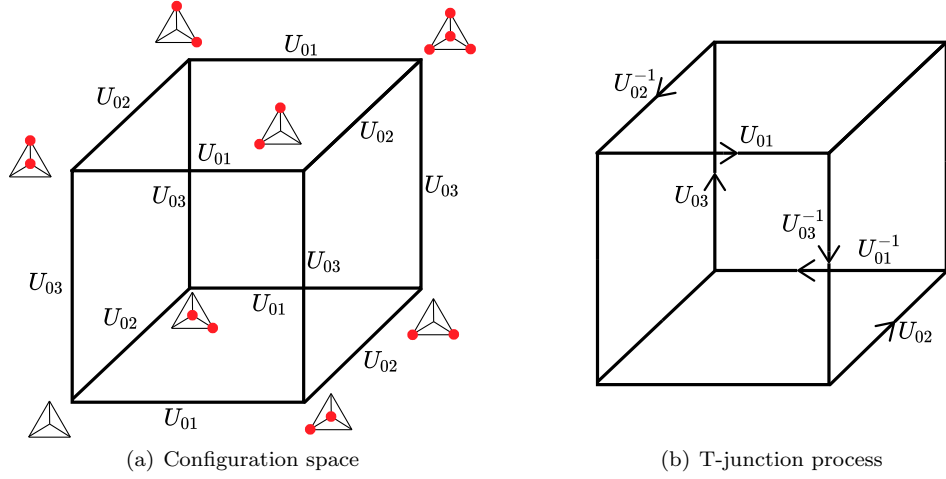


FIG. 7. (a) Configuration space for \mathbb{Z}_2 particles on a triangle with a central vertex. We analyze states within the same superselection sector as the vacuum. These states are interconnected through string operators U_{0i} where $i = 1, 2, 3$, delineating the 1-skeleton of a cube. It is important to note that transitions between states can be achieved by applying either U_{0i} or U_{0i}^{-1} , and generally, the operator U_{0i}^2 does not necessarily equal $+1$. Connections between states via U_{ij} are not explicitly shown in this diagram. (b) Visualization of the T-junction process in the configuration space. A specific initial state is selected (the outcome is independent of this choice), demonstrating how the T-junction process swaps the positions two particles.

where $j \in 0, 1, 2, \dots, k-1$.

A. Deriving generalized statistics via locality identities

1. \mathbb{Z}_2 particles in $(2+1)D$

As an example, we begin by considering the T-junction process in $(2+1)D$ with the fusion group $G = \mathbb{Z}_2$, demonstrating that its anyon statistics must take the form $\exp(i\Theta) = \pm 1, \pm i$. The configuration states are shown in Fig. 7(a). We start by presenting particular locality identities for demonstration:

$$\langle \triangleleft \mid [[U_{02}, U_{03}], U_{12}] \mid \triangleleft \rangle = 1. \quad (45)$$

In terms of $\theta(s, a)$, the above identity can be expanded as:

$$\begin{aligned} & \theta(U_{03}, \triangleleft) + \theta(U_{02}, \triangleleft) + \theta(U_{03}^{-1}, \triangleleft) \\ & + \theta(U_{02}^{-1}, \triangleleft) + \theta(U_{02}, \triangleleft) + \theta(U_{03}, \triangleleft) \\ & + \theta(U_{02}^{-1}, \triangleleft) + \theta(U_{03}^{-1}, \triangleleft) = 0 \pmod{2\pi}, \end{aligned} \quad (46)$$

where we have adjusted the notation from $\theta(s, a)$ to $\theta(U(s), a)$. This change allows us to extend the definition of θ for $U(s)^{-1}$ as:

$$\theta(U(s)^{-1}, a) := -\theta(U(s), a - \partial s), \quad (47)$$

which follows from Eqs. (19) and (20). More generally, θ can be defined for any sequence of $U(s)$ using the follow-

ing property:

$$\theta(VU(s)^\pm, a) := \theta(V, a \pm \partial s) + \theta(U(s)^\pm, a), \quad (48)$$

for all unitary operators V . Using Eq. (47), the locality identity (46) can be rewritten as:

$$\begin{aligned} & \theta(U_{03}, \triangleleft) + \theta(U_{02}, \triangleleft) - \theta(U_{03}, \triangleleft) \\ & - \theta(U_{02}, \triangleleft) + \theta(U_{02}, \triangleleft) + \theta(U_{03}, \triangleleft) \\ & - \theta(U_{02}, \triangleleft) - \theta(U_{03}, \triangleleft) = 0 \pmod{2\pi}, \end{aligned} \quad (49)$$

where we express θ solely in terms of U , without involving U^{-1} . Besides this locality identity, we can write down the following eight identities:

1. $\langle \triangleleft \mid [[U_{01}, U_{02}], U_{13}] \mid \triangleleft \rangle = 1.$
2. $\langle \triangleleft \mid [[U_{03}, U_{01}], U_{23}] \mid \triangleleft \rangle = 1.$
3. $\langle \triangleleft \mid [[U_{02}^{-1}, U_{03}^{-1}], U_{12}] \mid \triangleleft \rangle = 1.$
4. $\langle \triangleleft \mid [[U_{01}^{-1}, U_{02}^{-1}], U_{13}] \mid \triangleleft \rangle = 1.$
5. $\langle \triangleleft \mid [[U_{03}^{-1}, U_{01}^{-1}], U_{23}] \mid \triangleleft \rangle = 1.$
6. $\langle \triangleleft \mid \left([[U_{02}, U_{03}], U_{23}]^2 \mid \triangleleft \rangle = 1.$
7. $\langle \triangleleft \mid \left([[U_{01}, U_{02}], U_{12}]^2 \mid \triangleleft \rangle = 1.$
8. $\langle \triangleleft \mid \left([[U_{03}, U_{01}], U_{13}]^2 \mid \triangleleft \rangle = 1.$

In Appendix B, we explicitly demonstrate that summing over the 9 identities above yields the resulting equation:

$$\begin{aligned}
& 4 \left(\theta(U_{01}^{-1}, \triangle) + \theta(U_{03}, \triangle) + \theta(U_{02}^{-1}, \triangle) \right. \\
& \quad \left. + \theta(U_{01}, \triangle) + \theta(U_{03}^{-1}, \triangle) + \theta(U_{02}, \triangle) \right) \\
& = 0 \pmod{2\pi},
\end{aligned} \tag{50}$$

where the six θ terms can be combined into a total phase of a sequence of unitaries:

$$4\theta(U_{02}U_{03}^{-1}U_{01}U_{02}^{-1}U_{03}U_{01}^{-1}, \triangle) = 0 \pmod{2\pi}. \tag{51}$$

This sequence of unitaries precisely corresponds to the T-junction process as defined in Eq. (10) and is illustrated within the configuration state space in Fig. 7(b). Note that the coefficient 4 in Eq. (51) is crucial, as it constrains the phases to be

$$\theta(U_{02}U_{03}^{-1}U_{01}U_{02}^{-1}U_{03}U_{01}^{-1}, \triangle) = 0, \pi, \pm \frac{\pi}{2} \pmod{2\pi}, \tag{52}$$

indicating that the anyon with $G = \mathbb{Z}_2$ fusion can be a boson, a fermion, or an (anti-)semion. The coefficient in Eq. (51) depends on both the fusion group G and the spatial dimensions.

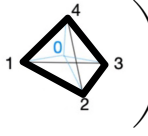
This computation can be generalized for $G = \mathbb{Z}_N$ straightforwardly. Specifically, in (2+1)D, the coefficient is $2N$ for even N and N for odd N , while in (3+1)D, the coefficient is 2 for even N and 1 for odd N , as discussed previously in Eq. (11). This is consistent with the topological spin of \mathbb{Z}_N anyons (related to the topological twist by $e^{2\pi i h}$) given by $h = \frac{p}{2N} \pmod{1}$ for integer $p = 0, 1, \dots, 2N-1$ for even N , and $p = 0, 2, 4, \dots, 2N-2$ for odd N in a bosonic theory, i.e., no transparent local fermion [49].

In the following sections, we present an algorithm that systematically determines these coefficients using the Smith normal form. In particular, we have reproduced the above quantization of topological spin for $G = \mathbb{Z}_N$ with $N \leq 10$ using our personal computers, while higher N demands more computational resources.

2. \mathbb{Z}_2 loops in (3+1)D

In addition to the well-known T-junction process for detecting the spins of particles, we now proceed to another more intricate example: the loop-flipping process for \mathbb{Z}_2 loops in (3+1)D. This process was first proposed in Ref. [44], where computers found a sequence of 36 unitaries to ensure invariance under any local perturbation. In Appendix B, we utilize our new method, which

involves summing over locality identities, to derive a sequence of 24 unitaries, μ_{24} , that satisfies the following equation analogous to Eq. (51):

$$2\theta \left(\mu_{24}, \text{loop} \right) = 0 \pmod{2\pi}, \tag{53}$$


with μ_{24} defined in Eq. (14) and illustrated in Fig. 4 and Fig. 5. Therefore, the total phase of this sequence must be 0 or $\pi \pmod{2\pi}$, implying that a loop with $G = \mathbb{Z}_2$ fusion can be either bosonic or fermionic [43, 44]. We further demonstrate that the total phase generated by the 36-unitary sequence from Ref. [44] matches the phase obtained from our μ_{24} sequence, up to some locality identities. In other words, both sequences yield the same loop statistics, but our process is more efficient, requiring fewer unitaries. We have verified that the 24-step sequence is optimal, as no shorter sequence exists.

B. Computational algorithm using the Smith normal form

In the previous section, we derived the T-junction process in (2+1)D and introduced the novel 24-step loop-flipping processes in (3+1)D. A natural question arises how to systematically determine specific linear combinations of the local identities such that the overall coefficients $\{\epsilon(s, a)\}$ in the expression $e = \sum_{s,a} \epsilon(s, a) \theta(s, a)$ result in a greatest common divisor (gcd) greater than one.

For smaller fusion groups, such as $G = \mathbb{Z}_2$, it is often feasible to rely on human intuition to manually determine the appropriate local identities to be summed in order to cancel certain $\theta(s, a)$ terms, ultimately ensuring that the remaining coefficients are all 2 or 4. We demonstrated this process in detail in Appendix B, where we effectively exploited the structure of \mathbb{Z}_2 to construct explicit summations that achieve the desired gcd properties.

For larger groups or more complex settings, it becomes challenging to manually determine the appropriate summation of local identities. Meanwhile, it turns out that finding such a summation can be efficiently handled by computational algorithms. The algorithm systematically determines the appropriate summation of locality identities by computing the Smith normal form of the corresponding matrix representation. By expressing the locality identities in matrix form, we can use the Smith normal form to identify combinations of rows that yield nontrivial gcd values for the coefficients $\epsilon(s, a)$. This method provides a systematic approach to finding the appropriate summations for larger fusion groups beyond \mathbb{Z}_2 , and allows us to optimize the result by finding the shortest unitary sequence.

The algorithm proceeds as follows: we first construct the matrix M , whose rows represent the locality identities, with entries corresponding to the coefficients of

the $\theta(s, a)$ terms in each identity. We then compute the Smith normal form (SNF) of M , which allows us to determine the invariant factors and, subsequently, the linear combinations of the original identities that yield the desired gcd properties for the coefficients $\epsilon(s, a)$.

To illustrate this process, let us consider a toy example with three θ terms, θ_1 , θ_2 , and θ_3 , and three locality identities:

$$\begin{aligned} \theta_1 + 2\theta_2 + 3\theta_3 &= 0 \pmod{2\pi}, \\ 4\theta_1 + 5\theta_2 + 6\theta_3 &= 0 \pmod{2\pi}, \\ 7\theta_1 + 8\theta_2 + 9\theta_3 &= 0 \pmod{2\pi}. \end{aligned} \quad (54)$$

These three locality identities are not independent, as the sum of the first and third identities equals twice the second identity. However, for the sake of demonstration, we proceed without recognizing this redundancy, as it can be challenging to identify such relationships in more extensive systems with thousands of identities in practice.

These locality identities can be represented as the **phase relation matrix**:

$$M = \begin{bmatrix} \theta_1 & \theta_2 & \theta_3 \\ 1 & 2 & 3 \\ 4 & 5 & 6 \\ 7 & 8 & 9 \end{bmatrix}, \quad (55)$$

where each row represents a locality identity. Row operations involving adding an integer multiple of one row to another do not change the row vector space spanned by these locality identities; they merely redefine the basis. However, column operations require more attention, as they necessitate the redefinition of phase labels for each column. Specifically, adding column k to column j requires a redefinition of phases as $\theta'_j = \theta_j$ and $\theta'_k = (-\theta_j + \theta_k)$:

$$M_{i,j}\theta_j + M_{i,k}\theta_k = (M_{i,j} + M_{i,k})\theta'_j + M_{i,k}\theta'_k \quad \forall i. \quad (56)$$

Next, we calculate the Smith normal form (SNF) of M , obtaining integer matrices L , R , and A such that

$$M = LAR, \quad (57)$$

where A is a diagonal integer matrix, and L and R are unimodular matrices (i.e., with determinant ± 1). For the matrix M given in Eq. (55), we decompose it as:

$$\begin{bmatrix} 1 & 2 & 3 \\ 4 & 5 & 6 \\ 7 & 8 & 9 \end{bmatrix} = \begin{bmatrix} 1 & 0 & 0 \\ 4 & -1 & 0 \\ 7 & -2 & 1 \end{bmatrix} \begin{bmatrix} 1 & 0 & 0 \\ 0 & 3 & 0 \\ 0 & 0 & 0 \end{bmatrix} \begin{bmatrix} 1 & 2 & 3 \\ 0 & 1 & 2 \\ 0 & 0 & 1 \end{bmatrix}. \quad (58)$$

We claim that this system exhibits \mathbb{Z}_3 generalized statistics, corresponding to the second diagonal entry in the matrix A . This corresponds to the process $\theta_2 + 2\theta_3$, which is represented by the second row of the matrix R .

To justify the physical interpretation of this computation, let us proceed step by step. We begin with the

matrix M in Eq. (55) and perform row operations over integers to obtain its Hermite normal form (HNF). We start by eliminating the entries below the first pivot, which is 1 in the first row and first column. First, we subtract $4 \times \text{Row 1}$ from Row 2 and subtract $7 \times \text{Row 1}$ from Row 3. The matrix then becomes:

$$M = \begin{bmatrix} \theta_1 & \theta_2 & \theta_3 \\ 1 & 2 & 3 \\ 0 & -3 & -6 \\ 0 & -6 & -12 \end{bmatrix}. \quad (59)$$

Next, we eliminate the entries below the second pivot. We focus on the second column, where the pivot is -3 . We add $2 \times \text{Row 2}$ to Row 3 to eliminate the entry below the pivot. The matrix becomes:

$$M = \begin{bmatrix} \theta_1 & \theta_2 & \theta_3 \\ 1 & 2 & 3 \\ 0 & -3 & -6 \\ 0 & 0 & 0 \end{bmatrix}. \quad (60)$$

To make the second pivot positive, we multiply Row 2 by (-1) :

$$M = \begin{bmatrix} \theta_1 & \theta_2 & \theta_3 \\ 1 & 2 & 3 \\ 0 & 3 & 6 \\ 0 & 0 & 0 \end{bmatrix}, \quad (61)$$

which is the final Hermite normal form.

Subsequently, we perform column operations, using the 1 in the first row to cancel out the entries 2 and 3 in the first row. Similarly, we use the 3 in the second row to cancel out the 6. According to the rule in Eq. (56), we reduce M to its Smith normal form:

$$M = \begin{bmatrix} \theta'_1 & \theta'_2 & \theta'_3 \\ 1 & 0 & 0 \\ 0 & 3 & 0 \\ 0 & 0 & 0 \end{bmatrix}, \quad (62)$$

with redefined phase labels as

$$\begin{aligned} \theta'_1 &= \theta_1 + 2\theta_2 + 3\theta_3, \\ \theta'_2 &= \theta_2 + 2\theta_3, \\ \theta'_3 &= \theta_3. \end{aligned} \quad (63)$$

The physical interpretation of Eq. (62) is that all locality identities can be reduced to three equations:

$$1\theta'_1 = 0, \quad 3\theta'_2 = 0, \quad 0\theta'_3 = 0. \quad (64)$$

This means that θ'_1 is fixed, θ'_3 can take any value, and θ'_2 must be $\frac{2\pi j}{3}$ for $j = 0, 1, 2$. In other words, this toy system exhibits \mathbb{Z}_3 statistics, corresponding to the unitary sequence labeled by $\theta'_2 = \theta_2 + 2\theta_3$.

Inspired by this example, we can derive the following theorem:

Theorem III.1. (Generalized statistics) Let M be the phase relation matrix for a given simplicial complex and a fusion group, and consider its Smith decomposition $M = LAR$. If any diagonal entry a_{ii} in A satisfies $a_{ii} \neq 0, 1$, then it gives rise to generalized statistics of type $\mathbb{Z}_{a_{ii}}$, with the i -th row of the matrix R specifying the corresponding unitary sequence. Namely, the generalized statistics T forms an Abelian group characterized by:

$$T = \bigoplus_{a_{ii} \neq 0,1} \mathbb{Z}_{a_{ii}}. \quad (65)$$

Remark III.1.1. The sum of θ terms in each row of R must originate from a sequence of unitary operators. This is because, in the original phase relation matrix M , each row corresponds to a (higher) commutator, which forms closed loops connecting the configuration states. Therefore, although each row of R may be divided by the greatest common divisor of the coefficients, it still represents a superposition of multiple closed loops. By the Eulerian path theorem, we can identify a sequence that generates these loops (allowing for retracing edges to cancel their contributions).

Remark III.1.2. In the Smith decomposition (57), the matrix A is uniquely determined, while the matrices L and R are not. However, any valid choice of R will yield the same generalized statistics, with the total phases differing only by linear combinations of locality identities. Typically, we choose R such that its entries contain as many zeros as possible, as this simplifies the corresponding unitary sequence.

The phase relation matrix M in Eq. (55) is a toy example. In practice, the computation can be much more involved. For instance, when determining the SNF, each diagonal element must divide the subsequent diagonal elements, which requires careful manipulation. The process of obtaining the HNF or SNF involves repeated use of the Euclidean algorithm to compute the greatest common divisor between matrix entries in each row or column. While the example is relatively simple, real-world applications often involve matrices with hundreds of rows and columns, making manual computation impractical. Fortunately, algorithms for computing the HNF and SNF have been optimized to handle these large-scale problems effectively.

In the following, let us estimate the computational overhead for this algorithm. The main cost comes from the size of the fusion group—larger group requires more variables. We can estimate the size of the fusion group that can be computed for each simplicial complex shown in Fig. 2. The size of the phase relation matrix M in Eq. (55) determines the computational time. Since we first perform the HNF decomposition and the number of rows (representing the locality identities on all initial states) is much greater than the number of columns (representing $\theta(s, a)$ terms), the computation speed is primarily determined by the number of columns. On a

personal computer, it is feasible to compute the HNF or SNF for matrices with approximately $\sim 10,000$ columns within a reasonable time.

The number of $\theta(s, a)$ terms is

$$|\text{number of simplices}| \times |\text{generators of } G| \times |\mathcal{A}|. \quad (66)$$

For example, in the (2+1)D T-junction process with fusion group $G = \mathbb{Z}_N$ on the simplicial complex shown in Fig. 2(b), there are 6 edges, G has a single generator, and there are N^3 configuration states. Thus, the number of $\theta(s, a)$ terms is $6N^3$. In this situation, we are able to compute the cases with $N \leq 10$.

Consider another example involving loop statistics with $G = \mathbb{Z}_N$ on the (3+1)D simplicial complex shown in Fig. 2(c). Here, there are 10 faces, G has a single generator, and there are N^6 configurations. The total number of $\theta(s, a)$ terms is $10N^6$, which limits our computations to $N \leq 4$.

Lastly, for membrane statistics with $G = \mathbb{Z}_N$ in the (3+1)D simplicial complex shown in Fig. 2(c), there are 5 tetrahedra (including the outer one), G has a single generator, and there are N^4 configurations. Therefore, the total number of $\theta(s, a)$ terms is $5N^4$, allowing us to compute the cases with $N \leq 8$.

C. Generalized statistics as anomalies: computational approach

Using the SNF algorithm presented above, we obtain the classification of the generalized statistics in various spatial dimensions as summarized in Sec. IB.

Below, we comment on the implications of several generalized statistics on the algebraic structure of the symmetry operators. We take the simplicial complex X for the excitation model to be the minimal triangulation of S^d embedded in d -dimensional space.⁶

- In (1+1)D with finite 0-form symmetry G , we get the generalized statistics T generated by the unitary sequence

$$Z_3(g) := [U(g)_{01}^{|g|}, U(g)_{02}], \quad (67)$$

with $g \in G$. This form of the invariant immediately implies that the nontrivial invariant $Z_3(g) = e^{i\Theta}$ becomes an obstruction to having

$$U(g)_{01}^{|g|} = 1, \quad (68)$$

implying that the symmetry operator on an interval must violate the original group fusion rule. Note

⁶ The minimal triangulation of S^d is formed by $d+1$ of d -simplices, which is identified as a boundary of single $(d+1)$ -simplex. Its vertices and edges form a complete graph K_{d+2} .

that an onsite symmetry satisfies $U(g)_{01}^{|g|} = 1$, since the onsite operators support at an interval again follows the G fusion rule. This immediately leads to a physical consequence that the operator $U(g)$ with the nontrivial invariant Θ cannot be realized by an onsite symmetry on the lattice. Physically, the invariant tells that the fusion of the operator $U(g)_{01}^{|g|}$ gives an electric charge of G symmetry localized at the end of the interval, which is a nontrivial point operator at the boundary.

- In (2+1)D with 0-form symmetry $G = \mathbb{Z}_N \times \mathbb{Z}_N$, the invariant is classified by $T = \mathbb{Z}_N \times \mathbb{Z}_N$. The classification is generated by a pair of invariants $Z_4(a), Z_4(b)$ shown in Eq. (12), with a, b the generators of $\mathbb{Z}_N \times \mathbb{Z}_N$. Though not manifest from their form, it turns out that either of the invariants $Z_4(a), Z_4(b)$ becomes an obstruction to the following $\mathbb{Z}_N \times \mathbb{Z}_N$ fusion algebra of symmetry operators:

$$U(a)_{ijk}^N = U(b)_{ijk}^N = [U(a)_{ijk}, U(b)_{ijk}] = 1. \quad (69)$$

This obstruction can be explicitly demonstrated by the SNF algorithm. That is, let us add the equations of the phases $\theta(s, a)$ originating from three equations (69) to the rows of the phase relation matrix M , and denote the new matrix by M' . Then, the SNF algorithm on M' classifies the invariants under these additional algebraic constraints. This invariant turns out to be trivial, meaning that the original invariants $Z_4(a), Z_4(b)$ must be trivial under the $\mathbb{Z}_N \times \mathbb{Z}_N$ fusion rule of $U(a), U(b)$. This shows that $Z_4(a), Z_4(b)$ obstructs the fusion rule (69). Based on a similar discussion to (1+1)D case, it implies that either of the invariants $Z_4(a), Z_4(b)$ becomes an obstruction to realizing the $\mathbb{Z}_N \times \mathbb{Z}_N$ symmetry by an onsite operator.

In the above examples, the generalized statistics define obstructions to a certain group theoretical identity of operators $U(s)$ under its fusion. It turns out that this is a symptom of the 't Hooft anomaly of the global symmetry G , defined as obstructions to gauging the symmetry. Roughly speaking, failure of the group identities such as Eq. (69) is directly interpreted as the failure of the Gauss law constraints in the gauge theory, where each unitary $U(s)$ is identified as a product of Gauss law operators. This leads to the absence of a gauge invariant Hilbert space after an attempt to promoting the global symmetry to the gauge symmetry. Such a perspective of the generalized statistics as the anomalies will be discussed in details in the following sections.

In (bosonic) quantum field theory, the 't Hooft anomalies of a finite $(d - p - 1)$ -form symmetry G in d spatial dimensions are classified by the group cohomology $H^{d+2}(B^{d-p}G, U(1))$, where $B^{d-p}G$ represents the Eilenberg–MacLane space of the group G . In all the examples we evaluated using the SNF algorithm, the generalized statistics T matches the group cohomology. This consistency leads us to the following conjecture:

Conjecture III.2. Consider p -dimensional excitations with a $(d - p - 1)$ -form symmetry and fusion group G in d spatial dimensions. Let X be a simplicial complex that triangulates the d -dimensional sphere S^d . Then, the generalized statistics T of p -dimensional excitations on X are classified by the cohomology of the Eilenberg–MacLane space:

$$T = H^{d+2}(B^{d-p}G, U(1)). \quad (70)$$

We remark that, in principle, any finite simplicial complex X on S^d could be chosen to compute the generalized statistics. We numerically observed that different triangulations of S^d yield the same result. This leads us to the above conjecture that the generalized statistics do not depend on a choice of the triangulation of S^d . Hence, we have decided to use minimal triangulation for convenience.

D. Stability of generalized statistics

Beyond the evidence of Conjecture III.2 provided above by computational methods, we present additional insights to support our conjecture. Assuming the independence of T under the choice of triangulations, one can see that both T and the group cohomology in Eq. (70) stabilize in the sense that for fixed p , both become independent of d for $d \geq d_{\text{crit}} := 2p + 3$.

Let us first see how the generalized statistics T stabilizes. When we define the generalized statistics of p -dimensional excitations, the excitations and unitaries are supported within finite $(p+1)$ -skeleton X_{p+1} that collects $0, \dots, (p+1)$ -simplices of X . According to dimension theory in point-set topology [87], every finite $(p+1)$ -dimensional simplicial complex, with Lebesgue covering dimension of $p+1$, can be embedded in S^{2p+3} . Therefore, any complex X_{p+1} can be embedded in a triangulation of S^{2p+3} . This implies that any invariants of p dimensional excitations can be realized by a unitary sequence in a suitable triangulation of S^{2p+3} . Assuming the independence on the triangulation of S^d , one can conclude that the generalized statistics T stabilizes for $d \geq d_{\text{crit}} = 2p + 3$.

Let us explicitly check this stability with several examples of small p . For particle statistics ($p = 0$), all 1-dimensional simplicial complexes can be embedded in S^d for $d \geq 3$. In other words, in spatial dimensions $d \geq 3$, particle statistics stabilizes and is characterized by a single \mathbb{Z}_2 invariant, distinguishing bosons from fermions. This result aligns with the fact in Lorentz invariant theories that the particles with fractional statistics can exist only in (1+1)D or (2+1)D, while the statistics is restricted to bosons or fermions in higher dimensions. Similarly, for loop excitations ($p = 1$), the critical dimension is $d_{\text{crit}} = 2p + 3 = 5$. In spatial dimensions $d \geq 5$, loop statistics stabilizes and is characterized by a single \mathbb{Z}_2 invariant that distinguishes between bosonic and fermionic

loops. An analogous result holds for membrane excitations ($p = 2$), where the generalized statistics stabilize at $d_{\text{crit}} = 7$.

Meanwhile, the (co)homology of the Eilenberg–MacLane space also stabilizes:

Theorem III.3. (13.2.2 of Ref. [88]) For any abelian group A , there exists a chain complex $Q_*(A)$ whose homology is isomorphic to the stable homology of the Eilenberg–MacLane space:

$$H_n(Q_*(A)) \cong H_{n+k}(K(A, k)), \quad k \geq n + 1 .$$

Using the universal coefficient theorem and the long exact sequence associated with $0 \rightarrow \mathbb{Z} \rightarrow \mathbb{R} \rightarrow \mathbb{R}/\mathbb{Z} \rightarrow 0$, we obtain the stabilization of the cohomology of the Eilenberg–MacLane space with coefficients in $\mathbb{R}/\mathbb{Z} = U(1)$:

$$H^{n+k}(B^k G, U(1)) = H^{2n+1}(B^{n+1} G, U(1)) , \quad (71)$$

for all $k \geq n + 1$. By choosing $n = p + 2$ and $k = d - p$, we find that $H^{d+2}(B^{d-p} G, U(1))$ stabilizes with respect to d for $k \geq n + 1$, or equivalently,

$$d \geq d_{\text{crit}} = 2p + 3 , \quad (72)$$

which matches precisely with the argument from the embedding theorem. Therefore, this consistency for the pattern of stability supports Conjecture III.2.

The group cohomology that appears in Conjecture III.2 classifies the topological responses in $(d + 2)$ dimensions that describes the anomaly inflow. We close this section with comments on the stable generalized statistics and the corresponding topological response:

- For particle statistics ($p = 0$) with the fusion group $G = \mathbb{Z}_N$, the stable generalized statistics for $d \geq 3$ is classified by $\mathbb{Z}_{\text{gcd}(2, N)}$; boson or fermion for even N . The statistics of the emergent particles are interpreted as a framing anomaly of the topological line operator, which is in turn understood as the 't Hooft anomaly of the $(d - 1)$ -form \mathbb{Z}_2 symmetry generated by this line operator. This 't Hooft anomaly is characterized by the response

$$\pi \int w_2 \cup B_d = \pi \int Sq^2(B_d) , \quad (73)$$

where B_d is the d -form \mathbb{Z}_N background gauge field with even N , and w_2 is the 2nd Stiefel-Whitney class.

- For loop statistics ($p = 1$) with the fusion group $G = \mathbb{Z}_N$, the stable generalized statistics for $d \geq 5$ is classified by $\mathbb{Z}_{\text{gcd}(2, N)}$; bosonic or fermionic loops for even N . The statistics is again interpreted as a framing anomaly of the topological surface operator, which is the 't Hooft anomaly of the $(d - 2)$ -form \mathbb{Z}_2 symmetry generated by this surface operator. The 't Hooft anomaly is characterized by the

response

$$\begin{aligned} \pi \int w_3 \cup B_{d-1} &= \pi \int w_2(dB_{d-1}/2) \\ &= \pi \int Sq^2(dB_{d-1}/2) , \end{aligned} \quad (74)$$

where B_{d-1} is the $(d - 1)$ -form \mathbb{Z}_N background gauge field with even N , and w_3 is the 3rd Stiefel-Whitney class. The first equality follows from $w_3 = Sq^1 w_2$ on orientable manifolds, and $Sq^1 B_{d-1} = dB_{d-1}/2$ where the right hand side uses a lift of \mathbb{Z}_2 cocycle B_{d-1} to \mathbb{Z}_4 cochain.

- For membrane statistics ($p = 2$) with the fusion group $G = \mathbb{Z}_N$, numerical computations suggest that the stable generalized statistics for $d \geq 7$ is classified by $\mathbb{Z}_{\text{gcd}(2, N)} \times \mathbb{Z}_{\text{gcd}(3, N)}$. We expect that the \mathbb{Z}_2 statistics with even N is again associated with the mixed gravitational 't Hooft anomaly involving the Stiefel-Whitney class,

$$\pi \int (w_4 + w_2^2) \cup B_{d-2} = \pi \int Sq^4(B_{d-2}) . \quad (75)$$

Meanwhile, for the \mathbb{Z}_3 statistics with N multiple of 3, we expect that the anomaly is associated with the Pontryagin class p_1

$$\frac{2\pi}{3} \int p_1 \cup B_{d-2} . \quad (76)$$

This implies that the membrane excitation is chiral—it has chiral central charge $c_- = -8$. See also Ref. [89] for a recent discussion on this response action. It would be interesting to verify the above expectations and find the corresponding generalized statistics on lattice models.

IV. STATISTICS AS OBSTRUCTION TO GAUGING

Let us make a direct connection between the generalized statistics and the 't Hooft anomaly of the lattice models. Suppose that a lattice model in d spatial dimensions has a finite $(d - p - 1)$ -form symmetry G . We argue that the invariant Θ gives an obstruction to gauging the global symmetry. This implies that Θ generally gives a microscopic definition of the 't Hooft anomaly.

For simplicity, let us study the system on a d -dimensional hypercubic lattice. We assume that the generators of the symmetry $g \in G$ is expressed by the product of the local unitary as

$$U_g(\Sigma_{p+1}) = \prod_{\Delta_{p+1} \in \Sigma_{p+1}} U_{\Delta_{p+1}, g} , \quad (77)$$

where $U_{\Delta_{p+1}, g}$ is a unitary support at a $(p + 1)$ -cube Δ_{p+1} which is local. We do not require that $\{U_g(\Delta_{p+1})\}$

commutes with each other; the above product is understood as ordering unitaries according to the action of finite depth local circuit that consists of local unitaries $\{U_g(\Delta_{p+1})\}$.

Let us briefly recall the procedure of gauging G on the lattice. The first step is to enlarge the Hilbert space by adding the G gauge fields on the p -cube. The next step is to impose the Gauss law constraints on the Hilbert space

$$G_{\Delta_{p+1},g} = 1, \quad (78)$$

with

$$G_{\Delta_{p+1},g} = U_{\Delta_{p+1},g} \prod_{\Delta' \in \partial \Delta_{p+1}} (A_{g,\Delta'})^\pm, \quad (79)$$

where $A_{g,\Delta'}$ is an operator generating the $g \in G$ gauge transformation on the gauge field on the p -cube Δ' , and \pm is the sign determined from the outgoing/ingoing orientation of the hypercubes Δ' . Then, one can express the symmetry operator as the product of Gauss law operators

$$U_g(\Sigma_{p+1}) = \prod_{\Delta_{p+1} \in \Sigma_{p+1}} G_{\Delta_{p+1},g}, \quad (80)$$

which turns on the $g \in G$ gauge field at the boundary of Σ_{p+1} .

One can then construct an excitation model (see Sec. II B 1) out of the Gauss law operators. Pick a simplicial complex X embedded in the space. Let us consider a set of operators $U_{g_j}(\sigma_{p+1})$ with a fixed set of generators $\{g_j\}$ of G , and with σ_{p+1} the $(p+1)$ -simplex of X . Each unitary is labeled by a pair $s = (\sigma_{p+1}, g_j)$, and define the set $\mathcal{S} = \{s\}$ with all possible choices of g_j and $\sigma_{p+1} \subset X$.

Then, consider a set of all states $\mathcal{A} = \{|a\rangle\}$ with the G gauge field configuration a , which can be generated by a sequence of unitaries $U(s)$ out of the fixed G symmetric state with the vanishing G gauge field $|0\rangle$.

One can see that the pair $(\mathcal{S}, \mathcal{A})$ forms the excitation model. Now we define an invariant as the sequence of unitaries $e^{i\Theta} = \langle 0 | \prod U(s)^\pm | 0 \rangle$ which is an element of E_{inv} . By definition, Θ is the product of the Gauss law operators $G_{\Delta_{p+1},g}$. So $\Theta \neq 0$ gives an obstruction to the commuting Gauss law operators $\{G_{\Delta_{p+1},g}\}$. In particular, a given symmetric state $|0\rangle$ cannot be promoted into a gauge invariant state, in the sense that $|0\rangle$ must vanish after acting the projection onto the Hilbert space satisfying all the Gauss law constraints. Therefore, Θ defines an obstruction to gauging the G symmetry of the given G symmetric state $|0\rangle$.

In our formalism, the invariant Θ is defined by evaluating the sequence of unitaries with the fixed initial symmetric state $|0\rangle$. Meanwhile, if we have $e^{i\Theta} = \prod U(s)^\pm$ as an operator equation without a reference to the fixed state, then the invariant defines the obstruction to gauging the symmetry in the whole Hilbert space.

V. STATISTICS AS OBSTRUCTION TO SHORT RANGE ENTANGLEMENT: DYNAMICAL CONSEQUENCE OF ANOMALIES

Here let us show that the generalized statistics in $T = E_{\text{inv}}/E_{\text{id}}$ define the obstructions to the short-range entanglement. That is, if the bosonic state $|\Psi\rangle$ preserves the global symmetry with the nontrivial invariant $\Theta \neq 0$ in T , then the state cannot be short-range entangled, $|\Psi\rangle \neq V(|0\rangle^n)$ for any choice of a finite depth circuit V and a product state $|0\rangle^n$. Given that the invariant Θ can be regarded as a microscopic definition of the 't Hooft anomaly, the obstruction to the SRE state is regarded as a dynamical consequence of the 't Hooft anomaly.

We generally show this statement by checking that SRE states must carry trivial invariants. Suppose that a state $|\Psi\rangle = V(|0\rangle^n)$ and the symmetry operators U has an invariant Θ . We can redefine the symmetry operators by $U' := V^{-1}UV$ and the input state $|\Psi'\rangle = |0\rangle^n$ without changing the invariant. Hence we take the input state as a product state $|\Psi\rangle = |0\rangle^n$ without loss of generality. Below we simply write U' as U .

The first step of the proof is to notice that the state with excitations $|a\rangle = U(s)|\Psi\rangle$ with $a = \partial s$ becomes a product state away from the location of the excitations.

We first show this statement when $U(s)$ generates the k -form symmetry with $k \geq 1$, i.e., the excitation has the dimension smaller than $d-1$. In that case, let us separate the system into $A \cup A^c$, where the subsystem A is the locus of the excitations a and A^c is its complement. Let us consider the projector Π_{A^c} onto the product state $|0\rangle^n$ within the subsystem A^c . One can write Π_{A^c} as the product of local projectors within A^c , $\Pi_{A^c} = \prod_{L_j \subset A^c} \Pi_{L_j}$, where the set of local regions $\{L_j\}$ satisfies $\bigcup_j L_j = A^c$. Since the operator $U(s)$ can be topologically deformed on $|\Psi\rangle$ as long as $a = \partial s$ is fixed, one can set s to avoid each region L_j by the deformation. This implies that $U(s)$ and Π_{L_j} are commutative within the state $|\Psi\rangle$, so $\Pi_{L_j} U(s) |\Psi\rangle = U(s) \Pi_{L_j} |\Psi\rangle = U(s) |\Psi\rangle$. This implies that $\Pi_{A^c} U(s) |\Psi\rangle = U(s) |\Psi\rangle$, so the state $U(s) |\Psi\rangle$ is expressed in the form of

$$U(s) |\Psi\rangle = |a\rangle_A \otimes |0\rangle_{A^c}, \quad (81)$$

where $|0\rangle_{A^c}$ is the product state at A^c , and $|a\rangle_A$ is the state whose Hilbert space is localized along the locations of excitations A .

Then, let us show Eq. (81) when $U(s)$ is the 0-form symmetry. In that case, take a symmetry operator $U(\bar{s})$ with $-a = \partial \bar{s}$ so that the product $U(\bar{s})U(s)$ becomes a closed symmetry operator that preserves the state $|\Psi\rangle$, $U(\bar{s})U(s) |\Psi\rangle \propto |\Psi\rangle$. This operator is chosen so that $\text{supp}(s)$, $\text{supp}(\bar{s})$ do not have an overlap on their bulk. We again separate the system into $A \cup A^c$, where A has a support near the boundary of $\text{supp}(s)$. A^c is naturally separated into the two subsystems by $A^c = A_{\text{in}}^c \cup A_{\text{out}}^c$, where A_{in}^c is supported inside $\text{supp}(s)$, while A_{out}^c is on the outside. Let us again write the projector onto the product state as $\Pi_{A^c} = \Pi_{A_{\text{in}}^c} \Pi_{A_{\text{out}}^c}$, and each projector

$\Pi_{A_{\text{in}}^c}, \Pi_{A_{\text{out}}^c}$ is given by the product of projectors at local regions $\{L_j^{\text{in}}\}, \{L_j^{\text{out}}\}$. The projectors $\Pi_{L_j^{\text{out}}}$ obviously commutes with $U(s)$ since their support do not overlap. For $\Pi_{L_j^{\text{in}}}$ since we have

$$\begin{aligned} U(\bar{s})U(s)\Pi_{L_j^{\text{in}}}|\Psi\rangle &= \Pi_{L_j^{\text{in}}}U(\bar{s})U(s)|\Psi\rangle \\ &= U(\bar{s})\Pi_{L_j^{\text{in}}}U(s)|\Psi\rangle, \end{aligned} \quad (82)$$

so $\Pi_{L_j^{\text{in}}}$ commutes with $U(s)$ on $|\Psi\rangle$, $U(s)\Pi_{L_j^{\text{in}}}|\Psi\rangle = \Pi_{L_j^{\text{in}}}U(s)|\Psi\rangle$. This implies that $\Pi_{A^c}U(s)|\Psi\rangle = U(s)|\Psi\rangle$, so we again obtain Eq. (81) for 0-form symmetry.

We remark that the discussion here assumes tensor product Hilbert space. There are also SPT phases with transparent excitations of nontrivial statistics, such as fermionic SPT phases or fermionic loop SPT phases. These phases require imposing suitable constraints from $d\rho = w_i$ for the “ w_i structure” ρ . These SPT phases would require Hilbert spaces that are not tensor product spaces, and thus, the discussion here does not apply to them.

A. Review: Anyons imply long-range entanglement

Let us demonstrate the obstruction to SRE states when the excitations are particles with fusion rule $G = \mathbb{Z}_2$. This is a review of the result in Refs. [90, 91]. See also Ref. [92] for recent discussions. Due to the structure of excited states (81), each state $|jk\rangle$ with a pair of particle excitations at vertices j and k has the form of

$$|jk\rangle = |j\rangle \otimes |k\rangle \otimes |0\rangle_{\overline{j,k}}, \quad (83)$$

where $|j\rangle, |k\rangle$ are local states around the excitations, and $|0\rangle_{\overline{j,k}}$ is the product state on the complement. This immediately implies that when j, k, l, m are distinct positions in the space, we have $\langle jl|U_{kj}|kl\rangle = \langle jm|U_{kj}|km\rangle$. Hence

$$\theta(U_{kj}, kl) = \theta(U_{kj}, km) \quad (84)$$

for distinct j, k, l, m . This immediately shows that the following invariant of the particles must be trivial,

$$\begin{aligned} \Theta &= \theta(U_{02}U_{03}^{-1}U_{01}U_{02}^{-1}U_{03}U_{01}^{-1}, 12) \\ &= -\theta(U_{01}, 02) + \theta(U_{03}, 02) - \theta(U_{02}, 03) \\ &\quad + \theta(U_{01}, 03) - \theta(U_{03}, 01) + \theta(U_{02}, 01) = 0. \end{aligned} \quad (85)$$

Therefore, the SRE state cannot support Abelian anyons of nontrivial self-statistics.

B. Example: Fermionic loops imply long-range entanglement

Next, let us study the cases where the excitations are loops. In a 3d space, we demonstrate that SRE states

cannot support the fermionic loops with the nontrivial invariant

$$\begin{aligned} e^{i\Theta} &= U_{014}U_{034}U_{023}U_{014}^{-1}U_{024}^{-1}U_{012}U_{023}^{-1}U_{013}^{-1} \\ &\quad \times U_{024}U_{014}U_{013}U_{024}^{-1}U_{034}^{-1}U_{023}U_{013}^{-1}U_{012}^{-1} \\ &\quad \times U_{034}U_{024}U_{012}U_{034}^{-1}U_{014}^{-1}U_{013}U_{012}^{-1}U_{023}^{-1}, \end{aligned} \quad (86)$$

where U_{jkl} is the generator of the \mathbb{Z}_2 1-form symmetry is supported on the a triangle with vertices j, k, l .

1. MPS representation of excitations in SRE states

For SRE states, one can assume that the excited state $|a\rangle$ has an expression $|a\rangle = |a\rangle_A \otimes |0\rangle_{A^c}$ with the 1d state $|a\rangle_A$ localized at the position of excitations. One can generally express the 1d state $|a\rangle_A$ using the matrix product state (MPS) representation.

Let us consider an MPS $|a\rangle_A$ on the 1d subsystem A , with the bipartition into $A = A_1 \sqcup A_2$. Accordingly, the excitation a allows a decomposition $a = a_1 + a_2$. The state then has the expression

$$|a\rangle_A = \sum_{\mu, \nu} |\psi\rangle_{\mu\nu}^{A_1} |\psi\rangle_{\nu\mu}^{A_2}, \quad (87)$$

where μ, ν are bond indices. Let us consider a symmetry operator $U(s)$ with $\partial s = -a_2 + a_2'$. That is, the unitary acts on the 2d subsystem S that contains A_2 on its boundary, and transforms $|a\rangle$ into a state $|a'\rangle$ with excitations at $A' = A_1 \sqcup A_2'$. The unitary acts on the state $|a\rangle$ by

$$U(s)|a\rangle = \sum_{\mu, \nu} |\psi\rangle_{\mu\nu}^{A_1} \otimes U(s) \left[|\psi\rangle_{\nu\mu}^{A_2} |0\rangle^{S \cap A_2^c} \right] \otimes |0\rangle^{S^c}. \quad (88)$$

Given that $U(s)|a\rangle$ again allows an expression $U(s)|a\rangle = |a\rangle_{A'} \otimes |0\rangle_{A'^c}$, the state $U(s) \left[|\psi\rangle_{\nu\mu}^{A_2} |0\rangle^{S \cap A_2^c} \right]$ has an expression

$$U(s) \left[|\psi\rangle_{\nu\mu}^{A_2} |0\rangle^{S \cap A_2^c} \right] = |\psi\rangle_{\nu\mu}^{A_2'} |0\rangle^{S \cap A_2'^c}. \quad (89)$$

That is, the operator $U(s)$ transforms the MPS $|\psi\rangle_{\nu\mu}^{A_2}$ into the new MPS $|\psi\rangle_{\nu\mu}^{A_2'}$ at the different location.

This motivates us to express the generic $|a\rangle_A$ in terms of the “patchwork” of MPS, see Fig. 8(a). Each state $|a\rangle_A$ is expressed in terms of the following MPS of two types:

- $|V\rangle^j$ is an MPS on a small interval $I_j \subset A$ that contains the vertex j .
- $|E\rangle^{jk}$ is an MPS on an interval $I_{jk} \subset A$ contained in the edge $e = \langle jk \rangle$. I_{jk} is adjacent to I_j, I_k .

If the excitation a has a support at the collection of edges $\langle jk \rangle, \langle kl \rangle, \dots$ that forms a closed loop, we have $A = I_j \sqcup$

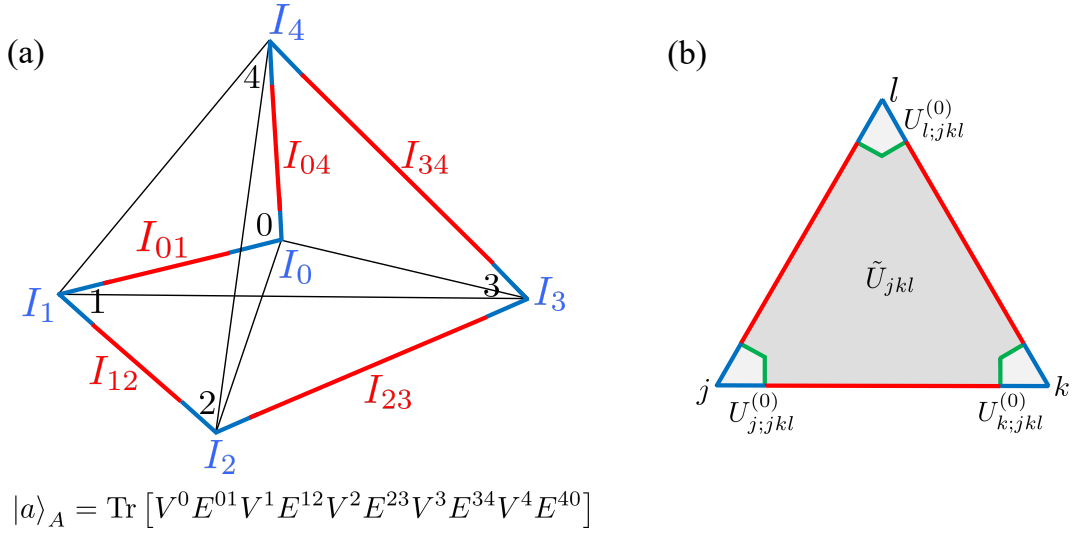


FIG. 8. (a): The excited state $|a\rangle_A$ is expressed as the patchwork of MPS at the intervals I_j, I_{jk} . I_j supports an MPS $|V\rangle^j$, I_{jk} supports an MPS $|E\rangle^{jk}$. (b): The support of each unitary on the triangle $jdkl$. $U_{j;jkl}^{(0)}$ acts nearby the vertex j whose boundary contains I_j .

$I_{jk} \sqcup I_k \sqcup I_{kl} \sqcup I_l \dots$ and the state $|a\rangle_A$ has an MPS representation as

$$|a\rangle_A = \text{Tr} [V^j E^{jk} V^k E^{kl} V^l \dots] . \quad (90)$$

The MPS $\{V^j, E^{jk}\}$ associated with the vertices and edges give the canonical choice of the states $\{|a\rangle\}$.

2. Decomposition of phases

According to the expression of states $|a\rangle_A$ in terms of the patch of MPS, it is convenient to separate the symmetry generator into the operators supported near the corner vertices j, k, l and the rest,

$$U_{jdkl} = U_{j;jkl}^{(0)} U_{k;jkl}^{(0)} U_{l;jkl}^{(0)} \times \tilde{U}_{jdkl} , \quad (91)$$

where $U_{j;jkl}^{(0)}$ is a small defect operator acting on the region I_j together with the subsystem of the surface $jdkl$ near the vertex. \tilde{U}_{jdkl} acts on the intervals I_{jk}, I_{kl}, I_{jl} and the bulk of the surface $jdkl$ except nearby the vertices. See Fig. 8 (b).

Consequently, the phase $U_{jdkl} |a\rangle = \theta(U_{jdkl}, a) |a'\rangle$ admits an expression⁷

$$\theta(U_{jdkl}, a) = \theta(U_{j;jkl}^{(0)}, a) + \theta(U_{k;jkl}^{(0)}, a) + \theta(U_{l;jkl}^{(0)}, a) + \theta(\tilde{U}_{jdkl}, a) . \quad (92)$$

Given that each state is given in the form of the patch of MPS, the phases θ achieve the following properties:

- The dependence of $\theta(\tilde{U}_{jdkl}, a)$ on a is through a restricted to edges jk, kl, jl . In other words, $\theta(\tilde{U}_{jdkl}, a) = \theta(\tilde{U}_{jdkl}, a')$ as long as $a = a'$ on edges jk, kl, jl . This is because this phase only depends on the MPS patch E^{jk}, E^{kl}, E^{jl} (and the small MPS patch for the intermediate state $\tilde{U}_{jdkl} |a\rangle$ connecting between I_{jk}, I_{kl}, I_{jl} , which is expressed as the green lines in Fig. 8 (b)). Note that this property does not hold for the original phase $\theta(U_{jdkl}, a)$ with the whole operator U_{jdkl} , since this would depend on other edges that end at vertices j, k or l through the MPS patch V^j, V^k, V^l .

⁷ To be precise, when we define the phases such as $\theta(U_{j;jkl}^{(0)}, a), \theta(\tilde{U}_{jdkl}, a)$, we are fixing the choice of the interme-

mediate states e.g., $\tilde{U}_{jdkl} |a\rangle_A$ in terms of the patch of MPS. This amounts to fixing the MPS at the intermediate edges expressed as the green lines in Fig. 8 (b).

- The dependence of $\theta(U_{j:ijkl}^{(0)}, a)$ on a is through a restricted to edges ending at the vertex j . In other words, $\theta(U_{j:ijkl}^{(0)}, a) = \theta(U_{j:ijkl}^{(0)}, a')$ as long as $a = a'$ on edges ending at j . This is because this phase only depends on the MPS patch V^j (and the choice of the surface $ijkl$ where we act U_{ijkl} , together with the small MPS patch for the intermediate state).

This allows us to write the above phases as $\theta(U, \{e\})$ where $\{e\}$ is the set of edges with excitations on which θ depends. We can then express the invariant as

$$\begin{aligned}
\Theta = & -\theta(U_{0:023}^{(0)}, 03, 02) - \theta(U_{3:023}^{(0)}, 03, 34) - \theta(U_{2:023}^{(0)}, 02, 12) - \theta(\tilde{U}_{023}, 03, 02) \\
& - \theta(U_{0:012}^{(0)}, 01, 03) - \theta(U_{1:012}^{(0)}, 01, 14) - \theta(U_{2:012}^{(0)}) - \theta(\tilde{U}_{012}, 01) \\
& + \theta(U_{0:013}^{(0)}, 03, 01) + \theta(U_{3:013}^{(0)}, 03, 34) + \theta(U_{1:013}^{(0)}, 01, 14) + \theta(\tilde{U}_{013}, 03, 01) \\
& - \theta(U_{0:014}^{(0)}, 01, 04) - \theta(U_{1:014}^{(0)}, 01, 13) - \theta(U_{4:014}^{(0)}, 04, 34) - \theta(\tilde{U}_{014}, 01, 04) \\
& - \theta(U_{0:034}^{(0)}, 01, 03) - \theta(U_{3:034}^{(0)}, 03, 13) - \theta(U_{4:034}^{(0)}) - \theta(\tilde{U}_{034}, 03) \\
& + \theta(U_{0:012}^{(0)}, 01, 03) + \theta(U_{1:012}^{(0)}, 01, 13) + \theta(U_{2:012}^{(0)}) + \theta(\tilde{U}_{012}, 01) \\
& + \theta(U_{0:024}^{(0)}, 02, 03) + \theta(U_{2:024}^{(0)}, 02, 12) + \theta(U_{4:024}^{(0)}) + \theta(\tilde{U}_{024}, 02) \\
& + \theta(U_{0:034}^{(0)}, 03, 04) + \theta(U_{3:034}^{(0)}, 03, 13) + \theta(U_{4:034}^{(0)}, 04, 24) + \theta(\tilde{U}_{034}, 03, 04) \\
& - \theta(U_{0:012}^{(0)}, 02, 01) - \theta(U_{2:012}^{(0)}, 02, 24) - \theta(U_{1:012}^{(0)}, 01, 31) - \theta(\tilde{U}_{012}, 02, 01) \\
& - \theta(U_{0:013}^{(0)}, 03, 02) - \theta(U_{3:013}^{(0)}, 03, 34) - \theta(U_{1:013}^{(0)}) - \theta(\tilde{U}_{013}, 03) \\
& + \theta(U_{0:023}^{(0)}, 02, 03) + \theta(U_{2:023}^{(0)}, 02, 24) + \theta(U_{3:023}^{(0)}, 03, 34) + \theta(\tilde{U}_{023}, 02, 03) \\
& - \theta(U_{0:034}^{(0)}, 03, 04) - \theta(U_{3:034}^{(0)}, 03, 32) - \theta(U_{4:034}^{(0)}, 04, 24) - \theta(\tilde{U}_{034}, 03, 04) \\
& - \theta(U_{0:024}^{(0)}, 03, 02) - \theta(U_{2:024}^{(0)}, 02, 32) - \theta(U_{4:024}^{(0)}) - \theta(\tilde{U}_{024}, 02) \\
& + \theta(U_{0:013}^{(0)}, 03, 02) + \theta(U_{3:013}^{(0)}, 03, 32) + \theta(U_{1:013}^{(0)}) + \theta(\tilde{U}_{013}, 03) \\
& + \theta(U_{0:014}^{(0)}, 01, 02) + \theta(U_{1:014}^{(0)}, 01, 31) + \theta(U_{4:014}^{(0)}) + \theta(\tilde{U}_{014}, 01) \\
& + \theta(U_{0:024}^{(0)}, 02, 04) + \theta(U_{2:024}^{(0)}, 02, 32) + \theta(U_{4:024}^{(0)}, 04, 14) + \theta(\tilde{U}_{024}, 02, 04) \\
& - \theta(U_{0:013}^{(0)}, 01, 03) - \theta(U_{1:013}^{(0)}, 01, 14) - \theta(U_{3:013}^{(0)}, 03, 23) - \theta(\tilde{U}_{013}, 01, 03) \\
& - \theta(U_{0:023}^{(0)}, 02, 01) - \theta(U_{2:023}^{(0)}, 02, 24) - \theta(U_{3:023}^{(0)}) - \theta(\tilde{U}_{023}, 02) \\
& + \theta(U_{0:012}^{(0)}, 01, 02) + \theta(U_{1:012}^{(0)}, 01, 14) + \theta(U_{2:012}^{(0)}, 02, 24) + \theta(\tilde{U}_{012}, 01, 02) \\
& - \theta(U_{0:024}^{(0)}, 02, 04) - \theta(U_{2:024}^{(0)}, 02, 21) - \theta(U_{4:024}^{(0)}, 04, 14) - \theta(\tilde{U}_{024}, 02, 04) \\
& - \theta(U_{0:014}^{(0)}, 02, 01) - \theta(U_{1:014}^{(0)}, 01, 21) - \theta(U_{4:014}^{(0)}) - \theta(\tilde{U}_{014}, 01) \\
& + \theta(U_{0:023}^{(0)}, 02, 01) + \theta(U_{2:023}^{(0)}, 02, 21) + \theta(U_{3:023}^{(0)}) + \theta(\tilde{U}_{023}, 02) \\
& + \theta(U_{0:034}^{(0)}, 03, 01) + \theta(U_{3:034}^{(0)}, 03, 23) + \theta(U_{4:034}^{(0)}) + \theta(\tilde{U}_{034}, 03) \\
& + \theta(U_{0:014}^{(0)}, 01, 04) + \theta(U_{1:014}^{(0)}, 01, 21) + \theta(U_{4:014}^{(0)}, 04, 34) + \theta(\tilde{U}_{014}, 01, 04) .
\end{aligned} \tag{93}$$

One can explicitly check that the above phases cancel out. Therefore, we get $\Theta = 0$, and the SRE state cannot support fermionic loops.

C. Nontrivial statistics imply long-range entanglement

One can extend the above discussions for the generic statistics of the p dimensional excitations embedded in d space dimensions. We can assume that the excitation model is defined on a certain simplicial complex X embed-

ded in the space. For SRE states, the excited state can be represented by a state $|a\rangle_A$ localized at the position of the p -dimensional excitations A .

1. Patchwork of tensor network states at the excitations

As a generalization of MPS patchwork state for the loop excitations, we assume that $|a\rangle_A$ admits an expression in terms of the tensor network state (TNS) at A . Note that A is a locus of a simplicial complex, so it can have e.g. a junction of hyper surfaces and generally is not a manifold.

This assumption leads to the canonical choice of the state $|a\rangle_A$ using a patch of TNS where a patch is defined on the vicinity of each simplex. To define a support of each patch TNS, we introduce a locus of each simplex X in the space. Let $D_j(\sigma_j)$ be a locus of the j -simplex σ_j with a radius r_j ; this is given by $\sigma_j \times D^{d-j}$ in d -dimensional space, where D^{d-j} is a $(d-j)$ -ball with radius r_j , and its center point $\sigma_j \times \{0\}$ corresponds to σ_j . See Fig. 9 (a). We also define the collection of these regions $D_j = \bigcup_{\sigma_j \in \mathcal{T}} D_j(\sigma_j)$ for the j -simplices $\{\sigma_j\}$. For convenience, we set the radius r_j to satisfy $r_{j-1} > \alpha r_j$ with a proper big constant $\alpha \gg 1$. Also, we require that the radius $\{r_j\}$ is large enough so that $A \subset \bigcup_{0 \leq j \leq p} D_j$.

We then define a patch of TNS $T_j^A(\sigma_j, a)$ with $0 \leq j \leq p$ support at $A \cap D_j(\sigma_j) \cap D_{j-1}^c \cap \dots \cap D_0^c$. This is the tensor network state support at a single j -simplex σ_j except for the vicinity of boundaries of σ_j . This TNS has bond indices at the boundary which will be contracted with other TNS at the adjacent patch. We represent the state $|a\rangle_A$ by

$$|a\rangle_A = \prod_{0 \leq j \leq p} \prod_{\sigma_j \in X} T_j^A(\sigma_j, a), \quad (94)$$

where the product denotes the contraction of bond indices. The conditions $r_{j-1} > \alpha r_j$ ensure that the support of each pair of TNS patch T_j^A has no overlap.

2. Decomposition of phases

Each $(p+1)$ -simplex $\sigma_{p+1} \in X$ can support a unitary $U(S(\sigma_{p+1}))$ that generates the global symmetry G . $S(\sigma_{p+1})$ denotes a vicinity of the simplex σ_{p+1} that supports the unitary. We require $S(\sigma_{p+1}) \subset D_{p+1}(\sigma_{p+1}) \sqcup (\bigcup_{0 \leq j \leq p} D_j)$.

Following the argument in Sec. VB2, we decompose the unitary $U(S(\sigma_{p+1}))$ into a sequence of smaller unitaries compatible with the patch structure of TNS. That is, we decompose the support of the unitary $S(\sigma_{p+1})$ into $S(\sigma_{p+1}) = S_{p+1} \sqcup S_p \sqcup S_{p-1} \sqcup \dots \sqcup S_0$, with

$$\begin{cases} S_{p+1} = S \cap D_{p+1}(\sigma_{p+1}) \cap D_p^c \cap \dots \cap D_0^c \\ S_j = S \cap D_j \cap D_{j-1}^c \cap \dots \cap D_0^c \end{cases} \quad \text{for } 0 \leq j \leq p. \quad (95)$$

Note that S_j with $0 \leq j \leq p$ consists of the disconnected components nearby each j -simplex of σ_{p+1} as

$$S_j = \bigsqcup_{\sigma_j \subset \sigma_{p+1}} S_j(\sigma_j). \quad (96)$$

We then rewrite the unitary $U(S(\sigma_{p+1}))$ as the sequence

$$U(S(\sigma_{p+1})) = \left(\prod_{\sigma_0 \subset \sigma_{p+1}} U(S_0(\sigma_0)) \right) \times \dots \times \left(\prod_{\sigma_p \subset \sigma_{p+1}} U(S_p(\sigma_p)) \right) \times U(S_{p+1}). \quad (97)$$

See Fig. 9 (b). Each unitary $U(S_j(\sigma_j))$ acts on a single TNS patch on the j -simplex σ_j with $0 \leq j \leq p$. Accordingly, the phase $U(S(\sigma_{p+1})) |a\rangle = \theta(U(S(\sigma_{p+1})), a) |a'\rangle$ admits an expression

$$\theta(U(S(\sigma_{p+1})), a) = \left(\sum_{\sigma_0 \subset \sigma_{p+1}} \theta(U(S_0(\sigma_0)), a) \right) + \dots + \left(\sum_{\sigma_p \subset \sigma_{p+1}} \theta(U(S_p(\sigma_p)), a) \right) + \theta(U(S_{p+1})). \quad (98)$$

Given that each small unitary $U(S_j(\sigma_j))$ acts within a single patch of the TNS, the phases θ achieve the following properties:

- The dependence of $\theta(U(S_j(\sigma_j)), a)$ (with $0 \leq j \leq p$) on a is through a restricted to the set of p -simplices $\{\sigma_p\}$ satisfying $\sigma_j \subset \sigma_p$. This is because the action of the unitary $U(S_j(\sigma_j))$ on A is only within the TNS patch $T_j^A(\sigma_j, a)$. $\theta(U(S_j(\sigma_j)), a)$ also depends on the choice of unitary $U(\sigma_{p+1})$,
- $\theta(U(S_{p+1}))$ does not depend on a , but only depends on the choice of $U(S_{p+1})$. Note that this creates the intermediate tensor network state on the boundary sphere of S_{p+1} inside the $(p+1)$ -simplex.

namely a choice of σ_{p+1} together with the group element $g \in G$ that corresponds to U .

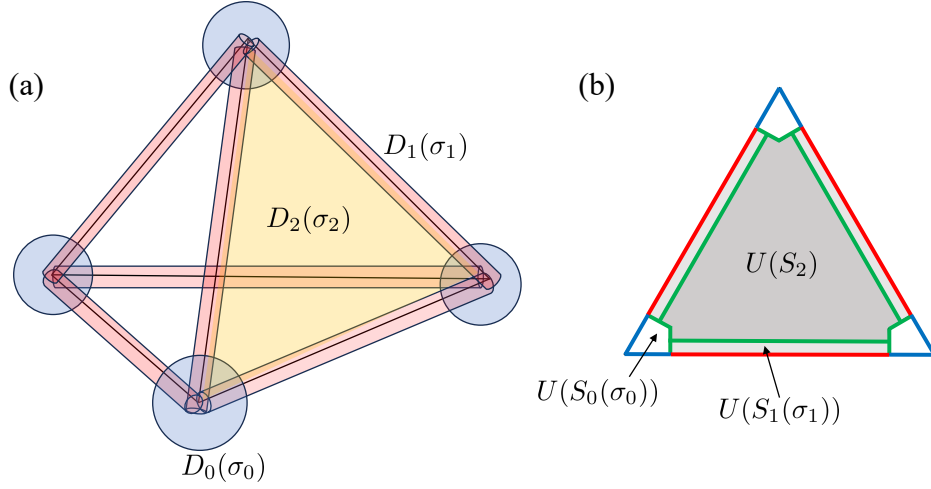


FIG. 9. (a): The disk locus of each simplex is denoted by $D_j(\sigma_j)$. Each TNS patch for the state $|a\rangle_A$ corresponds to extracting the TNS state inside each locus of σ_j with the locus of its boundary simplices excluded. (b): The decomposition of the unitary operator in the case of $p = 1$.

3. Trivial invariants in SRE states

Suppose that the sequence of unitaries $\langle a | \prod U(S) | a \rangle$ evaluated on a given excited state becomes the sum of phases θ which gives the element of E_{inv} ,

$$\Theta = \sum_{U(S(\sigma_{p+1})), a} \epsilon(U(S(\sigma_{p+1})), a) \times \theta(U(S(\sigma_{p+1})), a), \quad (99)$$

with $\epsilon(U(S(\sigma_{p+1})), a) \in \mathbb{Z}$. Recall that this phase $\Theta \in E_{\text{inv}}$ satisfies the Eqs. (24) and (25) given by

- The coefficients ϵ satisfy

$$\sum_a \epsilon(U(S(\sigma_{p+1})), a) = 0, \quad (100)$$

for any choice of $U(S(\sigma_{p+1}))$.

- The coefficients ϵ satisfy

$$\sum_{a|\sigma_j=a_*} \epsilon(U(S(\sigma_{p+1})), a) = 0, \quad (101)$$

with any choice of $U(S(\sigma_{p+1}))$ and a cochain a_* .

With this in mind, one can show that such Θ satisfying the invariance condition must have $\Theta = 0$ in the SRE state. Let us decompose the phases using Eq. (98) valid for the TNS patchwork state. In the sum of Θ , let us extract the part involving a fixed $U(S(\sigma_{p+1}))$, and then further pick the part of θ involving $S_j(\sigma_j)$ contained in $S(\sigma_{p+1})$ with $0 \leq j \leq p$. The extracted sum has the form

of

$$\begin{aligned} & \sum_a \epsilon(U(S(\sigma_{p+1})), a) \times \theta(U(S_j(\sigma_j)), a) \\ &= \sum_{a_*} \sum_{a|\sigma_j=a_*} \epsilon(U(S(\sigma_{p+1})), a) \times \theta(U(S_j(\sigma_j)), a). \end{aligned} \quad (102)$$

Here, recall that the phase $\theta(U(S_j(\sigma_j)), a)$ depends on a only through the reduced one $a|\sigma_j$ which is fixed in the second sum. We then have

$$\begin{aligned} & \sum_a \epsilon(U(S(\sigma_{p+1})), a) \times \theta(U(S_j(\sigma_j)), a) \\ &= \sum_{a_*} \left(\sum_{a|\sigma_j=a_*} \epsilon(U(S(\sigma_{p+1})), a) \right) \theta(U(S_j(\sigma_j)), a) = 0. \end{aligned} \quad (103)$$

So, the extracted sum with each choice of $U(S(\sigma_{p+1}))$ and $S_j(\sigma_j)$ in Θ vanishes due to Eq. (101).

Finally, one can also verify that the phases involving $\theta(U(S_{p+1}))$ also vanishes. The part of Θ that contains $\theta(U(S_{p+1}))$ is given by

$$\begin{aligned} & \sum_a \epsilon(U(S(\sigma_{p+1})), a) \times \theta(U(S_{p+1})) \\ &= \left(\sum_a \epsilon(U(S(\sigma_{p+1})), a) \right) \theta(U(S_{p+1})) = 0, \end{aligned} \quad (104)$$

where we used Eq. (100). Therefore, we get $\Theta = 0$ in the SRE state.

VI. DISCUSSIONS

In this paper, we established a universal microscopic description for the statistics of excitations in generic spacetime dimensions. The invariants are expressed as the Berry phase associated with families of excited states, transformed by sequences of unitaries that generate finite global symmetries and move the excitations. These invariants are generally quantized into discrete values, characterizing the generalized statistics of excitations in microscopic lattice models. For instance, this framework leads to the quantization of spins for Abelian anyons, which are microscopically defined via T-junctions. These invariants can be computed using algorithms with inputs such as the symmetry group and the configurations of excitations. This approach allows us to identify new invariants in microscopic lattice models, as well as a simplified expression for the invariants of fermionic loops in (3+1)D. These invariants can naturally be interpreted as obstructions to gauging the finite global symmetry G in microscopic lattice models, providing a microscopic definition of 't Hooft anomalies. We show that these anomalies have dynamical consequences, as nontrivial invariants forbid the existence of short-range entangled states.

One immediate direction for future work is to extend our framework of generalized statistics to include mixtures of $(d - p - 1)$ -form symmetries with distinct degrees p , which generally form higher-group symmetries. Even the simplest gapped phases, such as the \mathbb{Z}_2 toric code, exhibit a rich structure of higher-group symmetries with 't Hooft anomalies [64, 93–95]. For example, in (3+1)D, there may be string operators creating particle excitations alongside membrane operators creating loop excitations. Our SNF algorithm generates an additional invariant corresponding to the mutual braiding between particles and loops, supplementing the invariants for the self-statistics of particles and loops. For more general cases, it would be interesting to determine the invariants associated with these higher-group structures in topologically ordered phases.

While we mainly studied the finite invertible symmetries in this paper, there are other important class of symmetries which requires further study, such as the continuous symmetries. For instance, the (2+1)D gapped phases with continuous symmetries can exhibit electric Hall conductance, which is not associated with the 't Hooft anomaly of global symmetry in a usual sense. It would be interesting to see if the Hall conductance admits a similar microscopic characterization to our current paper, e.g., through the spin of the vortex of $U(1)$ symmetry. This would help clarify if the nontrivial Hall conductance gives obstructions to gauging continuous symmetries.

The other important class of symmetries not studied in this paper is the non-invertible symmetries, which includes the non-Abelian anyons. For instance, microscopic definitions of the anyon data of the non-Abelian topological order in (2+1)D has been discussed in Ref. [60]. Given

that the spins of Abelian anyons are shown to be quantized using the locality identities, it would be interesting to see if the anyon data of non-Abelian anyon systems are also quantized due to the locality of topological operators.

Recent development of non-invertible symmetries uncovered the existence of various invariants associated with the algebraic structure of the non-invertible symmetries. For instance, the defects of non-invertible symmetries can carry the invariant called the Frobenius-Schur indicator and its generalizations [96–98], and it would be interesting to characterize such invariants through the sequence of symmetry operators. Non-invertible symmetries allow us to define yet another invariants such as three-loop braiding of vortices in (3+1)D topological order [29], or the generalization of Hall conductance associated with continuous non-invertible symmetry [99]. It would be interesting to explore the characterization of these invariants.

While the global symmetries in our paper is assumed to be a finite depth circuit, some of global symmetries in the lattice models are not expressed as a circuit. This includes the crystalline symmetries such as lattice translations, or more generally symmetries generated by quantum cellular automata (QCA) [100–105]. It would be interesting to characterize the invariants for these symmetries.

Several open issues have arisen from our work, which deserves further study. The genuine Berry phase invariants T are conjectured to correspond to the cohomology of the Eilenberg–MacLane space $H^{d+2}(B^{d-p}G, U(1))$ classifying the anomalies of higher-form symmetries. It would be desirable to prove this correspondence using the explicit model of the Eilenberg–MacLane space.

While the invariants in this paper is valid for the gapped phases with exponentially decaying correlation length, it would be interesting to explore the invariants valid for the gapless phases as well. It is expected that the finite correlation length would modify the conditions for the stability of the invariants against local perturbations, but some of the invariants provided in this paper might survive in the gapless phases. In particular, it is plausible that the generalized statistics remains well-defined even in the gapless phases, as long as the excitations are gapped. For example, in gapless $U(1)$ quantum spin liquids the charge and flux particle excitations are gapped, and whether they are bosons or fermions distinguishes different phases [106, 107].

Also, while the invariants in this paper were defined with an explicit reference to a specific state in the Hilbert space, but it is expected that the anomalies can be characterized solely by the algebra of symmetry operators without explicit reference to the states [76]. It would be interesting to see if our invariants are promoted to operator equations independent of the choice of any states in the Hilbert space.

ACKNOWLEDGEMENTS

Y.-A.C wants to thank Qing-Rui Wang and Meng Cheng for sharing their unpublished note [61], and for the insightful discussions that inspired our Conjecture III.2. We also thank Andreas Bauer, Tyler D. Ellison, Dominic Else, Anton Kapustin, Kyle Kawagoe, Sahand Seifnashri, Wilbur Shirley, Nikita Sopenko, Nathanan Tantisadakarn, Bowen Yang, Peng Ye, and Carolyn Zhang for their discussions and valuable feedback.

Y.-A.C. is supported by the National Natural Science Foundation of China (Grant No. 12474491). R.K. is supported by the U.S. Department of Energy (Grant No. DE-SC0009988) and the Sivian Fund. P.-S.H. is supported by the Department of Mathematics at King's College London.

Appendix A: Simplicial complex, chains, and cochains

Simplicial complex is a useful mathematical toolkit that describes topological spaces by assembling fundamental building blocks called simplices. This allows us to describe the topological data of the space by purely combinatorial data of simplicial complex, making it easier to handle. Despite slight difference among several definitions of simplicial complex, we choose the simplest version used in this paper.

A simplex is a generalization of a triangle (2D) or tetrahedron (3D) to generic dimensions. n -simplex is the simplest geometric object that can represent an n dimensional shape in a given space. For instance, a 0-simplex is a point; a 1-simplex is an edge; a 2-simplex is a triangle; a 3-simplex is a tetrahedron. In general, an n -simplex is an n -dimensional object with $n + 1$ vertices. It also has $n + 1$ faces, each of which is an $(n - 1)$ -simplex.

A simplicial complex X is obtained by gluing simplices of different dimensions along their faces. First, we pick a finite set X_0 of vertices as labeled by $1, 2, \dots, k$. Second, we pick a finite set X_1 of edges and identify its two endpoints with two distinct vertices in X_0 . Third, we pick a finite set X_2 of 2-simplices and identify its three faces with three distinct edges in X_0 , and so on. We also impose an additional condition: for any two simplices σ, σ' in X , the sets of vertices of σ and σ' are not identical. The maximum integer d such that $X_d \neq \emptyset$ is called the dimension of X .

For any $\sigma_p \in X_p$, it has $p + 1$ distinct vertices in X_0 , which can be labeled by numbers $1 \leq i_0 < i_1 < \dots < i_p \leq k$. The j -th face ($0 \leq j \leq p$) of σ_p , as denoted by $\partial_j \sigma_p$, is defined as the $(p - 1)$ -simplex corresponds to vertices $i_0 < \dots < i_p$ except i_j . In total, we have the face maps $\partial_j : X_p \rightarrow X_{p-1}, 0 \leq j \leq p$.

The n -th chain group (with integer coefficient) is defined as the formal sum of n -simplices: $C_n(X) = \bigoplus_{\sigma \in X_n} \mathbb{Z}\sigma$. For every n -simplex σ , its homological boundary $\partial\sigma$ is defined as $\partial\sigma = \sum_{i=0}^n (-1)^i \partial_i \sigma \in C_{n-1}(X)$.

It naturally extends to a homomorphism $\partial : C_n(X) \rightarrow C_{n-1}(X)$. Its image is called the $(n - 1)$ -th boundary chain group, denoted by $B_{n-1}(X)$.

For any discrete Abelian group G , we can also formally multiply a group element $g \in G$ and a simplex $\sigma \in X_p$, the result denoted by $g\sigma$. Now, the n -th chain group with coefficient in G is defined by $C_n(X, G) = \bigoplus_{\sigma \in X_n} G\sigma$. To be specific, an element in $C_n(X, G)$ is written as $\sum_{\sigma \in X_n} g_\sigma \sigma$ with $g_\sigma \in G$. The homological boundary map $\partial : C_n(X, G) \rightarrow C_{n-1}(X, G)$ is defined by $\partial(g\sigma) = \sum_{i=0}^n (-1)^i g \partial_i \sigma$. The image of ∂ is called the $(n - 1)$ -th boundary chain group, denoted by $B_{n-1}(X, G)$, and is the group of configurations \mathcal{A} when we consider excitation models of dimension $n - 1$ and fusion group G in the simplicial complex X .

Appendix B: Derivations for particle and loop statistics with fusion group \mathbb{Z}_2

1. T-junction process in (2+1)D

In this section, we explicitly evaluate the summation of locality identities for the (2+1)D T-junction with $G = \mathbb{Z}_2$ as outlined in Sec. III A. This analysis shows that a particular combination of these locality identities results in four iterations of the T-junction process, thereby verifying the quantization of the T-junction into the fourth root of unity.

For convenience, we represent a configuration of excitations by a vertex of a graph. An edge connecting two vertices represents the action of a unitary operator that changes the configuration from one vertex to the other. The direction of the edge further specifies the initial and final configurations. All possible transformations of the states using the operators U_{0i} can be represented as a cube, as shown in Fig. 7(a).

Since $G = \mathbb{Z}_2$, for a fixed initial configuration of excitations, the actions of the unitaries U and U^{-1} yield the same final state. Each direction of an edge can be associated with two distinct unitaries, U or U^{-1} . Thus, each edge corresponds to four possible transformations, arising from the choice of edge direction and whether U or U^{-1} is applied. According to

$$\theta(U(s), a) = -\theta(U(s)^{-1}, a + \partial s), \quad (\text{B1})$$

for any $a \in \mathcal{A}$ and $s \in \mathcal{S}$. There are two relations among the four possible phases. Taking the leftmost vertical edge in Fig. 7(a) with U_{03} as an example, we have:

$$\begin{aligned} \theta(U_{03}, \triangle) + \theta(U_{03}^{-1}, \triangle) &= 0, \\ \theta(U_{03}, \triangle) + \theta(U_{03}^{-1}, \triangle) &= 0. \end{aligned} \quad (\text{B2})$$

Based on the above discussion, we describe the sum of phases using a cube with operators $\{U_{0j}\}$, where the directed edges indicate the initial and final states. We can

express the phases in Eq. (B2) diagrammatically on the edges of the cube as

$$\begin{array}{c}
 \begin{array}{cc}
 \begin{array}{c} \triangle \uparrow \\ U_{03} \\ \triangle \end{array} & = - & \begin{array}{c} \triangle \downarrow \\ U_{03}^{-1} \\ \triangle \end{array} , & \begin{array}{cc}
 \begin{array}{c} \triangle \downarrow \\ U_{03} \\ \triangle \end{array} & = - & \begin{array}{c} \triangle \uparrow \\ U_{03}^{-1} \\ \triangle \end{array} .
 \end{array}
 \end{array}
 \quad (B3)$$

The same relation holds for other edges in different directions.

Next, we consider the following locality identities acting on the vacuum state, represented by specific commutators of hopping operators whose supports do not overlap:

$$\begin{aligned}
 \text{Type 1: } & \langle \triangle \uparrow | [[U_{02}, U_{03}], U_{12}] | \triangle \uparrow \rangle = 0 \pmod{2\pi} , \\
 \text{Type 2: } & \langle \triangle \uparrow | [[U_{02}^{-1}, U_{03}^{-1}], U_{12}] | \triangle \uparrow \rangle = 0 \pmod{2\pi} , \\
 \text{Type 3: } & \langle \triangle \uparrow | [[U_{03}, U_{02}], U_{23}] | \triangle \uparrow \rangle = 0 \pmod{2\pi} .
 \end{aligned}
 \quad (B4)$$

Each identity involves a total of eight hopping operators within the cube of configuration states, forming two distinct oriented squares. The oriented squares associated with the Type 1 locality identity can be represented as follows:

$$\begin{array}{c}
 \begin{array}{c}
 \begin{array}{c} \triangle \uparrow \\ U_{02}^{-1} \\ \triangle \end{array} & \begin{array}{c} \triangle \uparrow \\ U_{02} \\ \triangle \end{array} \\
 \begin{array}{c} \triangle \uparrow \\ U_{03} \\ \triangle \end{array} & \begin{array}{c} \triangle \uparrow \\ U_{03}^{-1} \\ \triangle \end{array} \\
 \begin{array}{c} \triangle \uparrow \\ U_{02} \\ \triangle \end{array} & \begin{array}{c} \triangle \uparrow \\ U_{02}^{-1} \\ \triangle \end{array}
 \end{array}
 \quad = 0 \pmod{2\pi} , \quad (B5)
 \end{array}$$

where two squares correspond to the terms $\langle \triangle \uparrow | [U_{02}, U_{03}] | \triangle \uparrow \rangle$ and $-\langle \triangle \uparrow | [U_{02}, U_{03}] | \triangle \uparrow \rangle$, respectively. Similarly, the Type 2 locality identity can be visualized on the cube of configuration states as follows:

$$\begin{array}{c}
 \begin{array}{c}
 \begin{array}{c} \triangle \uparrow \\ U_{02} \\ \triangle \end{array} & \begin{array}{c} \triangle \uparrow \\ U_{02}^{-1} \\ \triangle \end{array} \\
 \begin{array}{c} \triangle \uparrow \\ U_{03} \\ \triangle \end{array} & \begin{array}{c} \triangle \uparrow \\ U_{03}^{-1} \\ \triangle \end{array} \\
 \begin{array}{c} \triangle \uparrow \\ U_{02} \\ \triangle \end{array} & \begin{array}{c} \triangle \uparrow \\ U_{02}^{-1} \\ \triangle \end{array}
 \end{array}
 \quad = 0 \pmod{2\pi} . \quad (B6)
 \end{array}$$

The Type 3 locality identity, on the other hand, is represented by two oriented squares located on the same face of the cube:

$$\begin{array}{c}
 \begin{array}{c}
 \begin{array}{c} \triangle \uparrow \\ U_{02}^{-1} \\ \triangle \end{array} & \begin{array}{c} \triangle \uparrow \\ U_{02} \\ \triangle \end{array} \\
 \begin{array}{c} \triangle \uparrow \\ U_{03} \\ \triangle \end{array} & \begin{array}{c} \triangle \uparrow \\ U_{03}^{-1} \\ \triangle \end{array} \\
 \begin{array}{c} \triangle \uparrow \\ U_{02} \\ \triangle \end{array} & \begin{array}{c} \triangle \uparrow \\ U_{02}^{-1} \\ \triangle \end{array}
 \end{array}
 \quad = 0 \pmod{2\pi} . \quad (B7)
 \end{array}$$

Note that each type of identity includes the one depicted above, along with two others that are related by the C_3 rotation along the axis extending from $\triangle \uparrow$ to $\triangle \uparrow$.

Below, we list all identities of the three types, which will be used in the derivation of the T-junction process.

$$\begin{aligned}
 \text{Type 1: } & \theta(U_{03}, \triangle \uparrow) + \theta(U_{02}, \triangle \uparrow) - \theta(U_{03}, \triangle \uparrow) - \theta(U_{02}, \triangle \uparrow) \\
 & - \theta(U_{03}, \triangle \uparrow) - \theta(U_{02}, \triangle \uparrow) + \theta(U_{03}, \triangle \uparrow) + \theta(U_{02}, \triangle \uparrow) = 0 \pmod{2\pi} , \\
 & \theta(U_{02}, \triangle \uparrow) + \theta(U_{01}, \triangle \uparrow) - \theta(U_{02}, \triangle \uparrow) - \theta(U_{01}, \triangle \uparrow) \\
 & - \theta(U_{02}, \triangle \uparrow) - \theta(U_{01}, \triangle \uparrow) + \theta(U_{02}, \triangle \uparrow) + \theta(U_{01}, \triangle \uparrow) = 0 \pmod{2\pi} , \\
 & \theta(U_{01}, \triangle \uparrow) + \theta(U_{03}, \triangle \uparrow) - \theta(U_{01}, \triangle \uparrow) - \theta(U_{03}, \triangle \uparrow) \\
 & - \theta(U_{01}, \triangle \uparrow) - \theta(U_{03}, \triangle \uparrow) + \theta(U_{01}, \triangle \uparrow) + \theta(U_{03}, \triangle \uparrow) = 0 \pmod{2\pi} .
 \end{aligned}
 \quad (B8)$$

$$\begin{aligned}
\text{Type 2: } & \theta \left(U_{03}, \begin{array}{c} \bullet \\ \triangle \\ \bullet \end{array} \right) + \theta \left(U_{02}, \begin{array}{c} \bullet \\ \triangle \\ \bullet \end{array} \right) - \theta \left(U_{03}, \begin{array}{c} \bullet \\ \triangle \\ \bullet \end{array} \right) - \theta \left(U_{02}, \begin{array}{c} \bullet \\ \triangle \\ \bullet \end{array} \right) \\
& - \theta \left(U_{03}, \begin{array}{c} \bullet \\ \triangle \\ \bullet \end{array} \right) - \theta \left(U_{02}, \begin{array}{c} \bullet \\ \triangle \\ \bullet \end{array} \right) + \theta \left(U_{03}, \begin{array}{c} \bullet \\ \triangle \\ \bullet \end{array} \right) + \theta \left(U_{02}, \begin{array}{c} \bullet \\ \triangle \\ \bullet \end{array} \right) = 0 \pmod{2\pi}, \\
& \theta \left(U_{02}, \begin{array}{c} \bullet \\ \triangle \\ \bullet \end{array} \right) + \theta \left(U_{01}, \begin{array}{c} \bullet \\ \triangle \\ \bullet \end{array} \right) - \theta \left(U_{02}, \begin{array}{c} \bullet \\ \triangle \\ \bullet \end{array} \right) - \theta \left(U_{01}, \begin{array}{c} \bullet \\ \triangle \\ \bullet \end{array} \right) \\
& - \theta \left(U_{02}, \begin{array}{c} \bullet \\ \triangle \\ \bullet \end{array} \right) - \theta \left(U_{01}, \begin{array}{c} \bullet \\ \triangle \\ \bullet \end{array} \right) + \theta \left(U_{02}, \begin{array}{c} \bullet \\ \triangle \\ \bullet \end{array} \right) + \theta \left(U_{01}, \begin{array}{c} \bullet \\ \triangle \\ \bullet \end{array} \right) = 0 \pmod{2\pi}, \\
& \theta \left(U_{01}, \begin{array}{c} \bullet \\ \triangle \\ \bullet \end{array} \right) + \theta \left(U_{03}, \begin{array}{c} \bullet \\ \triangle \\ \bullet \end{array} \right) - \theta \left(U_{01}, \begin{array}{c} \bullet \\ \triangle \\ \bullet \end{array} \right) - \theta \left(U_{03}, \begin{array}{c} \bullet \\ \triangle \\ \bullet \end{array} \right) \\
& - \theta \left(U_{01}, \begin{array}{c} \bullet \\ \triangle \\ \bullet \end{array} \right) - \theta \left(U_{03}, \begin{array}{c} \bullet \\ \triangle \\ \bullet \end{array} \right) + \theta \left(U_{01}, \begin{array}{c} \bullet \\ \triangle \\ \bullet \end{array} \right) + \theta \left(U_{03}, \begin{array}{c} \bullet \\ \triangle \\ \bullet \end{array} \right) = 0 \pmod{2\pi}.
\end{aligned} \tag{B9}$$

$$\begin{aligned}
\text{Type 3: } & \theta \left(U_{03}, \begin{array}{c} \bullet \\ \triangle \\ \bullet \end{array} \right) + \theta \left(U_{02}, \begin{array}{c} \bullet \\ \triangle \\ \bullet \end{array} \right) - \theta \left(U_{03}, \begin{array}{c} \bullet \\ \triangle \\ \bullet \end{array} \right) - \theta \left(U_{02}, \begin{array}{c} \bullet \\ \triangle \\ \bullet \end{array} \right) \\
& - \theta \left(U_{03}, \begin{array}{c} \bullet \\ \triangle \\ \bullet \end{array} \right) - \theta \left(U_{02}, \begin{array}{c} \bullet \\ \triangle \\ \bullet \end{array} \right) + \theta \left(U_{03}, \begin{array}{c} \bullet \\ \triangle \\ \bullet \end{array} \right) + \theta \left(U_{02}, \begin{array}{c} \bullet \\ \triangle \\ \bullet \end{array} \right) = 0 \pmod{2\pi}, \\
& \theta \left(U_{02}, \begin{array}{c} \bullet \\ \triangle \\ \bullet \end{array} \right) + \theta \left(U_{01}, \begin{array}{c} \bullet \\ \triangle \\ \bullet \end{array} \right) - \theta \left(U_{02}, \begin{array}{c} \bullet \\ \triangle \\ \bullet \end{array} \right) - \theta \left(U_{01}, \begin{array}{c} \bullet \\ \triangle \\ \bullet \end{array} \right) \\
& - \theta \left(U_{02}, \begin{array}{c} \bullet \\ \triangle \\ \bullet \end{array} \right) - \theta \left(U_{01}, \begin{array}{c} \bullet \\ \triangle \\ \bullet \end{array} \right) + \theta \left(U_{02}, \begin{array}{c} \bullet \\ \triangle \\ \bullet \end{array} \right) + \theta \left(U_{01}, \begin{array}{c} \bullet \\ \triangle \\ \bullet \end{array} \right) = 0 \pmod{2\pi}, \\
& \theta \left(U_{01}, \begin{array}{c} \bullet \\ \triangle \\ \bullet \end{array} \right) + \theta \left(U_{03}, \begin{array}{c} \bullet \\ \triangle \\ \bullet \end{array} \right) - \theta \left(U_{01}, \begin{array}{c} \bullet \\ \triangle \\ \bullet \end{array} \right) - \theta \left(U_{03}, \begin{array}{c} \bullet \\ \triangle \\ \bullet \end{array} \right) \\
& - \theta \left(U_{01}, \begin{array}{c} \bullet \\ \triangle \\ \bullet \end{array} \right) - \theta \left(U_{03}, \begin{array}{c} \bullet \\ \triangle \\ \bullet \end{array} \right) + \theta \left(U_{01}, \begin{array}{c} \bullet \\ \triangle \\ \bullet \end{array} \right) + \theta \left(U_{03}, \begin{array}{c} \bullet \\ \triangle \\ \bullet \end{array} \right) = 0 \pmod{2\pi}.
\end{aligned} \tag{B10}$$

By summing over all Type 1 identities, Type 2 identities, and twice the Type 3 identities, we obtain:

$$\begin{aligned}
& 4\theta \left(U_{03}, \begin{array}{c} \bullet \\ \triangle \\ \bullet \end{array} \right) - 4\theta \left(U_{02}, \begin{array}{c} \bullet \\ \triangle \\ \bullet \end{array} \right) + 4\theta \left(U_{01}, \begin{array}{c} \bullet \\ \triangle \\ \bullet \end{array} \right) \\
& - 4\theta \left(U_{03}, \begin{array}{c} \bullet \\ \triangle \\ \bullet \end{array} \right) + 4\theta \left(U_{02}, \begin{array}{c} \bullet \\ \triangle \\ \bullet \end{array} \right) - 4\theta \left(U_{01}, \begin{array}{c} \bullet \\ \triangle \\ \bullet \end{array} \right) = 0 \pmod{2\pi}.
\end{aligned} \tag{B11}$$

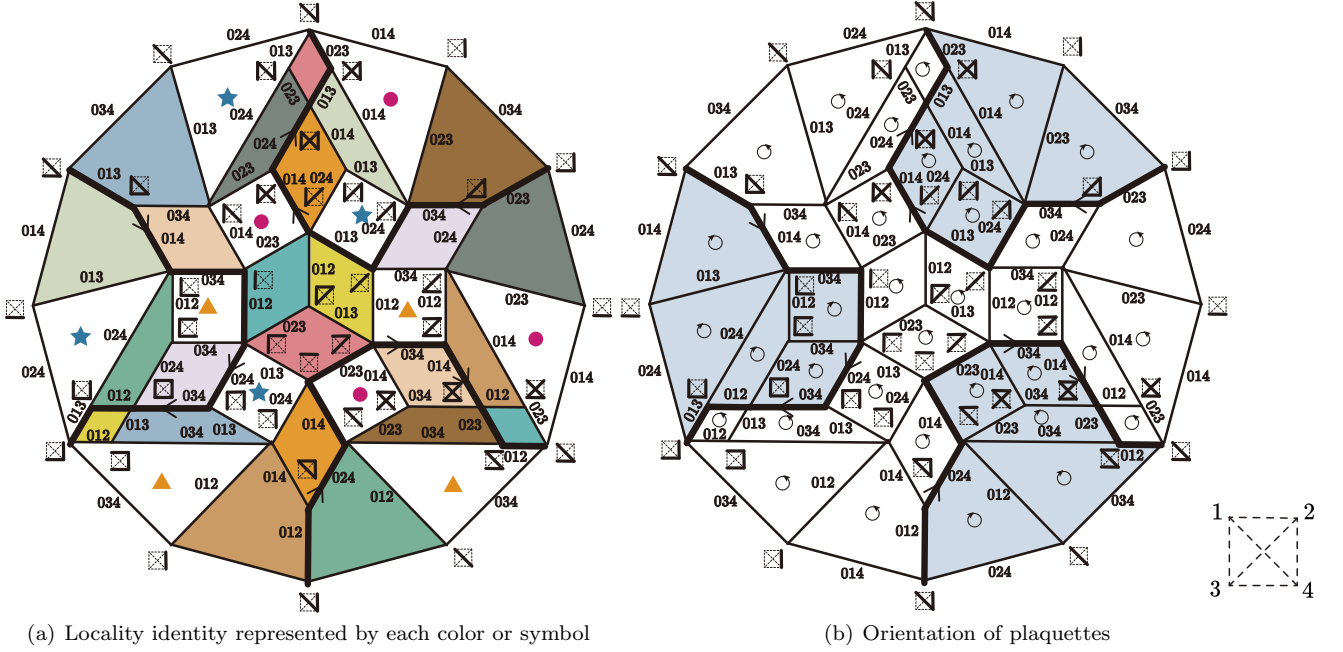
Using Eq. (B1), this expression can be simplified to

$$\begin{aligned}
& 4\theta \left(U_{03}, \begin{array}{c} \bullet \\ \triangle \\ \bullet \end{array} \right) + 4\theta \left(U_{02}^{-1}, \begin{array}{c} \bullet \\ \triangle \\ \bullet \end{array} \right) + 4\theta \left(U_{01}, \begin{array}{c} \bullet \\ \triangle \\ \bullet \end{array} \right) \\
& + 4\theta \left(U_{03}^{-1}, \begin{array}{c} \bullet \\ \triangle \\ \bullet \end{array} \right) + 4\theta \left(U_{02}, \begin{array}{c} \bullet \\ \triangle \\ \bullet \end{array} \right) + 4\theta \left(U_{01}^{-1}, \begin{array}{c} \bullet \\ \triangle \\ \bullet \end{array} \right) \\
& = 4\theta \left(U_{02} U_{03}^{-1} U_{01} U_{02}^{-1} U_{03} U_{01}^{-1}, \begin{array}{c} \bullet \\ \triangle \\ \bullet \end{array} \right) = 0 \pmod{2\pi}.
\end{aligned} \tag{B12}$$

This implies that four iterations of the T-junction process yield $0 \pmod{2\pi}$. The T-junction process is illustrated in Fig. 7(b).

2. Loop-flipping process in (3+1)D

In this section, we derive the unitary sequence used to detect loop statistics for the fusion group $G = \mathbb{Z}_2$ in (3+1)D. This derivation is inspired by Appendix D of Ref. [44]. Similar to the previous section, we first construct the graph space of configurations. In principle, there are six operators: U_{012} , U_{013} , U_{014} , U_{023} , U_{024} , and U_{034} , which create loops along the boundary of these faces, resulting in a total of $2^6 = 64$ configuration states within the same superselection sector as the vacuum state. For simplicity, we restrict our analysis to single-loop configurations, where the loop excitation is connected and does not have self-intersection. There are 37 single-loop configurations, represented as vertices in Fig. 10. Interestingly, the computation is even more straightforward than in the T-junction case. Since $G = \mathbb{Z}_2$, transitioning from one state to another allows us to apply either U or U^{-1} , as used in the locality identities in Eqs. (B5), (B6), and (B7). However, for loop excitations, we further constrain ourselves such that U_{0ij} can only create a loop on edge $\langle ij \rangle$, while U_{0ij}^{-1} can only annihilate it on the same edge.



(a) Locality identity represented by each color or symbol

(b) Orientation of plaquettes

FIG. 10. Each vertex represents a single-loop configuration on the tetrahedron $\langle 1234 \rangle$ with a central vertex 0, as shown in Fig. 2(c). Only the loop configuration along the edges between vertices 1, 2, 3, and 4 is depicted, as the configurations on the remaining edges can be inferred. The operator U_{0ij} creates a loop excitation on edge $\langle ij \rangle$, while U_{0ij}^{-1} annihilates it. This structure forms an \mathbb{RP}^2 space, as antipodal vertices represent the same configuration state [44]. (a) Each plaquette is labeled by a color or symbol, indicating that summing over plaquettes (according to the orientation in Fig. 10(b)) with the same color or symbol yields a locality identity. (b) The orientation of each plaquette used to express the local identity. Summing over all locality identities results in twice the 24-step process (represented by the black directed line), as the $\theta(U(s), a)$ terms on all other edges are canceled out.

The locality identities are represented by colors and symbols in Fig. 10(a). For example, the two yellow plaquettes correspond to the following locality identity:

$$\begin{aligned} & \theta(U_{012}^{-1}U_{013}^{-1}U_{012}U_{013}, \partial\langle 023 \rangle) + \theta(U_{013}^{-1}U_{012}^{-1}U_{013}U_{012}, \partial\langle 023 \rangle + \partial\langle 234 \rangle) \\ &= \theta(U_{012}^{-1}U_{013}^{-1}U_{012}U_{013}, \partial\langle 023 \rangle) - \theta(U_{012}^{-1}U_{013}^{-1}U_{012}U_{013}, \partial\langle 023 \rangle + \partial\langle 234 \rangle) \\ &= \theta([U_{234}, [U_{012}, U_{013}]], \partial\langle 023 \rangle) = 0 \pmod{2\pi}. \end{aligned} \quad (\text{B13})$$

Each color corresponds to a pair of plaquettes, and summing over two plaquettes with orientations given in Fig. 10(b) results in the locality identity for each color. On the other hand, each symbol (red circles, blue stars, yellow triangles) appears in four plaquettes. For instance, the red circles in Fig. 10(a) are present on four plaquettes spanning $\langle 014 \rangle$ and $\langle 023 \rangle$. The corresponding locality identity across these four plaquettes is more involved:

$$\begin{aligned} & \theta([U_{014}, U_{023}], \partial\langle 012 \rangle) + \theta([U_{014}, U_{023}], \partial\langle 024 \rangle) + \theta([U_{014}, U_{023}], \partial\langle 034 \rangle) + \theta([U_{014}, U_{023}], \partial\langle 013 \rangle) \\ &= 0 \pmod{2\pi}, \end{aligned} \quad (\text{B14})$$

which results from summing over four plaquettes following the orientations in Fig. 10(b). To show that Eq. (B14) is indeed a locality identity, we expand it as follows:

$$\begin{aligned} & \left(\theta(U_{023}, \partial\langle 012 \rangle) + \theta(U_{014}, \partial\langle 012 \rangle + \partial\langle 023 \rangle) - \theta(U_{023}, \partial\langle 012 \rangle + \partial\langle 014 \rangle) - \theta(U_{014}, \partial\langle 012 \rangle) \right) \\ & + \left(\theta(U_{023}, \partial\langle 024 \rangle) + \theta(U_{014}, \partial\langle 024 \rangle + \partial\langle 023 \rangle) - \theta(U_{023}, \partial\langle 024 \rangle + \partial\langle 014 \rangle) - \theta(U_{014}, \partial\langle 024 \rangle) \right) \\ & + \left(\theta(U_{023}, \partial\langle 034 \rangle) + \theta(U_{014}, \partial\langle 034 \rangle + \partial\langle 023 \rangle) - \theta(U_{023}, \partial\langle 034 \rangle + \partial\langle 014 \rangle) - \theta(U_{014}, \partial\langle 034 \rangle) \right) \\ & + \left(\theta(U_{023}, \partial\langle 013 \rangle) + \theta(U_{014}, \partial\langle 013 \rangle + \partial\langle 023 \rangle) - \theta(U_{023}, \partial\langle 013 \rangle + \partial\langle 014 \rangle) - \theta(U_{014}, \partial\langle 013 \rangle) \right). \end{aligned} \quad (\text{B15})$$

Next, the subsequent locality identities are added to the above equation to modify the configuration states a within the $\theta(U(s), a)$ terms appearing in the first three lines:

1. $\theta([U_{014}, U_{023}], U_{123}, \partial\langle 012 \rangle) = 0 \pmod{2\pi}$.
2. $\theta([U_{014}, U_{023}], U_{123}U_{124}, \partial\langle 024 \rangle) = 0 \pmod{2\pi}$.
3. $\theta([U_{014}, U_{023}], U_{134}, \partial\langle 034 \rangle) = 0 \pmod{2\pi}$.

Eq. (B15) is transformed to

$$\begin{aligned}
& \left(\theta(U_{023}, \partial\langle 012 \rangle + \partial\langle 123 \rangle) + \theta(U_{014}, \partial\langle 012 \rangle + \partial\langle 023 \rangle + \partial\langle 123 \rangle) \right. \\
& \quad \left. - \theta(U_{023}, \partial\langle 012 \rangle + \partial\langle 014 \rangle + \partial\langle 123 \rangle) - \theta(U_{014}, \partial\langle 012 \rangle + \partial\langle 123 \rangle) \right) \\
& + \left(\theta(U_{023}, \partial\langle 024 \rangle + \partial\langle 124 \rangle + \partial\langle 123 \rangle) + \theta(U_{014}, \partial\langle 024 \rangle + \partial\langle 023 \rangle + \partial\langle 124 \rangle + \partial\langle 123 \rangle) \right. \\
& \quad \left. - \theta(U_{023}, \partial\langle 024 \rangle + \partial\langle 014 \rangle + \partial\langle 124 \rangle + \partial\langle 123 \rangle) - \theta(U_{014}, \partial\langle 024 \rangle + \partial\langle 124 \rangle + \partial\langle 123 \rangle) \right) \\
& + \left(\theta(U_{023}, \partial\langle 034 \rangle + \partial\langle 134 \rangle) + \theta(U_{014}, \partial\langle 034 \rangle + \partial\langle 023 \rangle + \partial\langle 134 \rangle) \right. \\
& \quad \left. - \theta(U_{023}, \partial\langle 034 \rangle + \partial\langle 014 \rangle + \partial\langle 134 \rangle) - \theta(U_{014}, \partial\langle 034 \rangle + \partial\langle 134 \rangle) \right) \\
& + \left(\theta(U_{023}, \partial\langle 013 \rangle) + \theta(U_{014}, \partial\langle 013 \rangle + \partial\langle 023 \rangle) - \theta(U_{023}, \partial\langle 013 \rangle + \partial\langle 014 \rangle) - \theta(U_{014}, \partial\langle 013 \rangle) \right) \\
& = 0 \pmod{2\pi},
\end{aligned} \tag{B16}$$

where the terms with matched colors are completely canceled out in the last equality. Thus, we have demonstrated that Eq. (B14) indeed represents a valid locality identity.

Note that for the locality identity of each color or symbol, we have the freedom to multiply the overall minus sign, e.g., the locality identity on the yellow plaquettes in Eq. (B13) can be modified as:

$$\begin{aligned}
0 &= -\theta([U_{234}, [U_{012}, U_{013}], \partial\langle 023 \rangle) \\
&= -\theta(U_{012}^{-1}U_{013}^{-1}U_{012}U_{013}, \partial\langle 023 \rangle) - \theta(U_{013}^{-1}U_{012}^{-1}U_{013}U_{012}, \partial\langle 023 \rangle + \partial\langle 234 \rangle) \\
&= \theta(U_{013}^{-1}U_{012}^{-1}U_{013}U_{012}, \partial\langle 023 \rangle) + \theta(U_{012}^{-1}U_{013}^{-1}U_{012}U_{013}, \partial\langle 023 \rangle + \partial\langle 234 \rangle).
\end{aligned} \tag{B17}$$

The physical interpretation of this choice of locality identity is that it reverses the orientation of the yellow plaquettes in Fig. 10(b). This same argument applies to each symbol: we can simultaneously reverse the orientations of four plaquettes with the same symbol. We can derive different unitary sequences by altering the orientation of each color or symbol. However, all these sequences are equivalent, as they differ only by locality identities. Specifically, changing the orientation corresponds to adding (-2) times the locality identity, and the unitary sequence is the sum of all locality identities divided by 2. For example, by selecting a different orientation, we obtain the 36-step unitary sequence shown in Fig. 11, which exactly matches the sequence proposed in Ref. [44].

Finally, we used computers to enumerate all possible orientations for each locality identity. There are $2^{15} = 32768$ different configurations, corresponding to the three symbols and twelve colors. Our computations verified that the minimal number of steps required is 24. Therefore, the unitary sequence presented in Fig. 10 is optimal, meaning there is no shorter sequence capable of detecting the loop statistics.

Appendix C: Detailed analysis on the structure of E_{id}

Here we show the following statement. Suppose we have an invariant Θ in E_{inv} for an Abelian symmetry group G , expressed as

$$e^{i\Theta} = \langle a | U(s_n)^\pm \dots U(s_1)^\pm | a \rangle. \tag{C1}$$

Let us pick any element $s_0 \in \mathcal{S}$. Then the following ratio is an element of E_{id} :

$$e^{i\Phi} = \frac{\langle a | U(s_n)^\pm \dots U(s_1)^\pm | a \rangle}{\langle a + \partial s_0 | U(s_n)^\pm \dots U(s_1)^\pm | a + \partial s_0 \rangle}. \tag{C2}$$

In other words, we show that the phase $e^{i\Phi}$ can be expressed as the product of higher commutators of the form

$$\begin{aligned}
& \langle a' | [[U(s'_1), U(s'_2)], \dots], U(s'_m) | a' \rangle = 1, \\
& a' \in \mathcal{A}, s'_1, s'_2, \dots, s'_m \in \mathcal{S} | s'_1 \cap s'_2 \cap \dots \cap s'_m = \emptyset,
\end{aligned} \tag{C3}$$

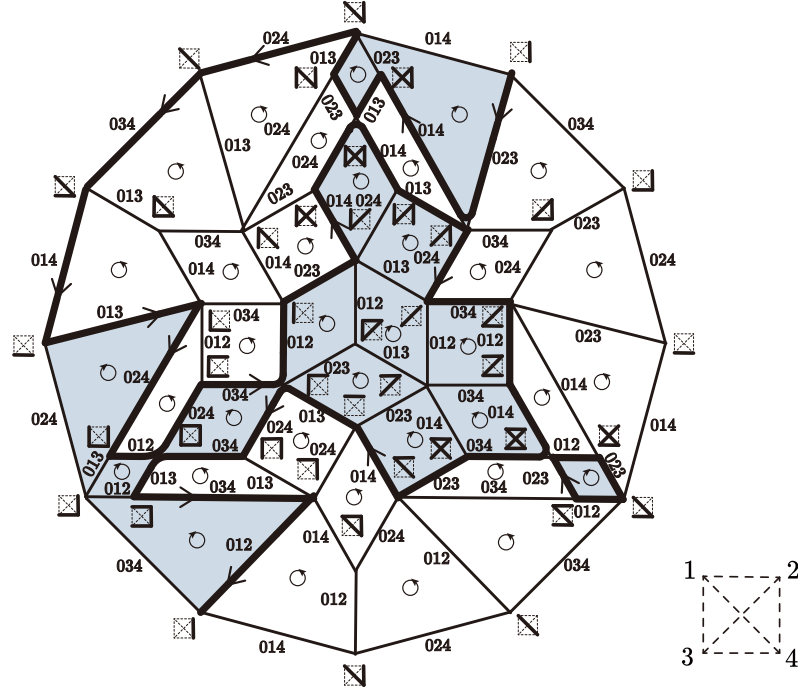


FIG. 11. The 36-step unitary sequence corresponding to \mathbb{Z}_2 loop statistics in (3+1)D. Compared to Fig. 10(b), the orientations of certain locality identities have been reversed. Any choice of orientation for each locality identity yields a valid sequence for detecting the loop statistics. This particular orientation corresponds to the 36-step process proposed in Ref. [44], where a different computational method was used to derive the sequence.

which is called the locality identity in the main text. Throughout the proof, we assume that X is a triangulation of a sphere.

We first rewrite the phase Φ in the following fashion:

$$\begin{aligned} \Phi &= \sum_{j=0}^{n-1} \theta(U(s_{j+1})^\pm, a + t_j) - \theta(U(s_{j+1})^\pm, a + \partial s_0 + t_j) \\ &= \sum_{j=0}^{n-1} \theta(U(s_{j+1})^\pm, a + t_j) - \theta(U(s_{j+1})^\pm, a + \partial s_0 + t_j) + \theta(U(s_0), a + t_{j+1}) - \theta(U(s_0), a + t_j), \end{aligned} \quad (\text{C4})$$

where $t_j = \sum_{k=1}^j \pm \partial s_k$. In the second equation, we used $t_n = t_0 = 0$. Noting that

$$\begin{aligned} &\arg(\langle a | [U(s_2), U(s_1)] | a \rangle) \\ &= \theta(s_1, a) + \theta(s_2, a + \partial s_1) - \theta(s_1, a + \partial s_2) - \theta(s_2, a), \end{aligned} \quad (\text{C5})$$

and $\theta(U(s), a) = -\theta(U(s)^{-1}, a + \partial s)$, we get

$$\Phi = \sum_{j=0}^{n-1} \langle a + t_j | [U(s_0), U(s_{j+1})] | a + t_j \rangle + \sum_{j=0}^{n-1} \langle a + t_{j+1} | [U(s_0), U(s_{j+1})]^{-1} | a + t_{j+1} \rangle, \quad (\text{C6})$$

where the sum breaks into the two parts depending on the sign on $U(s_j)^\pm$. Let us fix an element $s \in \mathcal{S}$. In the expression (C6), let us collect the commutators involving $U(s_j)^\pm$ with $s_j = s$. Focusing on these commutators, the sum is schematically written as

$$\Phi = \sum_{a'} \langle a' | [U(s_0), U(s)]^\pm | a' \rangle + \dots, \quad (\text{C7})$$

where \dots denotes the commutators involving $s_j \neq s$. If $\text{supp}(s_0) \cap \text{supp}(s) = \emptyset$, the commutator can be regarded as the locality identity. Hence we assume $\text{supp}(s_0) \cap \text{supp}(s')$ is nontrivial.

Let us first study the case with $s_0 \neq s'$. For $a', b' \in \mathcal{A}$, if $a' = b'$ at $\text{supp}(s_0) \cap \text{supp}(s')$, there exists $s_{ab} \in \mathcal{S}$ satisfying $U(s_{ab})|a'\rangle = |b'\rangle$ and $\text{supp}(s_0) \cap \text{supp}(s') \cap \text{supp}(s_{ab}) = \emptyset$. In that case one can convert a' into b' by the locality identity:

$$\frac{\langle a'| [U(s_0), U(s)]^\pm |a'\rangle}{\langle b'| [U(s_0), U(s)]^\pm |b'\rangle} = \langle [U(s_{ab}), [U(s_0), U(s)]^\pm] \rangle = 1. \quad (\text{C8})$$

This implies that the phase Φ in Eq. (C7) depends on a' only through the configuration of a' in the vicinity of the mutual support $\text{supp}(s_0) \cap \text{supp}(s)$. Concretely, the configuration of a' near the mutual support of the unitaries can be specified as follows. The mutual support $\text{supp}(s_0) \cap \text{supp}(s)$ generally becomes a p -simplex σ_p . Pick $(p+1)$ vertices v_0, \dots, v_p of this p -simplex σ_p . Then, a' in the expression (C7) can be represented by a $(p+1)$ -tuple of the restricted configurations $(a'|_{v_0}, \dots, a'|_{v_p})$. In other words, we can replace $|a'\rangle$ with a canonical representative of the state $|(a'|_{v_0}, \dots, a'|_{v_p})\rangle$ in \mathcal{A} whose restriction to vertices become the fixed ones. This can be done by using the locality identity, and leaves the value of Φ invariant.

Let us write the set of restricted configurations $a|_{v_j}$ as \mathcal{A}_{v_j} . We also introduce a shorthand notation $a|_{v_j} = \alpha_j$. We can express Φ as

$$\Phi = \sum_{\oplus_j \mathcal{A}_{v_j}} \epsilon_+(s, \{\alpha_j\}) \langle \{\alpha_j\} | [U(s_0), U(s)] | \{\alpha_j\} \rangle + \sum_{\oplus_j \mathcal{A}_{v_j}} \epsilon_-(s, \{\alpha_j\}) \langle \{\alpha_j\} | [U(s_0), U(s)]^{-1} | \{\alpha_j\} \rangle, \quad (\text{C9})$$

where ϵ_\pm is the positive integer coefficient counting the number of the commutator $\langle \{\alpha_j\} | [U(s_0), U(s)]^\pm | \{\alpha_j\} \rangle$ appears in the sum of Φ . Let us define ϵ as

$$\epsilon(s, \{\alpha_j\}) = \epsilon_+(s, \{\alpha_j\}) - \epsilon_-(s, \{\alpha_j\}). \quad (\text{C10})$$

Then, due to the condition of E_{inv} shown in Eq. (27) satisfied by the invariant Θ , ϵ satisfies

$$\sum_{\oplus_{j \neq k} \mathcal{A}_{v_j}} \epsilon(s, (\alpha_0, \dots, \alpha_p)) = 0, \quad (\text{C11})$$

for any $\alpha_k \in \mathcal{A}_{v_k}$, and any $0 \leq k \leq p$. The sum is over $\alpha_j \in \mathcal{A}_{v_j}$ with $j \neq k$ while α_k is fixed. Further, once we fix a choice of α_{v_k} , it fixes the configuration of the excitation at the p -simplex σ_p which we write a_{σ_p} . Then ϵ is nonzero iff $\alpha_0, \dots, \alpha_p$ all specify the same a_{σ_p} at σ_p . This allows us to write a refined version of Eq. (C11) as

$$\sum_{\oplus_{j \neq k} \mathcal{A}_{v_j}(a_{\sigma_p})} \epsilon(s, (\alpha_0, \dots, \alpha_p)) = 0, \quad (\text{C12})$$

where we defined $\mathcal{A}_{v_j}(a_{\sigma_p}) \subset \mathcal{A}_{v_j}$ as a set of α_j which has the fixed configuration a_{σ_p} at the simplex σ_p .

Eq. (C12) gives a number of constraints on $\epsilon(s, \{\alpha_j\})$. One can show that the solution to Eq. (C12) is generated by the following (overcomplete) basis; let us pick a pair of elements $\alpha_j^{(0)}, \alpha_j^{(1)}$ from each $\mathcal{A}_{v_j}(a_{\sigma_p})$. Then, the basis is given by

$$\epsilon(s, \{\alpha_j^{(n_j)}\}) = (-1)^{\sum_j n_j}, \quad (\text{C13})$$

with $n_j = 0, 1$, with the other ϵ zero.

Let us show that the basis (C13) corresponds to the trivial phase due to the locality identity. To see this, take a unitary $U(s_{\alpha_k})$ that shifts $\alpha_k^{(0)}$ to $\alpha_k^{(1)}$, but leaves the other α_j with $j \neq k$ invariant. Note that the mutual support of the unitaries $\text{supp}(s_0) \cap \text{supp}(s) \cap \text{supp}(s_{\alpha_k})$ becomes a 0-simplex v_k . In particular, this implies that

$$\left(\bigcap_{j=0}^p \text{supp}(s_{\alpha_j}) \right) \cap \text{supp}(s_0) \cap \text{supp}(s) = \emptyset. \quad (\text{C14})$$

Now, the basis (C13) corresponds to the invariant given by the following higher commutator:

$$\langle \{\alpha_j^{(0)}\} | [U(s_{\alpha_0}), [\dots, [U(s_{\alpha_p}), [U(s_0), U(s)]]]] | \{\alpha_j^{(0)}\} \rangle, \quad (\text{C15})$$

so each basis corresponds to the locality identity. Noticing this for each choice of a_{σ_p} at σ_p completes the proof for $s_0 \neq s'$.

When $s_0 = s'$, the proof is done in a similar logic: the difference is that the support of $[U(s_0), U(s)]$ is given by $\partial(\text{supp}(s))$, so we need to take $p+2$ vertices of a $(p+1)$ -simplex s to fix the configuration of excitations in the vicinity of the operator support. Let us write these vertices as v_0, \dots, v_{p+1} . The boundary $p+1$ -simplices of s are written as $\sigma_{\hat{0}}, \dots, \sigma_{\hat{p+1}}$, where $\sigma_{\hat{j}}$ does not contain the vertex v_j . We again write the set of restricted configurations $a|_{v_j} = \alpha_j$ as \mathcal{A}_{v_j} , with $0 \leq j \leq p+1$. One can again express Φ as

$$\Phi = \sum_{\bigoplus_j \mathcal{A}_{v_j}} \epsilon_+(s, \{\alpha_j\}) \langle \{\alpha_j\} | [U(s_0), U(s)] | \{\alpha_j\} \rangle + \sum_{\bigoplus_j \mathcal{A}_{v_j}} \epsilon_-(s, \{\alpha_j\}) \langle \{\alpha_j\} | [U(s_0), U(s)]^{-1} | \{\alpha_j\} \rangle, \quad (\text{C16})$$

where ϵ_{\pm} is the positive integer coefficient counting the number of the given commutator appears in the sum of Φ . We again define ϵ as

$$\epsilon(\{\alpha_j\}) = \epsilon_+(s, \{\alpha_j\}) - \epsilon_-(s, \{\alpha_j\}). \quad (\text{C17})$$

where we suppressed the dependence on s . Then, due to the condition of E_{inv} in Eq. (27) satisfied by the invariant Θ , ϵ satisfies

$$\sum_{\bigoplus_{j \neq k} \mathcal{A}_{v_j}} \epsilon(\alpha_0, \dots, \alpha_{p+1}) = 0, \quad (\text{C18})$$

for any $\alpha_k \in \mathcal{A}_{v_k}$, and any $0 \leq k \leq p+1$. The sum is over $\alpha_j \in \mathcal{A}_{v_j}$ with $j \neq k$ while α_k is fixed. Once we fix the restricted configuration α_k , it fixes the configuration of the excitation a at p -simplices $\{\sigma_{\hat{j}}\}$ except for $\sigma_{\hat{k}}$.

Let us define the set $\mathcal{A}_{v_k}(\{a_{\sigma_{\hat{j}}}\}) \subset \mathcal{A}_{v_k}$ as a set of α_k which has the fixed configurations of excitations $\{a_{\sigma_{\hat{j}}}\}$ at the p -simplices $\sigma_{\hat{0}}, \dots, \sigma_{\hat{p+1}}$ of s . Note that this set does not depend on $a_{\sigma_{\hat{k}}}$.

One can show that the solution to Eq. (C18) is generated by the following basis:

1. Let us fix a configuration of excitations $\{a_{\sigma_{\hat{j}}}\}$ at the p -simplices of s , and consider $\mathcal{A}_{v_k}(\{a_{\sigma_{\hat{j}}}\})$. Let us pick two elements $\alpha_k^{(0)}, \alpha_k^{(1)} \in \mathcal{A}_{v_k}(\{a_{\sigma_{\hat{j}}}\})$ for each $0 \leq k \leq p+1$. Then, the basis is given by

$$\epsilon(\{\alpha_j^{(n_j)}\}) = (-1)^{\sum_j n_j}, \quad (\text{C19})$$

with $n_j = 0, 1$, with the other ϵ zero.

2. Let us fix a choice of the vertex v_k . Take two configurations of the excitations $\{a_{\sigma_{\hat{j}}}\}, \{a'_{\sigma_{\hat{j}}}\}$, where $a_{\sigma_{\hat{j}}} = a'_{\sigma_{\hat{j}}}$ for $j \neq k$. Pick two elements $\alpha_k^{(0)}, \alpha_k^{(1)} \in \mathcal{A}_{v_k}(\{a_{\sigma_{\hat{j}}}\})$. Note that $\alpha_k^{(0)}, \alpha_k^{(1)} \in \mathcal{A}_{v_k}(\{a'_{\sigma_{\hat{j}}}\})$. For $l \neq k$, let us pick a set of elements $\{\alpha_l\}_{l \neq k}, \{\alpha'_l\}_{l \neq k}$ from $\{\mathcal{A}_{v_l}(\{a_{\sigma_{\hat{j}}}\})\}_{l \neq k}, \{\mathcal{A}_{v_l}(\{a'_{\sigma_{\hat{j}}}\})\}_{l \neq k}$. Then, the basis is given by

$$\begin{aligned} \epsilon(\alpha_k^{(0)}, \{\alpha_l\}_{l \neq k}) &= 1, \\ \epsilon(\alpha_k^{(1)}, \{\alpha_l\}_{l \neq k}) &= -1, \\ \epsilon(\alpha_k^{(0)}, \{\alpha'_l\}_{l \neq k}) &= -1, \\ \epsilon(\alpha_k^{(1)}, \{\alpha'_l\}_{l \neq k}) &= 1, \end{aligned} \quad (\text{C20})$$

with the other ϵ zero.

3. For each p -simplex $\sigma_{\hat{j}}$, let us take a pair of configurations of excitation $a_{\sigma_{\hat{j}}}^{(0)}, a_{\sigma_{\hat{j}}}^{(1)}$. For each configuration $\{a_{\sigma_{\hat{j}}}^{(n_j)}\}$ at p -simplices, we choose a single excitation configuration $\{\alpha_j\}_{\{n_j\}} \in \mathcal{A}(\{a_{\sigma_{\hat{j}}}^{(n_j)}\})$. These excitation configurations are chosen so that when $n_j = n'_j$ for $j \neq k$, we have $(\alpha_k)_{\{n_j\}} = (\alpha_k)_{\{n'_j\}}$. Then, the basis is given by

$$\epsilon(\{\alpha_j\}_{\{n_j\}}) = (-1)^{\sum_j n_j}. \quad (\text{C21})$$

Each type of the basis (C19) corresponds to the higher commutators:

1. For the first type of the basis, let us take a unitary $U(s_{\alpha_k})$ that transforms $\alpha_k^{(0)}$ into $\alpha_k^{(1)}$, leaving the other $\{\alpha_j\}$ invariant. Note that the mutual support of the unitaries $\text{supp}(s) \cap \text{supp}(s_{\alpha_k})$ becomes a 0-simplex v_k . In particular, this implies that

$$\left(\bigcap_{j=0}^{p+1} \text{supp}(s_{\alpha_j}) \right) \cap \text{supp}(s) = \emptyset. \quad (\text{C22})$$

Now, the basis (C19) corresponds to the invariant given by the following higher commutator:

$$\langle \{\alpha_j^{(0)}\} \left| [U(s_{\alpha_0}), [\dots, [U(s_{\alpha_{p+1}}), [U(s_0), U(s)]]]] \right| \{\alpha_j^{(0)}\} \rangle . \quad (\text{C23})$$

2. For the second type of the basis (C20), let us take a unitary $U(s_{\alpha_k})$ that transforms $\alpha_k^{(0)}$ into $\alpha_k^{(1)}$, leaving the other $\{\alpha_j\}$ invariant. Let us also take a unitary $U(s_{\hat{k}})$ that transforms $\{\alpha_l\}_{l \neq k}$ into $\{\alpha'_l\}_{l \neq k}$, leaving α_k invariant. The mutual support of the unitaries becomes $\text{supp}(s_{\alpha_k}) \cap \text{supp}(s) = v_k$, $\text{supp}(s_{\hat{k}}) \cap \text{supp}(s) = \sigma_{\hat{k}}$. We then have

$$\text{supp}(s_{\alpha_k}) \cap \text{supp}(s_{\hat{k}}) \cap \text{supp}(s) = \emptyset . \quad (\text{C24})$$

The basis (C20) corresponds to the invariant given by the following higher commutator:

$$\langle \alpha_k^{(0)}, \{\alpha_l\}_{l \neq k} \left| [U(s_{\alpha_k}), [U(s_{\hat{k}}), [U(s_0), U(s)]]] \right| \alpha_k^{(0)}, \{\alpha_l\}_{l \neq k} \rangle . \quad (\text{C25})$$

3. For the third type of the basis (C21), let us take a unitary $U(s_{\hat{k}})$ that transforms $\{\alpha_j\}_{\{n_j\}}$ into $\{\alpha_j\}_{\{n'_j\}}$, with $n'_k = n_k + 1 \pmod{2}$, and $n_j = n'_j$ with $j \neq k$. Note that the mutual support $\text{supp}(s) \cap \text{supp}(s_{\hat{k}})$ becomes a p -simplex $\sigma_{\hat{k}}$. This implies that

$$\left(\bigcap_{j=0}^{p+1} \text{supp}(s_j) \right) \cap \text{supp}(s) = \emptyset . \quad (\text{C26})$$

The basis (C21) corresponds to the invariant given by the following higher commutator:

$$\langle \{\alpha_j\}_{\{n_j=0\}} \left| [U(s_{\hat{0}}), [\dots, [U(s_{\widehat{p+1}}), [U(s_0), U(s)]]]] \right| \{\alpha_j\}_{\{n_j=0\}} \rangle . \quad (\text{C27})$$

This completes the proof that Φ is given by linear combinations of the locality identities.

-
- [1] S.N. Bose, “Plancks gesetz und lichtquantenhypothese,” *Zeitschrift für Physik* **26**, 178–181 (1924).
- [2] A. Einstein, “Quantentheorie des einatomigen idealen gases,” *Albert Einstein: Akademie-Vorträge*, 237–244 (2005).
- [3] L. Landau, “Theory of the Superfluidity of Helium II,” *Phys. Rev.* **60**, 356–358 (1941).
- [4] L. Onsager, “Statistical hydrodynamics,” *Il Nuovo Cimento (1943-1954)* **6**, 279–287 (1949).
- [5] V. L. Ginzburg and L. D. Landau, “On the Theory of superconductivity,” *Zh. Eksp. Teor. Fiz.* **20**, 1064–1082 (1950).
- [6] J. Bardeen, L. N. Cooper, and J. R. Schrieffer, “Theory of superconductivity,” *Phys. Rev.* **108**, 1175–1204 (1957).
- [7] Zheng-Cheng Gu and Xiao-Gang Wen, “Symmetry-protected topological orders for interacting fermions: Fermionic topological nonlinear σ models and a special group supercohomology theory,” *Phys. Rev. B* **90**, 115141 (2014).
- [8] Davide Gaiotto and Anton Kapustin, “Spin TQFTs and fermionic phases of matter,” *Int. J. Mod. Phys. A* **31**, 1645044 (2016), arXiv:1505.05856 [cond-mat.str-el].
- [9] Lakshya Bhardwaj, Davide Gaiotto, and Anton Kapustin, “State sum constructions of spin-TFTs and string net constructions of fermionic phases of matter,” *JHEP* **04**, 096 (2017), arXiv:1605.01640 [cond-mat.str-el].
- [10] Maissam Barkeshli, Yu-An Chen, Po-Shen Hsin, and Naren Manjunath, “Classification of (2 + 1)d invertible fermionic topological phases with symmetry,” *Phys. Rev. B* **105**, 235143 (2022).
- [11] Frank Wilczek, “Quantum mechanics of fractional-spin particles,” *Phys. Rev. Lett.* **49**, 957–959 (1982).
- [12] R. B. Laughlin, “Anomalous quantum hall effect: An incompressible quantum fluid with fractionally charged excitations,” *Phys. Rev. Lett.* **50**, 1395–1398 (1983).
- [13] Horst L. Stormer, “Nobel lecture: The fractional quantum hall effect,” *Rev. Mod. Phys.* **71**, 875–889 (1999).
- [14] Gregory Moore and Nicholas Read, “Nonabelions in the fractional quantum hall effect,” *Nuclear Physics B* **360**, 362–396 (1991).
- [15] Michael H. Freedman, Michael Larsen, and Zhenghan Wang, “A modular functor which is universal for quantum computation,” *Communications in Mathematical Physics* **227**, 605–622 (2002).
- [16] Michael Freedman, Alexei Kitaev, Michael Larsen, and Zhenghan Wang, “Topological quantum computation,” *Bulletin of the American Mathematical Society* **40**, 31–38 (2003).

- [17] A.Yu. Kitaev, “Fault-tolerant quantum computation by anyons,” *Annals of Physics* **303**, 2–30 (2003).
- [18] Chetan Nayak, Steven H. Simon, Ady Stern, Michael Freedman, and Sankar Das Sarma, “Non-abelian anyons and topological quantum computation,” *Rev. Mod. Phys.* **80**, 1083–1159 (2008).
- [19] Edward Witten, “Quantum field theory and the jones polynomial,” *Communications in Mathematical Physics* **121**, 351–399 (1989).
- [20] Alexei Kitaev, “Anyons in an exactly solved model and beyond,” *Annals Phys.* **321**, 2–111 (2006).
- [21] Alexei Kitaev and Liang Kong, “Models for gapped boundaries and domain walls,” *Communications in Mathematical Physics* **313**, 351–373 (2012).
- [22] Liang Kong, “Anyon condensation and tensor categories,” *Nuclear Physics B* **886**, 436–482 (2014).
- [23] Maissam Barkeshli, Parsa Bonderson, Meng Cheng, and Zhenghan Wang, “Symmetry fractionalization, defects, and gauging of topological phases,” *Phys. Rev. B* **100**, 115147 (2019).
- [24] Michael A. Levin and Xiao-Gang Wen, “String-net condensation: A physical mechanism for topological phases,” *Phys. Rev. B* **71**, 045110 (2005).
- [25] Eric C. Rowell, “From quantum groups to unitary modular tensor categories,” (2006), [arXiv:math/0503226](https://arxiv.org/abs/math/0503226) [[math.QA](https://arxiv.org/abs/math/0503226)].
- [26] “On classification of modular tensor categories,” *Communications in Mathematical Physics* **292**, 343–389 (2009).
- [27] Liang Wang and Zhenghan Wang, “In and around abelian anyon models*,” *Journal of Physics A: Mathematical and Theoretical* **53**, 505203 (2020).
- [28] Julia Plavnik, Andrew Schopieray, Zhiqiang Yu, and Qing Zhang, “Modular tensor categories, subcategories, and galois orbits,” *Transformation Groups* (2023), [10.1007/s00031-022-09787-9](https://doi.org/10.1007/s00031-022-09787-9).
- [29] Chenjie Wang and Michael Levin, “Braiding statistics of loop excitations in three dimensions,” *Phys. Rev. Lett.* **113**, 080403 (2014).
- [30] Shenghan Jiang, Andrej Mesáros, and Ying Ran, “Generalized modular transformations in $(3+1)D$ topologically ordered phases and triple linking invariant of loop braiding,” *Phys. Rev. X* **4**, 031048 (2014).
- [31] Chao-Ming Jian and Xiao-Liang Qi, “Layer construction of 3d topological states and string braiding statistics,” *Phys. Rev. X* **4**, 041043 (2014).
- [32] Juven C. Wang, Zheng-Cheng Gu, and Xiao-Gang Wen, “Field-theory representation of gauge-gravity symmetry-protected topological invariants, group cohomology, and beyond,” *Phys. Rev. Lett.* **114**, 031601 (2015).
- [33] Chenjie Wang, Chien-Hung Lin, and Michael Levin, “Bulk-boundary correspondence for three-dimensional symmetry-protected topological phases,” *Phys. Rev. X* **6**, 021015 (2016).
- [34] Peng Ye and Zheng-Cheng Gu, “Topological quantum field theory of three-dimensional bosonic abelian-symmetry-protected topological phases,” *Phys. Rev. B* **93**, 205157 (2016).
- [35] Pavel Putrov, Juven Wang, and Shing-Tung Yau, “Braiding statistics and link invariants of bosonic/fermionic topological quantum matter in 2+1 and 3+1 dimensions,” *Annals of Physics* **384**, 254–287 (2017).
- [36] AtMa P. O. Chan, Peng Ye, and Shinsei Ryu, “Braiding with borromean rings in $(3+1)$ -dimensional spacetime,” *Phys. Rev. Lett.* **121**, 061601 (2018).
- [37] Qing-Rui Wang, Meng Cheng, Chenjie Wang, and Zheng-Cheng Gu, “Topological quantum field theory for abelian topological phases and loop braiding statistics in $(3+1)$ -dimensions,” *Phys. Rev. B* **99**, 235137 (2019).
- [38] Zhi-Feng Zhang and Peng Ye, “Compatible braidings with hopf links, multiloop, and borromean rings in $(3+1)$ -dimensional spacetime,” *Phys. Rev. Res.* **3**, 023132 (2021).
- [39] Zhi-Feng Zhang and Peng Ye, “Topological orders, braiding statistics, and mixture of two types of twisted bf theories in five dimensions,” *Journal of High Energy Physics* **2022**, 138 (2022).
- [40] Zhi-Feng Zhang, Qing-Rui Wang, and Peng Ye, “Continuum field theory of three-dimensional topological orders with emergent fermions and braiding statistics,” *Phys. Rev. Res.* **5**, 043111 (2023).
- [41] Ryan Thorngren, “Framed Wilson Operators, Fermionic Strings, and Gravitational Anomaly in 4d,” *JHEP* **02**, 152 (2015), [arXiv:1404.4385](https://arxiv.org/abs/1404.4385) [[hep-th](https://arxiv.org/abs/1404.4385)].
- [42] Po-Shen Hsin, Wenjie Ji, and Chao-Ming Jian, “Exotic Invertible Phases with Higher-Group Symmetries,” (2021), [arXiv:2105.09454](https://arxiv.org/abs/2105.09454) [[cond-mat.str-el](https://arxiv.org/abs/2105.09454)].
- [43] Yu-An Chen and Po-Shen Hsin, “Exactly solvable lattice Hamiltonians and gravitational anomalies,” *SciPost Phys.* **14**, 089 (2023).
- [44] Lukasz Fidkowski, Jeongwan Haah, and Matthew B. Hastings, “Gravitational anomaly of $(3+1)$ -dimensional F_2 toric code with fermionic charges and fermionic loop self-statistics,” *Phys. Rev. B* **106**, 165135 (2022).
- [45] Srivatsa Tata, Ryohei Kobayashi, Daniel Bulmash, and Maissam Barkeshli, “Anomalies in $(2+1)d$ fermionic topological phases and $(3+1)d$ path integral state sums for fermionic spts,” *Communications in Mathematical Physics* **397**, 199–336 (2022).
- [46] Ryohei Kobayashi, Kantaro Ohmori, and Yuji Tachikawa, “On gapped boundaries for spt phases beyond group cohomology,” *Journal of High Energy Physics* **2019** (2019), [10.1007/jhep11\(2019\)131](https://doi.org/10.1007/jhep11(2019)131).
- [47] Theo Johnson-Freyd, “ $(3+1)D$ topological orders with only a \mathbb{Z}_2 -charged particle,” *arXiv preprint* [arXiv:2011.11165](https://arxiv.org/abs/2011.11165) (2020).
- [48] Yu-An Chen and Sri Tata, “Higher cup products on hypercubic lattices: Application to lattice models of topological phases,” *Journal of Mathematical Physics* **64**, 091902 (2023).
- [49] Po-Shen Hsin, Ho Tat Lam, and Nathan Seiberg, “Comments on one-form global symmetries and their gauging in 3d and 4d,” *SciPost Phys.* **6**, 039 (2019).
- [50] Yu-Xin Yang, Meng Cheng, and Ji-Yao Chen, “Chiral spin liquid in a generalized kitaev honeycomb model with z_4 1-form symmetry,” *arXiv preprint* [arXiv:2408.02046](https://arxiv.org/abs/2408.02046) (2024).
- [51] Michael Levin and Zheng-Cheng Gu, “Braiding statistics approach to symmetry-protected topological phases,” *Phys. Rev. B* **86**, 115109 (2012).
- [52] Tyler D. Ellison, Yu-An Chen, Arpit Dua, Wilbur Shirley, Nathanan Tantivasadakarn, and Dominic J. Williamson, “Pauli stabilizer models of twisted quantum doubles,” *PRX Quantum* **3**, 010353 (2022).
- [53] Tyler D. Ellison, Yu-An Chen, Arpit Dua, Wilbur Shirley, Nathanan Tantivasadakarn, and Dominic J.

- Williamson, “Pauli topological subsystem codes from Abelian anyon theories,” *Quantum* **7**, 1137 (2023).
- [54] Wilbur Shirley, Yu-An Chen, Arpit Dua, Tyler D. Ellison, Nathanan Tantivasadakarn, and Dominic J. Williamson, “Three-dimensional quantum cellular automata from chiral semion surface topological order and beyond,” *PRX Quantum* **3**, 030326 (2022).
- [55] Li-Mei Chen, Tyler D. Ellison, Meng Cheng, Peng Ye, and Ji-Yao Chen, “Chiral spin liquid in a F_3 kitaev model,” *Phys. Rev. B* **109**, 155161 (2024).
- [56] Blazej Ruba and Bowen Yang, “Homological invariants of pauli stabilizer codes,” *Communications in Mathematical Physics* **405**, 126 (2024).
- [57] Zijian Liang, Yijia Xu, Joseph T. Iosue, and Yu-An Chen, “Extracting topological orders of generalized pauli stabilizer codes in two dimensions,” *PRX Quantum* **5**, 030328 (2024).
- [58] Zijian Liang, Bowen Yang, Joseph T Iosue, and Yu-An Chen, “Operator algebra and algorithmic construction of boundaries and defects in $(2+1)$ d topological pauli stabilizer codes,” arXiv preprint arXiv:2410.11942 (2024).
- [59] Michael Levin and Xiao-Gang Wen, “Fermions, strings, and gauge fields in lattice spin models,” *Phys. Rev. B* **67**, 245316 (2003).
- [60] Kyle Kawagoe and Michael Levin, “Microscopic definitions of anyon data,” *Phys. Rev. B* **101**, 115113 (2020).
- [61] Qing-Rui Wang and Meng Cheng, Unpublished note.
- [62] Anton Kapustin and Ryan Thorngren, “Higher Symmetry and Gapped Phases of Gauge Theories,” *Prog. Math.* **324**, 177–202 (2017), arXiv:1309.4721 [hep-th].
- [63] Francesco Benini, Clay Córdova, and Po-Shen Hsin, “On 2-Group Global Symmetries and their Anomalies,” *JHEP* **03**, 118 (2019), arXiv:1803.09336 [hep-th].
- [64] Maissam Barkeshli, Yu-An Chen, Po-Shen Hsin, and Ryohei Kobayashi, “Higher-group symmetry in finite gauge theory and stabilizer codes,” *SciPost Physics* **16** (2024), 10.21468/scipostphys.16.4.089.
- [65] Elliott H. Lieb and Derek W. Robinson, “The finite group velocity of quantum spin systems,” *Communications in Mathematical Physics* **28**, 251 – 257 (1972).
- [66] Matthew B. Hastings and Tohru Koma, “Spectral gap and exponential decay of correlations,” *Commun. Math. Phys.* **265**, 781–804 (2006), arXiv:math-ph/0507008.
- [67] Elliott Lieb, Theodore Schultz, and Daniel Mattis, “Two soluble models of an antiferromagnetic chain,” *Annals of Physics* **16**, 407–466 (1961).
- [68] Masaki Oshikawa, “Commensurability, excitation gap, and topology in quantum many-particle systems on a periodic lattice,” *Phys. Rev. Lett.* **84**, 1535–1538 (2000).
- [69] M. B. Hastings, “Lieb-schultz-mattis in higher dimensions,” *Physical Review B* **69** (2004), 10.1103/physrevb.69.104431.
- [70] Ryohei Kobayashi, Ken Shiozaki, Yuta Kikuchi, and Shinsei Ryu, “Lieb-schultz-mattis type theorem with higher-form symmetry and the quantum dimer models,” *Physical Review B* **99** (2019), 10.1103/physrevb.99.014402.
- [71] Dominic V. Else and Ryan Thorngren, “Topological theory of lieb-schultz-mattis theorems in quantum spin systems,” *Phys. Rev. B* **101**, 224437 (2020).
- [72] Meng Cheng and Nathan Seiberg, “Lieb-Schultz-Mattis, Luttinger, and ’t Hooft - anomaly matching in lattice systems,” *SciPost Phys.* **15**, 051 (2023), arXiv:2211.12543 [cond-mat.str-el].
- [73] Sahand Seifnashri, “Lieb-schultz-mattis anomalies as obstructions to gauging (non-on-site) symmetries,” *SciPost Physics* **16** (2024), 10.21468/scipostphys.16.4.098.
- [74] Robbert Dijkgraaf and Edward Witten, “Topological Gauge Theories and Group Cohomology,” *Commun. Math. Phys.* **129**, 393 (1990).
- [75] Xie Chen, Zheng-Cheng Gu, Zheng-Xin Liu, and Xiao-Gang Wen, “Symmetry protected topological orders and the group cohomology of their symmetry group,” *Phys. Rev. B* **87**, 155114 (2013), arXiv:1106.4772 [cond-mat.str-el].
- [76] Dominic V. Else and Chetan Nayak, “Classifying symmetry-protected topological phases through the anomalous action of the symmetry on the edge,” *Phys. Rev. B* **90**, 235137 (2014).
- [77] Chenjie Wang and Michael Levin, “Topological invariants for gauge theories and symmetry-protected topological phases,” *Phys. Rev. B* **91**, 165119 (2015).
- [78] Nathanan Tantivasadakarn, “Dimensional reduction and topological invariants of symmetry-protected topological phases,” *Phys. Rev. B* **96**, 195101 (2017).
- [79] Carolyn Zhang, “Topological invariants for symmetry-protected topological phase entanglers,” *Phys. Rev. B* **107**, 235104 (2023).
- [80] Yu-An Chen, Anton Kapustin, and Djordje Radicević, “Exact bosonization in two spatial dimensions and a new class of lattice gauge theories,” *Annals Phys.* **393**, 234–253 (2018).
- [81] Yu-An Chen and Anton Kapustin, “Bosonization in three spatial dimensions and a 2-form gauge theory,” *Phys. Rev. B* **100**, 245127 (2019).
- [82] Tyler D. Ellison and Lukasz Fidkowski, “Disentangling interacting symmetry-protected phases of fermions in two dimensions,” *Phys. Rev. X* **9**, 011016 (2019).
- [83] Yu-An Chen, “Exact bosonization in arbitrary dimensions,” *Phys. Rev. Research* **2**, 033527 (2020).
- [84] Yu-An Chen, Tyler D. Ellison, and Nathanan Tantivasadakarn, “Disentangling supercohomology symmetry-protected topological phases in three spatial dimensions,” *Phys. Rev. Research* **3**, 013056 (2021).
- [85] Yu-An Chen and Yijia Xu, “Equivalence between fermion-to-qubit mappings in two spatial dimensions,” *PRX Quantum* **4**, 010326 (2023).
- [86] Clay Córdova, Daniel S. Freed, and Constantin Teleman, “Gapped theories have torsion anomalies,” (2024), arXiv:2408.15148 [hep-th].
- [87] James R. Munkres, *Topology: a First Course* (Prentice-Hall, Inc., 1975) section 7-9.
- [88] Jean-Louis Loday, *Cyclic Homology*, 2nd ed., Grundlehren der mathematischen Wissenschaften (Springer Berlin, Heidelberg, 1997) pp. XIX, 516, chapter 13, section 2.
- [89] Xinping Yang and Meng Cheng, “Gapped boundary of $(4+1)$ d beyond-cohomology bosonic spt phase,” *Phys. Rev. B* **110**, 045137 (2024).
- [90] S. Bravyi, M. B. Hastings, and F. Verstraete, “Lieb-robinson bounds and the generation of correlations and topological quantum order,” *Physical Review Letters* **97** (2006), 10.1103/physrevlett.97.050401.
- [91] Dorit Aharonov and Yonathan Touati, “Quantum circuit depth lower bounds for homological codes,” (2018), arXiv:1810.03912 [quant-ph].
- [92] Zhi Li, Dongjin Lee, and Beni Yoshida, “How

- much entanglement is needed for emergent anyons and fermions?” (2024), [arXiv:2405.07970 \[quant-ph\]](#).
- [93] Anton Kapustin and Ryan Thorngren, “Fermionic SPT phases in higher dimensions and bosonization,” *JHEP* **10**, 080 (2017), [arXiv:1701.08264 \[cond-mat.str-el\]](#).
- [94] Maissam Barkeshli, Yu-An Chen, Sheng-Jie Huang, Ryohei Kobayashi, Nathanan Tantivasadakarn, and Guanyu Zhu, “Codimension-2 defects and higher symmetries in (3+1)D topological phases,” *SciPost Phys.* **14**, 065 (2023).
- [95] Maissam Barkeshli, Po-Shen Hsin, and Ryohei Kobayashi, “Higher-group symmetry of (3+1)d fermionic \mathbb{Z}_2 gauge theory: Logical ccz, cs, and t gates from higher symmetry,” *SciPost Physics* **16** (2024), [10.21468/scipostphys.16.5.122](#).
- [96] Ryan Thorngren and Yifan Wang, “Fusion category symmetry i: Anomaly in-flow and gapped phases,” (2019), [arXiv:1912.02817 \[hep-th\]](#).
- [97] Carolyn Zhang and Clay Córdova, “Anomalies of (1 + 1)D categorical symmetries,” (2023), [arXiv:2304.01262 \[cond-mat.str-el\]](#).
- [98] Clay Cordova, Po-Shen Hsin, and Carolyn Zhang, “Anomalies of Non-Invertible Symmetries in (3+1)d,” (2023), [arXiv:2308.11706 \[hep-th\]](#).
- [99] Po-Shen Hsin, Ryohei Kobayashi, and Carolyn Zhang, “Fractionalization of coset non-invertible symmetry and exotic hall conductance,” *SciPost Physics* **17** (2024), [10.21468/scipostphys.17.3.095](#).
- [100] Hoi Chun Po, Lukasz Fidkowski, Takahiro Morimoto, Andrew C. Potter, and Ashvin Vishwanath, “Chiral floquet phases of many-body localized bosons,” *Phys. Rev. X* **6**, 041070 (2016).
- [101] D. Gross, V. Nesme, H. Vogts, and R. F. Werner, “Index theory of one dimensional quantum walks and cellular automata,” *Communications in Mathematical Physics* **310**, 419–454 (2012).
- [102] Jeongwan Haah, Lukasz Fidkowski, and Matthew B. Hastings, “Nontrivial quantum cellular automata in higher dimensions,” *Communications in Mathematical Physics* **398**, 469–540 (2023).
- [103] Jie-Yu Zhang, Meng-Yuan Li, and Peng Ye, “Higher-order cellular automata generated symmetry-protected topological phases and detection through multi point strange correlators,” *PRX Quantum* **5**, 030342 (2024).
- [104] Lukasz Fidkowski and Matthew B. Hastings, “Pumping chirality in three dimensions,” *Phys. Rev. B* **109**, 235142 (2024).
- [105] Lukasz Fidkowski, Jeongwan Haah, and Matthew B Hastings, “A qca for every spt,” [arXiv preprint arXiv:2407.07951 \(2024\)](#).
- [106] Chong Wang and T. Senthil, “Time-reversal symmetric $U(1)$ quantum spin liquids,” *Phys. Rev. X* **6**, 011034 (2016).
- [107] Po-Shen Hsin and Alex Turzillo, “Symmetry-enriched quantum spin liquids in (3 + 1)d,” *JHEP* **09**, 022 (2020), [arXiv:1904.11550 \[cond-mat.str-el\]](#).